

**THE Na⁺/H⁺ EXCHANGER NHE1 PLAYS A PERMISSIVE ROLE IN
REGULATING EARLY NEURITE MORPHOGENESIS**

by

DAVID MATTHEW MONIZ

B.Sc., The University of British Columbia, 2005

A THESIS SUBMITTED IN PARTIAL FULFILMENT OF THE REQUIREMENTS FOR THE
DEGREE OF

MASTER OF SCIENCE

in

THE FACULTY OF GRADUATE STUDIES

(Cell and Developmental Biology)

THE UNIVERSITY OF BRITISH COLUMBIA

(Vancouver)

November, 2008

© David Matthew Moniz, 2008

Abstract

The ubiquitously expressed plasma membrane Na^+/H^+ exchanger isoform 1 (NHE1) plays an important role in directed cell migration in non-neuronal cells, an effect which requires both the ion translocation and actin cytoskeleton anchoring functions of the protein. In the present study, an analogous role for NHE1 as a modulator of neurite outgrowth was evaluated *in vitro* utilizing NGF-differentiated PC12 cells as well as mouse neocortical neurons in primary culture. Examined at 3 d.i.v., endogenous NHE1 was found to be expressed in growth cones, where it gave rise to an elevated intracellular pH in actively-extending neurites. Application of the NHE inhibitor cariporide at an NHE1-selective concentration (1 μM) resulted in reductions in neurite extension and elaboration while application of 100 μM cariporide, to inhibit all known plasmalemmal NHE isoforms, failed to exert additional inhibitory effects, suggesting a dominant role for the NHE1 isoform in modulating neurite outgrowth. In addition, whereas transient overexpression of full-length NHE1 enhanced neurite outgrowth in a cariporide-sensitive manner in both NGF-differentiated PC12 cells and WT neocortical neurons, neurite outgrowth was reduced in NGF-differentiated PC12 cells overexpressing NHE1 mutants deficient in either ion translocation activity or actin cytoskeleton anchoring, suggesting that both functional domains of NHE1 are important for modulating neurite elaboration. A role for NHE1 in modulating neurite outgrowth was confirmed in neocortical neurons obtained from NHE1^{-/-} mice which displayed reduced neurite outgrowth when compared to neurons obtained from their NHE1^{+/+} littermates. Further, neurite outgrowth in NHE1^{-/-} neurons was rescued by transient overexpression of full-length NHE1 but not with mutant NHE1 constructs again suggesting that both functional domains of NHE1 are important for modulating neurite outgrowth. Finally, the growth promoting effects of netrin-1 but not BDNF or IGF-1 were abolished by cariporide in WT neocortical neurons and while both BDNF and IGF-1 were able to promote neurite outgrowth in

NHE1^{-/-} neurons, netrin-1 was unable to elicit this effect. Taken together, these results indicate that NHE1 is a permissive regulator of early neurite morphogenesis and also plays a novel role in netrin-1-stimulated neurite outgrowth.

Table of Contents

	Page
Abstract	ii
Table of Contents	iv
List of Tables	vii
List of Figures	viii
Acknowledgements	x
1.0 Introduction	1
1.1 Neuronal morphogenesis	1
1.1.1 General characteristics	1
1.1.2 Actin cytoskeleton and actin regulating proteins	1
1.1.3 Regulation of Neurite Outgrowth	3
1.1.3.1 Environmental Cues	4
1.1.3.1.1 BDNF	4
1.1.3.1.2 IGF-1	5
1.1.3.1.3 Netrin-1	7
1.1.3.2 Intracellular Signaling Pathways	8
1.1.3.2.1 Calcium	8
1.1.3.2.2 cAMP	10
1.1.3.2.3 RhoGTPases	11
1.1.3.3 Other Mechanisms	13
1.1.3.3.1 Linker Proteins	14
1.1.3.3.1.1 Adhesion Proteins	14
1.1.3.3.1.2 Ion Transporters and Ion Channels	15
1.2 Sodium Proton Exchangers	16
1.2.1 General Characteristics	16
1.2.2 NHE1	17
1.2.2.1 Ion Translocation	18
1.2.2.2 Structural Functions of NHE1	20
1.2.2.2.1 Actin Cytoskeleton Anchor	20
1.2.2.2.2 Scaffold for Signaling Complexes	21
1.2.2.3 Role in Directed Cell Migration	22
1.3 Summary and Objectives	23
2.0 Materials and Methods	32
2.1 Cell Culture	32
2.1.1 PS120 Cells	32
2.1.2 PC12 Cells	33
2.1.3 Mouse Neocortical Neurons	34
2.1.3.1 Primary Culture of E16 Neocortical Neurons	34
2.1.3.2 NHE1 ^{-/-} neurons	35
2.1.3.2.1 Breeding	35
2.1.3.2.2 Genotyping	36
2.1.3.2.3 Primary Culture of P0.5 Neocortical Neurons	37
2.2 Transient Transfection	38

2.2.1 DNA Constructs	38
2.2.2 Transfection Protocols	38
2.2.2.1 PS120 cells	38
2.2.2.2 PC12 Cells	39
2.2.2.3 Primary neurons	40
2.3 Immunocytochemistry and Morphometric Analysis	41
2.3.1 Fixing	41
2.3.2 Staining	41
2.3.3 Morphometric analyses	42
2.3.3.1 Wide field microscopy	42
2.3.3.1.1 Equipment and image acquisition	42
2.3.3.1.2 Criteria for inclusion	43
2.4 Live cell imaging	44
2.4.1 Microspectrofluorimetry	44
2.4.1.1 Experimental solutions	45
2.4.1.2 Imaging equipment	46
2.4.1.3 Dye loading conditions	47
2.4.1.4 Image analysis	48
2.4.1.5 Calibration and calculation of pH_i	48
2.4.2 Time-lapse DIC microscopy	50
2.5 Protein extraction and Western blot analysis	50
2.5.1 Protein isolation	50
2.5.1.1 Whole brain lysate	51
2.5.1.2 PC12 cells	51
2.5.2 Western Blot Analysis	52
3.0 Results	62
3.1 Role of NHE1 in NGF-induced neurite outgrowth in PC12 cells	62
3.1.1 Endogenous NHE1 is expressed in PC12 cell growth cones	62
3.1.2 Application of cariporide at an NHE1 selective concentration reduces neurite outgrowth	63
3.1.2.1 Application of cariporide at a concentration to inhibit all known plasmalemmal NHE isoforms has no additional effect on neurite outgrowth	63
3.1.2.2 Inhibition of neurite outgrowth by 100 μ M cariporide is reversible	64
3.1.3 Transient transfection of either full-length NHE1 or mutant NHE1 constructs modulates neurite outgrowth	65
3.1.3.1 Functional characterization of the full-length and mutant NHE1 constructs	65
3.1.3.2 Transient transfection of full-length NHE1 enhances neurite outgrowth	66
3.1.3.3 Transient transfection of mutant NHE1 constructs reduces neurite outgrowth in NGF-differentiated PC12 cells	67
3.1.4 pH_i Measured in the growth cones of PC12 cells	68
3.1.4.1 pH_i in actively extending neurites is higher than that found at the cell body	68
3.1.4.2 Application of 5 μ M cariporide reduces pH_i in the growth cones of actively extending neurites	69
3.1.4.2.1 Application of cariporide results in a transient cessation of neurite outgrowth	70

3.1.5 NHE1 is involved in the organization of the actin cytoskeleton at the growth cones of NGF-differentiated PC12 cells.....	71
3.1.5.1 Cariporide reduces the total but not the mean length of filopodia at the growth cone.....	71
3.1.5.2 Filopodia number is affected by modulating NHE1 activity.....	72
3.1.5.2.1 Cariporide reduces the number of filopodia at the growth cone	72
3.1.5.2.2 Transient transfection of full-length NHE1 increases the number of filopodia at the growth cone in a cariporide-sensitive manner.....	72
3.1.5.2.3 Transient transfection of NHE1-E266I or NHE1-KR/A does not lead to an increase in the number of filopodia at the growth cone	73
3.2 Role of NHE1 in non-stimulated neurite outgrowth in mouse neocortical neurons.....	74
3.2.1 Neurite outgrowth in wild-type E16 neocortical neurons.....	74
3.2.1.1 Endogenous NHE1 is expressed in the growth cones of E16 neurons	74
3.2.1.2 E16 neurons treated with NHE1 inhibitors exhibit reduced neurite outgrowth	75
3.2.1.3 Transient overexpression of full-length NHE1 enhances neurite outgrowth in a cariporide-sensitive manner	76
3.2.2 Neurite outgrowth in NHE1 ^{-/-} P0.5 mouse neocortical neurons.....	77
3.2.2.1 NHE1 ^{-/-} neurons do not express endogenous NHE1	77
3.2.2.2 Neurite outgrowth is reduced in neurons obtained from NHE1 ^{+/-} mice and to a greater extent in neurons obtained from NHE1 ^{-/-} mice	78
3.2.2.3 Transient overexpression of full-length NHE1 rescues neurite outgrowth in neurons obtained from NHE1 ^{-/-} mice in a cariporide-sensitive manner	78
3.2.2.4 Transient overexpression of either NHE1-E266I or NHE1-KR/A fails to rescue the phenotype of NHE1 ^{-/-} neurons	79
3.3 NHE1 is involved in stimulated neurite outgrowth in mouse neocortical neurons	80
3.3.1 1 μM cariporide abolishes netrin-1 enhanced neurite outgrowth but not outgrowth stimulated by BDNF or IGF-1	80
3.3.2 Netrin-1 fails to stimulate neurite outgrowth in NHE1 ^{-/-} neurons while BDNF and IGF-1 enhance outgrowth.....	81
4.0 Discussion	133
4.1 NHE1 ion translocation and neurite outgrowth.....	135
4.1.1 NHE1 may be creating an [ion] _i microdomain within the growth cone to promote actin dynamics	136
4.1.2 NHE1 may create an acidified extracellular microenvironment to promote the strength of collagen-integrin bonds.....	138
4.1.3 NHE1 may be functioning cooperatively with other ion transporters and/or channels to mediate localized growth cone swelling.....	139
4.2 Potential involvement of the structural functions of NHE1 in regulating neurite outgrowth	141
4.3 NHE1 activity modulates netrin-1 but not BDNF- or IGF-1-enhanced neurite outgrowth	143
4.4 Future directions	147
5.0 References.....	154

List of Tables

	Page
Table 1 Proteinase K digestion buffers.....	54
Table 2 PCR reaction Master Mix.....	55
Table 3 Antibodies used in the experiments.....	56
Table 4 Compositions of experimental solutions for live-cell imaging	57
Table 5 Composition of solutions used during Western Blot analysis.....	58
Table 6 Composition of the SDS-PAGE gels used to separate proteins	69

List of Figures

	Page
Figure 1 Schematic representation of the stages in neurite outgrowth.....	24
Figure 2 Cytoskeletal organization of a growth cone.....	26
Figure 3 Transmembrane organization and regulation of the mammalian Na ⁺ /H ⁺ exchangers NHE1 and NHE3.....	28
Figure 4 Ion transporters at the leading edge of migrating cells.....	30
Figure 5 Sample calibration plot for BCECF.....	60
Figure 6 Endogenous expression of NHE1 in PC12 cells.....	83
Figure 7 Inhibition of NHE1 with cariporide reduces NGF-induced neurite outgrowth in PC12 cells.....	85
Figure 8 Representative PC12 cells showing reduced neurite outgrowth in response to cariporide treatment.....	87
Figure 9 The effects of 100 μM cariporide on neurite outgrowth are reversible.....	89
Figure 10 Functional Characterization of full-length and mutant NHE1 constructs expressed in NHE-deficient PS120 cells.....	91
Figure 11 Quantification of the effects of overexpressing full-length or mutant NHE1 constructs on neurite outgrowth.....	93
Figure 12 Representative PC12 cells showing the effects of overexpressing WT or mutant NHE1s on neurite outgrowth in NGF-differentiated PC12 cells.....	95
Figure 13 pH _i in actively extending neurites is elevated compared to that found at the cell body.....	97
Figure 14 Cariporide (5 μM) caused reversible reductions in pH _i measured simultaneously at the cell body and in the growth cones of actively extending neurites.....	99
Figure 15 Cariporide treatment halts neurite outgrowth and results in the loss of filopodia at the growth cone.....	101
Figure 16 NHE1 regulates filopodia number in PC12 cell growth cones.....	104
Figure 17 Quantification of the effects of modulating NHE1 activity and expression on growth cone filopodia.....	105

Figure 18	NHE1 is endogenously expressed at the growth cones of WT E16 mouse neocortical neurons	107
Figure 19	Quantification of the effects of cariporide and EIPA on neurite outgrowth in WT E16 mouse neocortical neurons	109
Figure 20	Representative WT E16 neurons show reduced neurite outgrowth in response to NHE1 inhibitors.....	111
Figure 21	Overexpression of full-length NHE1 in WT E16 mouse neocortical neurons enhances neurite outgrowth	113
Figure 22	Quantification of the effect of overexpressing NHE1 in WT E16 mouse neocortical neurons.....	115
Figure 23	NHE1 ^{-/-} neurons do not express endogenous NHE1	117
Figure 24	NHE1 ^{+/-} neurons have intermediate neurite outgrowth and sensitivity to 1 μM cariporide compared to NHE1 ^{+/+} and NHE1 ^{-/-} neurons	119
Figure 25	Quantification of neurite outgrowth in NHE1 ^{-/-} neurons transiently overexpressing full-length NHE1 or one of the NHE1 mutant constructs	121
Figure 26	Reduced neurite outgrowth in NHE1 ^{-/-} neurons can be rescued by transient overexpression of WT NHE1 but not by overexpression of NHE1 mutant constructs	123
Figure 27	Quantification of the effect of 1 μM cariporide on netrin-1, BDNF and IGF-1 enhanced neurite outgrowth in NHE1 ^{+/+} mouse neocortical neurons.....	125
Figure 28	Effects of cariporide on increases in neurite outgrowth induced by netrin-1, BDNF and IGF-1 in NHE1 ^{+/+} P0.5 mouse neocortical neurons.....	127
Figure 29	Quantification of neurite outgrowth in NHE1 ^{-/-} P0.5 mouse neocortical neurons treated with netrin-1, BDNF or IGF-1	129
Figure 30	Netrin-1 fails to enhance neurite outgrowth in NHE1 ^{-/-} P0.5 mouse neocortical neurons.....	131
Figure 31	DCC and NHE1 are expressed in close proximity in the growth cones of WT E16 mouse neocortical neurons	150
Figure 32	DCC is required for netrin-1-stimulated neurite outgrowth in WT E16 mouse neocortical neurons	152

Acknowledgements

First and foremost I would like to thank Dr. John Church for his endless gifts of patience, guidance and support throughout my entire project. His approach to supervision allowed me a wide degree of latitude to pursue my research as I saw fit, while directing me during the times when I lost the plot and began to head off-course. I would also like to thank the members of my supervisory committee Drs. Calvin Roskelley, Timothy O'Connor and Masayuki Numata for sharing their time, advice and scientific knowledge throughout my project and Drs. Kurt Haas and Douglas Allan for being a part of my examination committee.

I am also grateful to Drs. Mark Ozog, Tony Kelly and Wun Chey Sin for sharing their expertise in the lab and helping with the design and implementation of key experiments critical for the work presented in this thesis. I would also like to thank Jessica Tyler and Nicola Tam for their help with various aspects of data analysis and quantification. To the members of the Dept. of Cellular and Physiological Sciences and the Life Sciences Institute it has been a pleasure getting to know and working with many of you; without your camaraderie and support I would not have enjoyed my time here as thoroughly as I did. Finally I would like to thank my family for their unconditional love and support.

1.0 Introduction

1.1 Neuronal morphogenesis

1.1.1 General characteristics

One of the principal characteristics of neuronal differentiation is the induction of membrane protrusions that develop and become discernable as axons and dendrites (hereafter collectively termed "neurites") as the neuron becomes polarized (Fig. 1; [1, 2]). The growth of neurites is lead by a highly motile structure at the extending tip, the growth cone, which receives and processes signals from the extracellular environment to direct the rate as well as the direction of neurite outgrowth [2-10]. Neurite outgrowth can be divided into 3 distinct stages which are all essential for the proper growth and pathfinding of neurites to form the intricate neural networks required for proper functioning [1, 2, 4, 11]. In the first stage, budding protrusions, which are rich in actin, extend from spherical neural progenitor cells and effectively become the growth cones of the immature neurites [1, 2, 4, 11]. The second stage is the elongation phase where neurites extend from the cell body uniformly in all directions and also begin to branch from already existing neurites [1, 2, 4, 11]. During the third stage, the neurons become polarized, an event which is characterized by the accelerated growth of one neurite, which is now the cell's axon [1, 12-15]. The mechanisms underlying growth cone motility are still poorly understood but are thought to be similar to mechanisms involved in directed migration of non-neuronal cells.

1.1.2 Actin cytoskeleton and actin regulating proteins

Structurally, growth cones are organized into three distinctive domains central, transition and peripheral which differ in the composition of the cytoskeletal components [4, 6, 8, 11, 16].

Within the central domain of the growth cone a relatively high concentration of microtubules

extending from the cell body up the length of the neurite provide support and stability to the growth cone as well aiding in trafficking of materials to and from the cell body [4, 9, 11, 17]. Additionally, microtubules extend into the transitional zone where they interact with and are able to re-orient towards localized accumulations of F-actin in response to growth cone turning [4, 9, 11, 17]. The peripheral zone primarily contains actin fibers organized into discrete structures called lamellipodia and filopodia [4, 8, 9, 11, 17]. Filopodia, which contain projections of tight actin bundles, extend from the growth cone and interact with various guidance cues ultimately directing the path for the neurite (Fig. 2; [2, 18, 19]). In contrast, lamellipodia consist of networks of cross-linked actin fibers resulting in flat broad structures in between the individual filopodia, localizing scaffolding complexes at the leading edge to mediate actin polymerization required to drive the growth of the neurites (Fig. 2; [2, 18, 19]).

The mechanisms underlying actin dynamics during neurite outgrowth are thought to be analogous to the mechanisms involved in leading edge membrane protrusion and directed cell migration in fibroblasts. Actin dynamics within migrating fibroblasts are largely directed by the activities of small Rho-family GTPases which ultimately signal to a number of key actin regulatory proteins [20-22]. Chief among these are actin depolymerising factor (ADF) working in conjunction with cofilin which depolymerise F-actin at the minus end thereby freeing monomers for further polymerization, and the actin related protein complex (Arp 2/3) which nucleates actin monomers to prepare them for polymerization [8, 19]. ADF/cofilin, which are activated by LIMK downstream of Rac1 activation as well as calcium and cAMP signaling (see sections 1.3.2.1, 1.3.2.2 and 1.3.2.3 below) are expressed within growth cones and it has been shown that inhibition of ADF/cofilin activity inhibits neurite outgrowth [8, 23]. The Arp 2/3 complex, activated by Neuronal Wiskott-Aldrich Syndrome Protein (N-WASP), a downstream

effector of Cdc42, is required for dendritic spine morphogenesis in hippocampal neurons and is a key component in the formation of filopodia at the growth cone [19, 24, 25].

1.1.3 Regulation of neurite outgrowth

The regulation of neurite outgrowth is a complex process involving a variety of mechanisms including localized protein synthesis within the growth cone and along the neurite [26-29] as well as neuronal activity in developing neurons [30-36]. In addition, a number of environmental cues, intracellular signaling cascades as well as interactions between the actin cytoskeleton and the plasma membrane play important roles in regulating and directing neurite outgrowth (see sections 1.3.1, 1.3.2 and 1.3.3 respectively below).

Localized protein expression within the growth cones of growing neurites promotes neurite outgrowth by ensuring that, as the growth cone extends further away from the cell body, it maintains a supply of proteins essential for continued growth of the neurite [29, 32, 35]. For example, localized protein expression within the growth cones of extending neurites has been shown to maintain a steady supply of β -actin in response to a variety of neurotrophic factors to ensure the continued availability of actin polymers (see [29] for a review). In addition, a report by Kirkland and Franklin [32] showed that the rate of protein synthesis and degradation are linked within the growth cone and without this link, any suppression of protein synthesis could potentially lead to cell atrophy as proteins would be degraded faster than they could be produced.

An established link between neuronal activity and neurite outgrowth has also been established in a number of studies on *Xenopus* retinal neurons, whereby neuronal activity-dependent dendritic growth and remodelling was shown to be important for neural network formation during development [30, 31, 33, 34, 36]. Neuronal activity is important for regulating

the activities of the Rho GTPases thereby modulating the reorganization of the actin cytoskeleton to promote the formation of the dendritic arbour during synaptogenesis [30, 31, 33, 34, 36].

1.1.3.1 Environmental cues

A variety of environmental cues have been found to promote neurite outgrowth during development including the neurotrophins (nerve growth factor (NGF), brain-derived neurotrophic factor (BDNF; see section 1.3.1.1 below), neurotrophin 3 (NT-3) and neurotrophin 4 (NT-4); for reviews see [37]) as well as a number of guidance cues which function in growth cone pathfinding (e.g. Semaphorins, Slits, Ephrins and Netrin-1 (see section 1.3.1.3 below); for a review see [38] and [39]). Additionally, a number of seemingly unrelated growth factors which have widespread effects throughout the body have also been shown to promote neurite outgrowth during development (e.g. fibroblast growth factor (FGF) and insulin-like growth factor-1 (IGF-1, see section 1.3.1.2 below, for reviews see [38, 40]).

1.1.3.1.1 BDNF

BDNF has been shown to be a key modulator of neurite outgrowth in a number of neuronal types during development as well as being an important regulator of synaptic plasticity in adult neurons (for reviews see [41-43]). The predominant effect that BDNF seems to elicit during neurite outgrowth is an increase in the number and length of primary neurites with minimal effects on the extent of neurite branching [44-46]. In a report by Beck *et al.* [44] application of BDNF to explanted rat dopaminergic neurons stimulated the formation of primary neurites with little effect seen on the formation of branched neurites. In addition, Hanamura *et al.* [45]

reported that thalamic explants from embryonic day 16 (E16) rats had increased rates of axonal outgrowth, with little effect seen in dendritic growth, in response to exogenously applied BDNF.

Growth promoting effects elicited by BDNF are predominantly via interactions of BDNF with the high affinity tyrosine receptor kinase B (TrkB) [37, 42, 47]. Interaction between BDNF and TrkB initiate a number of signaling cascades (including phosphatidylinositol 3-kinase (PI3K), phospholipase C- γ (PLC γ) and the Ras-mediated cascade) which ultimately lead to changes in actin cytoskeleton dynamics essential for neurite initiation and elongation (see [41, 42] for reviews). One of the major effects of activation of both the PI3K and Ras-mediated cascades is the downstream activation of the Rho GTPases [37]. BDNF activation of TrkB leading to the activation of PI3K has been shown to activate guanine exchange factors (GEFs) which activate Rac1 and Cdc42 leading to actin modifications (see [37, 42] for reviews and section 1.3.2.3 below). PLC γ signaling, on the other hand, has been shown to hydrolyse phosphatidylinositol 4,5-bisphosphate (PIP2) into inositol 3 phosphate (IP3) and diacylglycerol [37]. IP3 subsequently binds to the IP3 receptor in the endoplasmic reticulum (ER) leading to the release of intracellular calcium stores which is itself an important modulator of neurite outgrowth (see section 1.3.2.1 below; [48, 49] and [37] for reviews).

1.1.3.1.2 IGF-1

It is established that signaling via IGF-1 is an important modulator of neurite outgrowth and elaboration in the developing nervous system (for reviews see [46, 50]). IGF-1 is produced by a variety of neurons within the CNS (including cortical cells) with an expression peak seen during periods of neuron proliferation and neurite outgrowth (for reviews see [46, 50]). The effects of IGF-1 are mediated through an interaction with a tyrosine receptor kinase on the cell surface

leading to an enhancement of both neurite length as well as elaboration of both axons and dendrites [46, 51]. IGF-1 has been postulated to be primarily involved in embryonic neurite outgrowth as the expression levels have been shown to peak around embryonic day 14 (E14) with an approximate 3-4 fold decrease at birth [52]. Interestingly however, it has been reported that mice which overexpress IGF-1 have increased postnatal outgrowth with minimal anatomic abnormalities observed, while mice in which IGF-1 expression has been ablated have a significant reduction in brain size and function with the most prominent effects seen in the cerebral cortex and cerebellum (for a review see [50]).

Upon binding to its receptor, IGF-1 initiates a number of signaling cascades important for cell survivability and outgrowth (for a review see [53]). A number of studies have linked the activation of PI3K via IGF-1 binding to the IGF-1 receptor as being essential for neurite outgrowth promotion [51, 53, 54]. A report by Laurino *et al.* [54] showed that the plasmalemmal expansion induced by IGF-1 action was dependent on the activation of the PI3K cascade and inhibition of the pathway prevented expansion and concomitantly inhibited neurite outgrowth. Additionally, activation of PI3K downstream of IGF-1 has been linked with the activation of Rac1 ultimately promoting actin cytoskeletal dynamics within the growth cone [53]. IGF-1 also activates the mitogen activated protein kinase (MAPK) signaling pathway leading to the activation of extracellular related protein kinase 1 and 2 (ERK1/2) which has a well established role in mediating neurite outgrowth as well as being a key regulator of NHE1 activity (see [53] for a review; see also [55] and section 2.3.1.1 below). Interestingly, IGF-1 has been found to inhibit the activation of glycogen synthase kinase 3 β (GSK3 β) in neuronal cells; when activated, GSK3 β leads to the hyperphosphorylation of Tau, a microtubule associated protein, and subsequently to neuronal degeneration [40].

1.1.3.1.3 Netrin-1

Netrin-1, a member of the highly conserved family of laminin-related proteins, is a well established guidance cue involved with axon pathfinding as well as mediating neurite outgrowth in the developing nervous system (for reviews see [39, 56, 57]). A number of studies have found that the interaction of netrin-1 with the deleted in colorectal cancer (DCC) receptor is required for the netrin-1-dependent enhancement of outgrowth, while the interaction between netrin-1 and an additional receptor, uncontrolled-5 (Unc-5), generally leads to growth cone repulsion [39, 58-63]. Netrin-1/DCC signaling in large part ultimately induces cytoskeletal rearrangements via the activation of Cdc42 and Rac1 with a concomitant decrease in the activation of RhoA (see section 1.3.2.3 below; [39, 64-69]). Interestingly, on netrin-1 binding to DCC, the cytosolic pool of DCC is recruited to the plasma membrane where it functions as a scaffold for a number of signaling cascades [39, 65, 66, 69, 70]. Of note is the recruitment of the adaptor protein Nck1 to the membrane which serves as a scaffold to recruit Cdc42, Rac1 and their effectors p21 associated kinase-1 (PAK1) and N-WASP to the activated DCC receptor, thereby leading to the formation of an intracellular signaling complex that provides a link between DCC and Rho GTPases in regulating the actin cytoskeleton [66, 70].

In addition to Rho GTPases, a variety of second messengers regulate the growth-promoting effects of netrin-1 (see [39] for a review). In particular, elevations in growth cone calcium (via increases in calcium influx and/or calcium release from intracellular stores; see section 1.3.2.1 below) and $[cAMP]_i$, which has long been known to promote the morphological maturation of primary neurons (see section 1.3.2.2 below), have been suggested to play important roles in netrin-1-induced neurite outgrowth [39, 71-74]. Although the involvement of cAMP appears to be cell-type specific and the precise role of PKA remains in question [68, 75,

76], netrin-1 has been found to increase $[cAMP]_i$ in growth cones to promote growth cone elaboration, attractive turning and/or neurite outgrowth in some types of neurons [77-79].

1.1.3.2 Intracellular signaling pathways

The regulation of neurite outgrowth is dependent on the activation of a number of intracellular signaling pathways (for reviews see [55, 72]). Each of the factors discussed above initiates a signaling cascade within the cell which requires the activation of second messengers to elicit the promotion of neurite outgrowth. Of immediate importance to the work presented in this thesis are the actions of the calcium, cAMP, and Rho GTPase signaling pathways.

1.1.3.2.1 Calcium

Calcium signaling within neurons plays important roles in growth cone guidance in addition to promoting neurite outgrowth in the developing nervous system (for reviews see [55, 72, 80]). The levels of free ionized calcium in the cell are tightly regulated by a combination of calcium influx through voltage-gated calcium channels (e.g. L-type calcium channels), calcium efflux via transporters (such as the Na^+/Ca^{2+} exchanger) as well as by calcium release from intracellular stores (e.g. in the endoplasmic reticulum; [81-83]). Several reports have indicated that the level of calcium in the cell is required to be maintained within an optimal range to promote neurite outgrowth and that deviation from the optimum concentration in either direction leads to an inhibition of neurite outgrowth [81-83]. In a report by Tang *et al.* [83] transient, rather than sustained, increases in calcium levels enhanced neurite outgrowth in both chick DRG and *Xenopus* spinal neurons and inhibition of either calcium influx or the mobilization of calcium from intracellular stores blocked neurite outgrowth. In addition, Lohmann *et al.* [84] showed

that blocking localized calcium transients within the growth cone resulted in dendritic retractions in E18-19 chick retinal ganglion cells, however, blockade of whole cell calcium transients did not appear to have an effect on neurite outgrowth. These findings suggest that localized calcium levels within the growth cone are an important modulator of neurite outgrowth during development. Calcium transients have also been implicated as being important modulators of axon regeneration following spinal cord injury. Ziv and Spira [85] reported that axotomized *Aplysia* neurons experienced elevated calcium levels at the site of the axotomy which ultimately lead to the formation of a new growth cone and subsequent regrowth of the neurite. In addition, they found that by ectopically inducing high calcium levels the axotomized neurons formed growth cones, resulting in neurite outgrowth at branch points [85].

Calcium signals through a number of pathways to elicit the growth promoting effects seen in neurons (see [80] for a review). A key downstream effector in the calcium pathway is calmodulin (CaM) and the calmodulin dependent kinase II (CaMKII) which acts as both a cytoplasmic protein which has been shown to modulate actin organization and also as a nuclear transcriptional regulator [49, 80, 86, 87]. Chen *et al.* [87] reported that elevations in calcium levels activated CaMKII and subsequently led to formation of filopodia at the growth cone, while inhibition of CaMKII prevented this formation. In addition, it has been reported that CaM binding to calcium activates the phosphatase calcineurin which can dephosphorylate GAP-43 leading to destabilization of filamentous actin (F-actin) and thus neurite outgrowth by releasing actin monomers for further actin polymerization (see [88] for a review).

Calcium has also been implicated as an important modulator of the actin cytoskeleton independent of CaM by playing a role in inhibiting retrograde actin flow (for a review see [88]). By inhibiting the retrograde flow of actin, actin monomers are sequestered within the growth

cone where they can be polymerized into F-actin to promote neurite outgrowth [88]. In addition, increases in calcium have been shown to dephosphorylate and thereby activate ADF which promotes actin depolymerization at the minus end to free monomers for further polymerization at the plus end (see [80] for a review). Calcium transients have also been shown to modulate the activities of the Rho GTPases (see section 1.3.2.3 below) within the growth cone, thereby promoting the actin dynamics necessary for the promotion of neurite outgrowth ([89]; also see [88] for a review). For example, it has been reported that increased calcium levels in the growth cone lead to the dissociation of Rac from the GDP dissociation inhibitor Rho-GDI and thereby promote the translocation of Rac to the plasma membrane where it becomes activated and initiates lamellipodia formation [89].

1.1.3.2.2 cAMP

Many reports have shown the importance of cAMP signaling during neurite outgrowth and during axon regeneration following both spinal cord and traumatic brain injuries and it has been suggested that the main activity of cAMP appears to be modulation of neurite initiation with only a minor role in neurite elongation [90-93]. A recent report by Aglah *et al.* [90] also proposed that elevated cAMP levels may be necessary to overcome inhibition to neurite outgrowth elicited by myelin associated glycoprotein (MAG), Nogo-A and oligodendrocyte-myelin glycoprotein (OMG) following spinal cord injury and thereby may improve axon regeneration [90]. In addition, Atkins *et al.* [94] showed that following induction of traumatic brain injury in rats, a decrease in cellular cAMP levels resulted in the inhibition of neurite regeneration and ultimately to the formation of cortical contusions in the animals. Inhibiting the activity of phosphodiesterase IV (PDEIV), an enzyme which degrades cellular cAMP, resulted in

an increase in cAMP levels within the cell and ultimately to the regeneration of neurites and a reduction in cortical contusions following traumatic brain injury [94].

The major downstream effector of cAMP is the cAMP-dependent protein kinase A (PKA) which, once activated, has a multitude of downstream effects (for reviews see [95] and [96]). Indeed many studies have shown that PKA is expressed in growth cones and inhibiting its activity abrogates the effects of cAMP on neurite initiation (e.g. see [93, 97]; also see [95, 96]). The predominant effect of PKA in mediating neurite outgrowth appears to be its ability to modulate the activities of a number of actin cytoskeleton-associated proteins and thereby induce changes in cytoskeletal dynamics important for neurite outgrowth (see [95, 96] for reviews). Indeed it has been shown that PKA is able to decrease the phosphorylation state and thereby activate ADF/cofilin during neurite outgrowth to increase actin turnover in the growth cone [95]. In addition, PKA has been shown to play a role in activating Rac1 and Cdc42 to promote lamellipodia and filopodia formation, respectively, while inhibiting the activity of RhoA (see section 1.3.2.3 below and [95, 96]). PKA also elicits calcium transients within neuron growth cones by activating L-type calcium channels as well as activating IP3 receptors in the ER, thereby mobilizing intracellular calcium stores [95, 97] and, as discussed in section 1.3.2.1 above, calcium plays a major role in mediating neurite outgrowth and the coupling of these two pathways may be an important regulatory step in the activities of both.

1.1.3.2.3 Rho GTPases

Ridley and Hall [98, 99] first established the importance of Rho GTPase activity in promoting the actin cytoskeletal dynamics essential for cell motility and migration in non-neuronal cells. Rho GTPases cycle between an inactive guanine diphosphate (GDP) bound state and an active

guanine triphosphate (GTP) bound state via the activities of guanine nucleotide exchange factors (GEFs), which replace the GDP with GTP, and GTPase activating proteins (GAPs) which catalyze the conversion of GTP to GDP (see [2] for a review). During neuritogenesis the activities of the Rho GTPases RhoA, Rac1 and Cdc42 have been especially well-studied and have been shown to play a critical role regulating the actin filament dynamics necessary to promote neurite outgrowth [100-102]. While the activation of RhoA and its downstream effector RhoA associated kinase (ROCK) has been shown to promote motility in non-neuronal cells, it has been shown that during neuritogenesis, inhibition of RhoA is essential for the initiation and extension of neurites, while the activation of Rac1 and Cdc42 has been shown to be required for neurite outgrowth and the formation of actin-based structures such as microspines, lamellipodia and filopodia in growth cones and along neurites (see [2, 101]). In addition, the activation of Cdc42 and/or Rac1 is typically associated with a reciprocal downregulation of RhoA [22, 103, 104].

The Rho GTPases activate a number of downstream effectors which modulate the actin cytoskeleton upon activation (see [2, 101, 105]). During neuronal morphogenesis, Rac1 typically activates PAK1, which subsequently activates LIMK leading to the phosphorylation, and subsequent inactivation of, ADF/cofilin, thereby promoting the formation of lamellipodia [2, 20, 101]. However, a report by Lamoureaux *et al.* [106] suggested that, while Rac1 activation is important for growth cone function and the development of lamellipodia, it plays a minor role in the assembly of the neurite during elongation. On the other hand, Cdc42 activates N-WASP, leading to the activation of Arp 2/3 resulting in *de novo* F-actin assembly and filopodia formation in the growth cone [2, 20, 101]. In addition, a report by Wang *et al.* [107] showed that both Rac1 and Cdc42 activated IQ motif containing GTPase activating protein-3 (IQGAP3),

leading to the crosslinking of F-actin within the growth cones of hippocampal neurons, and that this activation was essential for axon outgrowth within these cells. The combined activities of Rac1 and Cdc42 thus work cooperatively to elongate F-actin within the growth cone and along the extending neurite to promote neurite outgrowth.

In contrast, activation of RhoA followed by the subsequent activation of its major downstream effector ROCK, promotes the formation of stress fibers and disrupts the disassembly of focal adhesions (FAs) and has been implicated in neurite retraction (reviewed by [22, 101]). Interestingly, Dubreuil *et al.* [108] showed that following spinal cord injury, RhoA and ROCK become hyperactivated leading to inhibition of neurite regeneration and also to an increase in cell apoptosis. Inhibition of neurite outgrowth could be abrogated by the inhibition of either RhoA directly or by inhibition of ROCK further highlighting the inhibitory role RhoA plays in neurite outgrowth [108]. Additionally, a recent report by Moore *et al.* [109] indicated that inhibition of RhoA is required for netrin-1 stimulated recruitment of DCC to the plasma membrane where it is then able to form the signaling complex discussed above (section 1.3.1.3).

1.1.3.3 Other mechanisms

Although there are numerous mechanisms which likely contribute to early neurite morphogenesis, for the purposes of the work presented in this thesis, the role of the actin cytoskeleton anchoring within the spatially restricted region of the growth cone will be highlighted. In migrating non-neuronal cells it has been shown that the actin cytoskeleton is tethered to the plasma membrane at the leading edge via interactions with integral membrane proteins and linker proteins which can either bind directly or indirectly to plasma membrane proteins (see [110] for a review).

1.1.3.3.1 Linker proteins

Linker proteins, which include talin, ankyrin, ezrin radixin moesin (ERM) and protein band 4.1 proteins, serve as a vital link between the actin cytoskeleton and the plasma membrane [110, 111]. These proteins bind to integral plasma membrane proteins and to F-actin at the leading edge of migrating cells and serve to anchor the actin cytoskeleton in these spatially restricted domains [110, 111]. Of importance to neurite outgrowth, ERM proteins have been found localized to the growth cones of extending neurites where they may play a role in anchoring the actin cytoskeleton and thereby permit actin cytoskeleton dynamics to be localized within the growth cone [112]. In their inactive conformation, ERM proteins bind head to tail which blocks the binding sites of the protein, and upon phosphorylation, ERM proteins effectively open up their binding sites to serve as an anchor between the actin cytoskeleton and the plasma membrane [110, 113, 114]. Among the integral membrane proteins with which linker proteins interact to anchor the actin cytoskeleton to the plasma membrane are adhesion proteins (e.g. intracellular cell adhesion molecules (ICAMs), integrins and CD44) as well as ion transport proteins (e.g. Na⁺/H⁺ exchangers (NHEs) and anion exchangers (AEs)) (see [110] for a review).

1.1.3.3.1.1 Adhesion proteins

Adhesion proteins play a pivotal role in anchoring the actin cytoskeleton to the plasma membrane and, as a result of their interactions with the extracellular matrix (ECM), also serve as an indirect link between the actin cytoskeleton and the ECM (see [115]). A number of reports have indicated that the association of ERM proteins with adhesion molecules is required for the localization of the adhesion molecules to the membrane where they are able to function in the formation of adhesion complexes ([115-118]; see also [110]). In a report by Serrador *et al.* [117]

they showed that the association of ERM proteins with ICAM-1 and ICAM-2 localizes the adhesion molecules to the leading edge of migrating T lymphocytes where they help mediate cellular migration. Inhibition of ERM binding to either ICAM disrupted their localization to the leading edge and resulted in disrupted cell migration [117].

1.1.3.3.1.2 Ion transporters and ion channels

Ion transporters, including ion exchangers and P-type ATPases, as well as ion channels have been found which act to anchor the actin cytoskeleton to the plasma membrane at the leading edge of migrating fibroblasts [110]. Linking the actin cytoskeleton to ion transporters and ion channels has been proposed to potentially serve two functions. First, it is thought that tethering the actin cytoskeleton to ion transporters/channels serves to localize the transporters/channels at the leading edge of migrating cells where their localized activities aid in the creation of discrete [ion]_i microdomains within this region [119]. Second, it is thought that by tethering the actin cytoskeleton within these ionic microdomains, ion transporters/channels may provide an appropriate ionic environment to allow the activation of actin regulatory proteins thus promoting actin cytoskeletal dynamics required for migration [119]. Of importance to the work presented in this thesis, Na⁺/H⁺ exchanger isoform 1 (NHE1) has been shown to bind to ERM proteins at the leading edge of migrating fibroblasts, an interaction which is important for directed cell migration in these cells [120, 121].

1.2 Sodium proton exchangers

1.2.1 General characteristics

Na^+/H^+ exchangers (NHEs) are integral membrane proteins which mediate the electroneutral exchange of intracellular H^+ for extracellular Na^+ and thereby play a critical role in maintaining intracellular acid-base balance, Na^+ homeostasis as well as cell volume control [122-125]. To date nine mammalian isoforms have been identified (NHE1-9) which play a role in maintaining both cytosolic and organellar ion and volume dynamics [126]. NHE isoforms fall broadly into 2 categories: 1) isoforms predominately localized to the plasma membrane (NHE1-5) and 2) isoforms which are predominately localized to the endomembrane system within the cell (NHE6-9) [126]. Interestingly, even though NHE3 and NHE5 are predominately localized to the plasma membrane, recent evidence has suggested that they may also enter recycling endosomes (see [126] for a review). The NHE isoforms which are predominately localized to the plasma membrane are also differentially expressed in different tissue types (for reviews see [126] and [127]). For example NHE3 is found expressed predominately in the epithelia of the gastrointestinal tract while NHE5 is expressed in neuron enriched regions of the brain [123, 126, 127]. The exception to this is NHE1, which, like the organellar NHE isoforms (NHE6-9) has a ubiquitous expression in virtually all cell types [123, 126, 127].

NHE isoforms have two functional domains, an *N*-terminal membrane spanning domain and a *C*-terminal cytosolic domain (Fig. 3; [123, 124, 126, 128, 129]). The *N*-terminal domain exhibits a common membrane topology amongst all of the known isoforms and contains 12 membrane-spanning segments and serves as the site of ion translocation [123, 124, 126, 128, 129]. The *C*-terminal domain, however, is more variable and contains numerous sites for phosphorylation and for the binding of ancillary proteins which, in turn, regulate transport

activity [119, 123-126, 128-130]. Extensive work has been done on characterizing the *C*-terminal domains of both NHE1 and NHE3 (Fig. 2; see also [123]) and it is thought the *C*-terminal domains of NHE2 and NHE4 share sequence homology with the *C*-terminus of NHE1 while the *C*-terminal domain of NHE5 shares sequence homology to the *C*-terminus of NHE3. The *C*-terminal domains of the organellar NHEs, however, are not well understood as of yet.

1.2.2 NHE1

NHE1 was originally cloned and characterized as the growth factor activatable Na^+/H^+ exchanger in fibroblasts [131]. Although NHE1 is expressed throughout the plasma membrane, several studies have shown that it localizes to lamellipodia at the leading edge of migrating fibroblasts where its activity has been shown to play a permissive role mediating cell proliferation, growth and motility, effects which require both functional domains of the protein (for reviews see [119, 124, 130]). Within the rat central nervous system (CNS), NHE1 has been shown to be expressed in virtually all regions of the CNS with the highest levels within the hippocampus and cerebral cortex suggesting that it may be a key regulator of intracellular pH (pH_i) within the CNS [132]. Additionally, a report by Tolkovsky and Richards [133] found that sympathetic neurons isolated from rat superior cervical ganglia maintained pH_i within the soma and along neurites by a mechanism predominated by NHE1 activity.

As noted above (Section 1.3.3.1.2), NHE1 plays an important role in regulating leading edge membrane protrusion and directed migration in a variety of non-neuronal cells, however a role for NHE1 in the migration and/or development of central neurons has not as of yet been established. However, there are suggestions that NHE1 may be involved in CNS development based on observations in mice which harbor a spontaneous mutation within the NHE1 allele

[134]. A study by Cox *et al.* [134] found that mice with a phenotype characterized by persistent short-wave epilepsy (*swe*) exhibited a spontaneous mutation in the *Nhe1* allele. A genetic map identified a point mutation within the *Nhe1* allele which resulted in a premature stop codon ultimately leading to a non-functional truncated *Nhe1* transcription product [134]. These mice exhibited epileptic seizures, truncal instability, ataxia and a notable loss of cerebellar deep nuclei neurons which was coincident with the onset of ataxia, suggesting that NHE1 may be an important modulator of neuronal development [134]. Interestingly, when these mice were backcrossed into wild-type C57BL/6 mice, a congenic strain (B6.SJL-+/*swe*) was developed and it was found that mice heterozygous for the mutation (+/*swe*) were indistinguishable from their wild-type littermates, however mice homozygous for the mutation (*swe/swe*) showed the same phenotypic characteristics [134].

1.2.2.1 Ion translocation

The ubiquitous expression of NHE1 suggests that its ion translocation activity plays a major role in cellular acid-base and Na^+ ion homeostasis, as well as the maintenance of cell volume in most if not all cell-types [110, 123, 126]. Ion translocation through NHE1 is a passive process driven by the transmembrane Na^+ gradient. However ion translocation activity is tightly controlled by numerous signal transduction cascades which converge on the C-terminal regulatory domain as well as by pH_i itself [124, 128, 129]. At normal resting pH_i , the ion transport site within the N-terminal transmembrane domain is allosterically hindered thereby preventing the binding of H^+ ions to the transport site [124, 128, 129]. However, a proton modifier site proximal to the ion transport site has been shown to bind H^+ in response to a decrease in pH_i (i.e. an increase in $[\text{H}^+]_i$) and in turn this binding confers an allosteric modification to the ion transport site thereby

activating ion exchange activity [135-137]. Decreases in pH_i have been found to be sufficient to activate NHE1 ion exchange activity independent of activation from signaling cascades highlighting the important role for NHE1 in pH_i homeostasis [125, 128, 129].

In addition to activation of NHE1 in response to decreases in pH_i , it has also been shown that a variety of growth factors, signaling via tyrosine receptor kinases (e.g. IGF-1, EGF) or G-protein coupled receptors (e.g. α -thrombin, serotonin), can activate NHE1 [131, 135, 138, 139]. Growth factor activation of NHE1 is dependent on the phosphorylation of serine and threonine residues within the distal portion of the C-terminal tail which shifts the set point for activation allowing NHE1 exchange activity under more alkaline conditions (see [124, 128] for reviews). Phosphorylation of NHE1 has been shown to potentially involve several different kinases including MAPK signaling to ERK1/2, CaMKII, and Nck-interacting kinase (NIK; see [128, 140, 141] for reviews). For example, a report by Takahashi *et al.* ([142]) found that a downstream effector of the ERK1/2 pathway, p90 ribosomal S6 kinase (p90^{rsk}), was able to directly phosphorylate NHE1 and activate ion exchange activity in rat vascular smooth muscle cells. Interestingly, there have also been reports that NHE1 is activated downstream of RhoA through phosphorylation via ROCK in fibroblasts; in turn, this activation of NHE1 has been suggested to be essential for RhoA function [143, 144].

Other signaling molecules, including CaM and PIP2, also regulate NHE1 activity in many cell types. In NHE1 deficient Chinese hamster lung fibroblast cells (PS120 cells), transiently transfected with full-length human NHE1, for example, CaM binds to the C-terminal domain of NHE1 in a calcium-dependent manner and inhibition of the CaM binding suppresses the activation of exchange activity in response to growth factors [145-147]. Thus, the CaM binding site on NHE1 serves as an auto-inhibitory domain in the absence of CaM, and CaM

binding to this site removes the inhibition resulting in the activation of exchange activity [145-147]. In addition, PIP₂, which binds to two proximal regions within the C-terminal domain, is a key regulator of exchange activity, and it was reported by Aharonovitz *et al.* [148] that prevention of this interaction at either site inhibits exchange activity (also see [124, 128, 149] for reviews). Interestingly, although NHE1 is ubiquitously expressed in all cell and tissue types, it appears to be differentially regulated in different cell types. For example, while cAMP/PKA has been found to have either no effect on or cause inhibition of NHE1 in many cell types [150-152], Yao *et al.* ([153]) found that functional Na⁺/H⁺ exchange in mouse hippocampal neurons required cAMP/PKA activation. A similar finding was made in trout red blood cells in which βNHE, a homologue of NHE1, was found to be activated in response to cAMP/PKA [154].

1.2.2.2 Structural functions of NHE1

In addition to mediating H⁺ and Na⁺ homeostasis and cell volume control, NHE1 functions as a plasma membrane tether for the actin cytoskeleton as well as a scaffold for the assembly of macromolecular signaling complexes [110, 130]. Both of these structural functions contribute to the role of NHE1 in regulating leading edge membrane protrusion and directed motility in non-neuronal cell types [110, 130].

1.2.2.2.1 Actin cytoskeleton anchor

ERM proteins interact with the C-terminal tail of NHE1 and thereby anchor the actin cytoskeleton to NHE1 and the plasma membrane [120, 121, 130]. The anchoring of NHE1 to the actin cytoskeleton maintains NHE1 localization at the leading edge of migrating cells where

its translocation activity helps to create an appropriate environment for the actin cytoskeletal dynamics important for cell motility and migration (see [119, 130] for reviews)

1.2.2.2.2 Scaffold for signaling complexes

NHE1 is emerging as an important plasma membrane scaffolding protein that localizes signaling complexes to the leading edge of migrating cells [119, 130]. The *C*-terminal domain of NHE1 contains binding sites for a number of functionally distinct signaling molecules which may coordinate signal relays at the leading edge [119, 124, 128-130]. As discussed in section 2.2.2.1 above, ERM proteins bind to NHE1 and serve to anchor the actin cytoskeleton to NHE1. In addition, PIP2 binds to regions in close proximity to the ERM binding sites and it has been proposed that the close association of ERM with PIP2 maintains the ERM proteins in the open configuration required to bind to NHE1 and actin [125] (see also [148]). PIP2 is also a key modulator of actin cytoskeleton remodeling by coordinating with active Cdc42 to activate N-WASP, resulting in increased actin nucleation and filament formation by Arp 2/3 ([155]; see also [130]). In addition, NHE1 binds NIK, which regulates actin dynamics by binding to its adapter protein Nck which subsequently is able to activate N-WASP ([156] and see [130] also). The *C*-terminal domain of NHE1 also contains binding sites for CaM, calcineurin homologous protein (CHP), the adapter protein 14-3-3 and carbonic anhydrase II (CAII). In addition to their roles in regulating NHE1 activity (see [119] for a review), CaM, 14-3-3 and PIP2 are also known to facilitate the formation of large multi-protein signaling complexes at the plasma membrane [130]. Interactions between NHE1 and these proteins may therefore result in NHE1 being associated with additional signaling complexes at the leading edge in migrating cells thereby further enhancing its role as a scaffolding protein.

1.2.2.3 Role in directed cell migration

NHE1 is a key modulator of directed cell migration in a variety of cell types, a function which requires both the ion translocation as well as the actin cytoskeletal anchoring functions of the protein [120, 121]. Denker and Barber ([120]) showed that NHE1-deficient PS120 fibroblast cells had disrupted cell migration, a phenotype which could be rescued by transfecting the cells with full-length NHE1. However, transfecting the cells with either ion translocation-deficient or ERM binding-deficient mutants maintained the disrupted cell migration but by slightly different mechanisms. In cells transfected with the ion translocation dead mutant, there was a disruption in the cell's ability to disassemble FAs and stress fibers resulting in slowed migration [120]. In cells transfected with the ERM binding-deficient mutant, however, migration was disrupted as a result of the cells being unable to properly polarize and form a primary leading edge lamellipodia, instead forming several membrane protrusions around the cell [120, 121]. In analogous studies on transformed Madine-Darby Canine Kidney (MDCK-F) cells [157], and in metastatic breast cancer cells [158, 159], NHE1 ion translocation and actin cytoskeletal anchoring functions were required for the proper formation of invasive pseudopodia, an essential requirement for tumor cell invasion and metastasis (also see [160] for a review).

The role that NHE1 plays in directing cell migration is likely two-fold. First, as discussed in section 2.2.2.1, NHE1 serves as an anchor for the actin cytoskeleton, and this association is thought to spatially restrict both NHE1 and actin to the leading edge lamellipodia in migrating cells [110, 119, 125, 130]. In addition, ion translocation via NHE1 creates $[ion]_i$ microdomains within the spatially restricted region of the primary lamellipodia, thus creating an optimal environment for the activities of actin regulatory proteins, such as ADF/cofilin which have been shown to exhibit pH sensitivity in non-neuronal cells (see [161]), to modulate actin

cytoskeleton dynamics necessary for cell migration [110, 119, 125, 130]. Additionally, ion translocation may function with other ion transporters (such as the $\text{Cl}^-/\text{HCO}_3^-$ exchanger) at the leading edge to mediate salt and concomitant osmotic water-uptake via aquaporins, leading to swelling of the membrane and subsequent protrusion of the leading edge (Fig. 4; see [162, 163] for reviews). While the exact mechanism by which NHE1 modulates directed cell migration is not completely understood, it is likely a combination of these mechanisms which allow NHE1 to modulate cell motility.

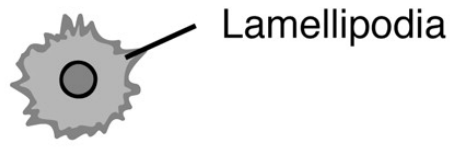
1.3 Summary and objectives

Although the mechanisms involved in growth cone motility during neurite outgrowth are not well understood, there are similarities between growth cone motility and directed cell migration in non-neuronal cells. Actin cytoskeletal dynamics at the leading edge of migrating fibroblasts have been shown to be regulated, at least in part, by NHE1 ion translocation activity as well as the structural functions of NHE1. The goal of this thesis is to investigate if NHE1 is playing a similar role in modulating neurite outgrowth.

Figure 1. Schematic representation of the stages in neurite outgrowth

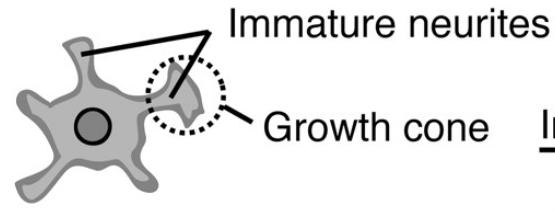
During stage 1 membrane protrusions, resembling lamellipodia, extend from the cell body. In stage 2 these protrusions form into discrete neurites with a mature growth cone at the tip. Polarization occurs at stage 3 and is characterized by the accelerated extension of the axon from the cell body. Adapted from Yoshimura *et al.* [14].

Stage 1



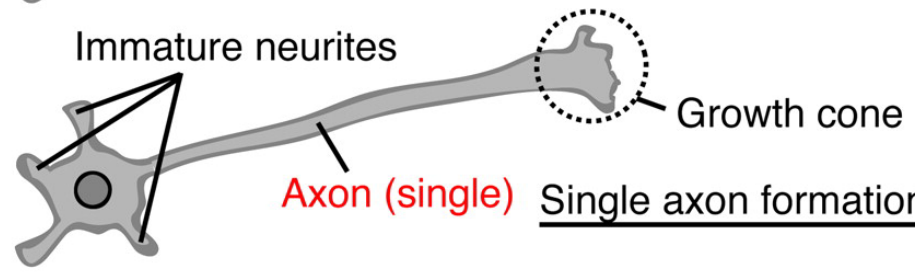
Lamellipodia formation

Stage 2



Immature neurites formation

Stage 3



Single axon formation

Figure 2. Cytoskeletal organization of a growth cone

Lamellipodia and filopodia are found at the extending tips of developing neurites (growth cones); filopodia also develop on dendritic shafts in younger neurons, where they may be precursors of dendritic spines. In lamellipodia and filopodia, light grey represents F-actin, which is also represented by <<<< in the *insets* representing the polarity of F-actin (– end <<< + end). In the *insets*, white arrows represent actin polymerization at the leading edges and open arrows represent retrograde F-actin flow. Taken from Luo [2].

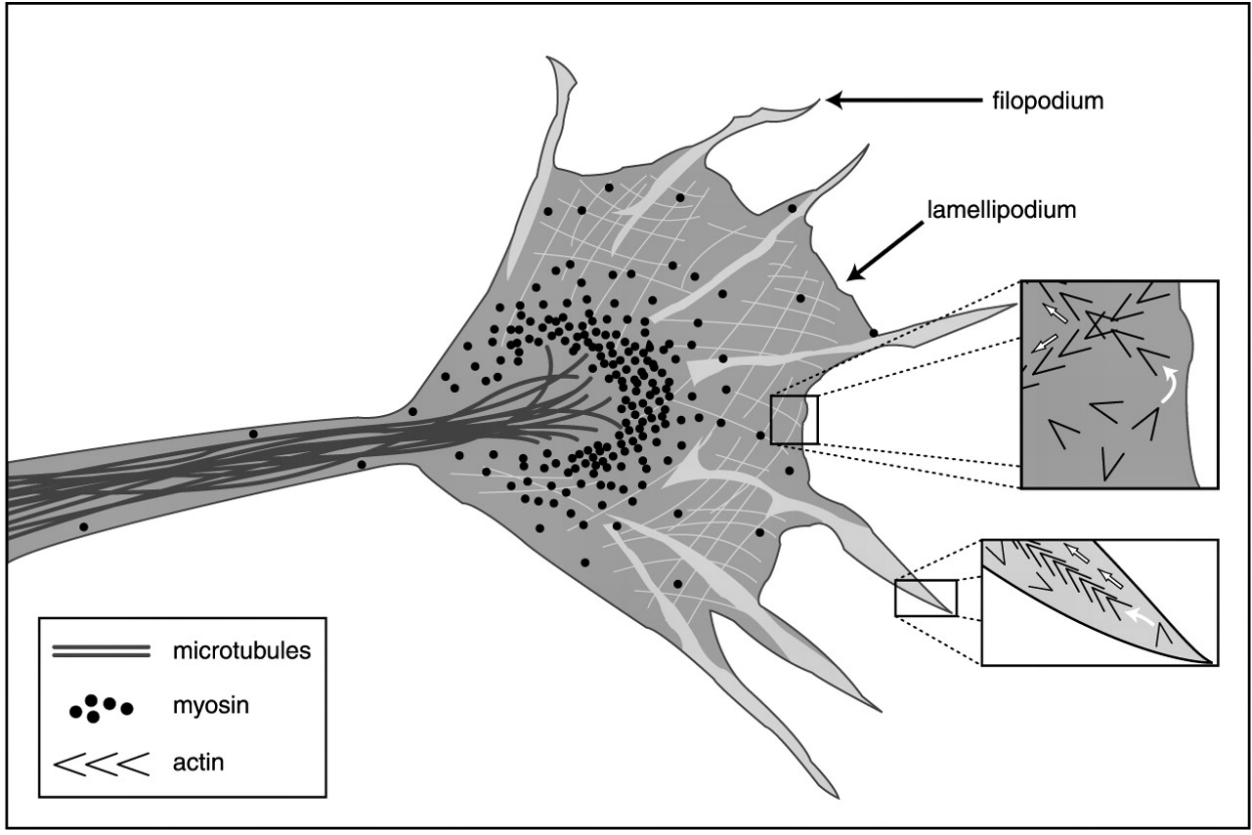


Figure 3. Transmembrane organization and regulation of the mammalian Na^+/H^+ exchangers NHE1 and NHE3

The topologies of NHE1 and NHE3 showing the relatively highly conserved transmembrane *N*-terminal domain and the more variable *C*-terminal cytosolic regulatory domain. The topologies of NHE2 and NHE4 are thought to resemble NHE1 while the topology of NHE5 is believed to be similar to that of NHE3. *R-loop* re-entrant loop; *PIP₂* phosphatidylinositol 4,5-bisphosphate; *CHP* calcineurin B homolog protein; *CaM* Ca^{2+} -calmodulin; *NIK* Nck-interacting kinase; *CAII* carbonic anhydrase II; *PTH* parathyroid hormone; *DPPIV* dipeptidyl peptidase IV; *ROK* rho-associated kinase; *NHERF* NHE regulatory factor; *AC* adenylate cyclase. Taken from Orłowski and Grinstein [123].

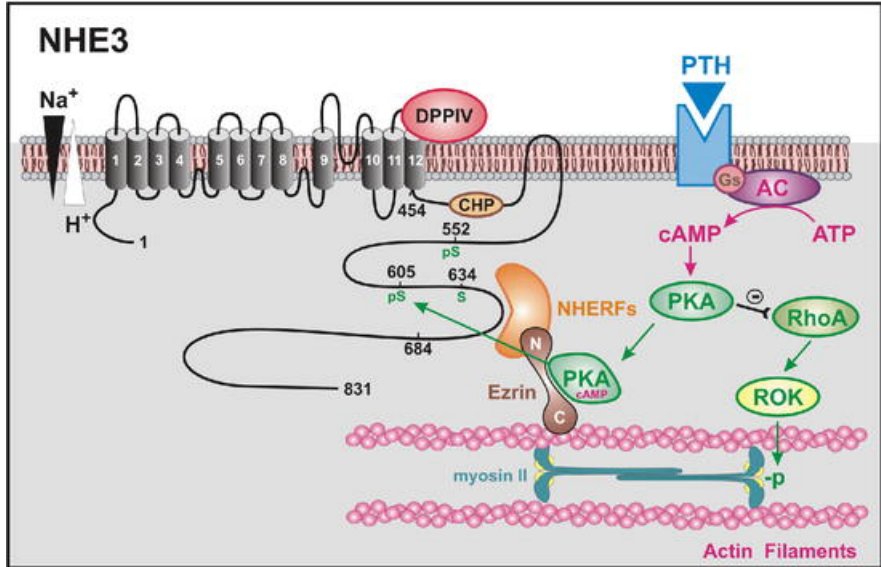
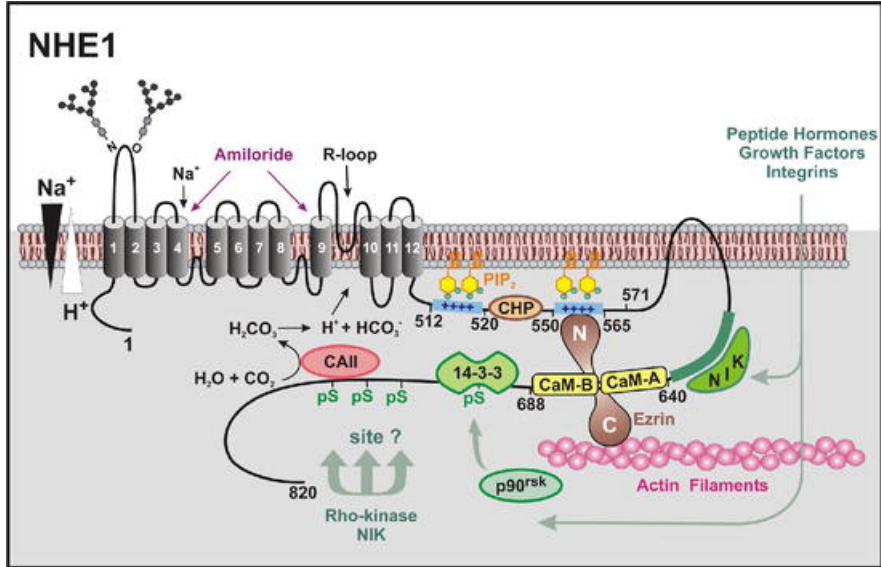
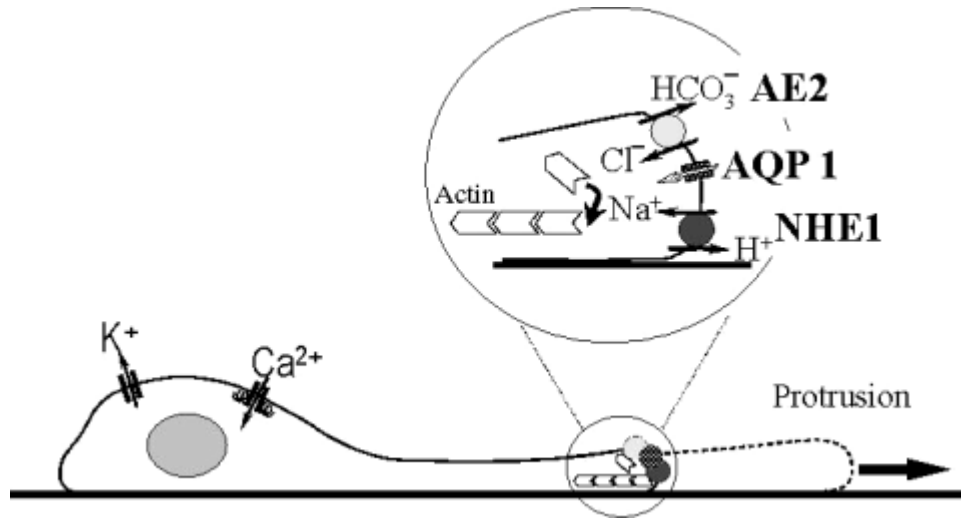


Figure 4. Ion transporters at the leading edge of migrating cells

Salt uptake mediated by the cooperative action of Na^+/H^+ (NHE1) and $\text{Cl}^-/\text{HCO}_3^-$ (AE2) exchangers at the leading edge of migrating fibroblasts is thought to lead to osmotic water entry facilitated by the aquaporin AQP1 resulting in localized membrane swelling and contributing to the extension of the lamellipodium. Taken from Stock and Schwab [163]



2.0 Materials and methods

2.1 Cell culture

2.1.1 PS120 cells

Pouyssegur *et al.* [164] previously described a cell-line which does not possess any Na^+/H^+ exchange activity. The cell-line was derived from a Chinese hamster lung fibroblast (CCL39) cell line subjected to multiple rounds of treatments which result in cytoplasmic acidification [164]. A line of clones, termed PS120, was found to be resistant to these H^+ -suicide treatments and was found to not possess functional Na^+/H^+ exchange activity, as determined by $^{22}\text{Na}^+$ uptake assays [164]. These cells are often used as a control for assays to determine the role of Na^+/H^+ activity in cell migration and also as a Na^+/H^+ deficient cell in which to test the function of Na^+/H^+ exchange mutants [110, 120, 143, 165-167].

PS120 cells were maintained in high-glucose Dulbecco's Modified Eagle Medium with GlutaMAX (DMEM; Invitrogen Canada Inc., Burlington, ON) supplemented with 10% fetal bovine serum (FBS; Invitrogen Canada Inc.) at 37°C in a 5% CO_2 atmosphere. When cells reached >90% confluency they were passaged to new culture dishes by first washing with phosphate buffered saline (PBS) to remove the serum followed by the addition of 0.25% Trypsin (Invitrogen Canada Inc.) for 2 min at 37°C . Following the incubation, the trypsin was inactivated by the addition of full-growth medium at a ratio of 3 parts media:1 part trypsin solution. Cells were subsequently plated in new culture plates at a cell suspension to media ratio of 3:1 and maintained in the incubator. For experiments utilizing PS120 cells, the cells were lifted off the culture plate using the trypsin protocol noted above and the cells were plated on glass coverslips at a density of 2×10^5 cells mL^{-1} and maintained in the high-glucose DMEM with GlutaMAX supplemented with 10% FBS for 48 h before the experiments

2.1.2 PC12 cells

PC12 cells are an established cell line commonly used as a model *in vitro* system to study neuronal growth and differentiation (e.g. see [168-173]). PC12 cells were derived from a pheochromocytoma arising from the chromaffin cells of the adrenal medulla of adult rats [170]. When treated with nerve growth factor (NGF), PC12 cells exhibit sympathetic neuron-like morphological changes complete with the extension of neurites from the cell body in addition to the production of neurotransmitters of the catecholamine family [170].

PC12 cells, obtained from The American Type Culture Collection (ATCC, Manassas, VA), were maintained in 60 mm plastic tissue culture plates (Thermo Fisher Scientific, Ottawa ON) at 37°C under a 5% CO₂ atmosphere in high glucose DMEM with GlutaMAX supplemented with 10% horse serum, 5% FBS and penicillin (100 units mL⁻¹) / streptomycin (100 µg mL⁻¹) (Sigma-Aldrich Canada Ltd., Oakville, ON). Cells which reached approximately 90% confluency in the 60 mm dishes were passaged to new 60 mm dishes by first removing the old medium and replacing it with fresh DMEM. The cells were lifted off the plate and resuspended in the fresh media by the use of a 22G needle attached to an appropriately-sized syringe (BD Biosciences, Mississauga, ON). By using 22G needles, large cell clumps were broken up so that predominantly single cells were passed along to the new plates. The resuspended cells were diluted in fresh DMEM at a 1:4 cells to media ratio and plated in new 60 mm dishes and returned to the incubator.

For differentiation, PC12 cells were again resuspended, as described above, in high-glucose DMEM supplemented with 1% FBS and penicillin/streptomycin, and seeded at a low density of 1.3×10^5 cells mL⁻¹ on glass coverslips coated with 10 µg cm⁻² collagen (BD Biosciences). To coat the coverslips, collagen was diluted with PBS and the solution was

applied to the coverslip and let sit for at least 15 min. The coverslips were then washed with PBS before cells were plated. Cells were treated for up to 72 h with NGF (50 ng mL⁻¹, Cedarlane Laboratories, Burlington, ON) with the medium replaced every 24 h with fresh NGF-containing medium.

2.1.3 Mouse neocortical neurons

2.1.3.1 Primary culture of E16 neocortical neurons

Dissociated mouse neocortical neurons were isolated using a modified method described by Mazzoni and Kenigsberg [174]. Female C57BL/6 pregnant mice at 13-15 days gestation were obtained from Charles River Laboratories, Inc. (Wilmington, MA) and housed under conditions of controlled temperature (20⁰C-22⁰C) and lighting (lights on 0600-1900). Food (Lab Diet, PMI Feeds Inc., St. Louis, MO) and water were available *ad libitum*. All procedures conformed to guidelines established by the Canadian Council on Animal Care and were approved by the University of British Columbia Animal Care Committee.

To isolate neocortical neurons, the animals were anesthetized with 3% halothane in air, decapitated and their brains were rapidly removed and placed in ice-cold (4⁰C) Hanks Balanced Salt Solution (HBSS, Invitrogen Canada Inc.) supplemented with 10% FBS and penicillin (100 units mL⁻¹) / streptomycin (100 µg mL⁻¹). The hemispheres were separated, freed of meninges and the neocortices were isolated and placed in ice-cold HBSS supplemented with 10% FBS and penicillin/streptomycin. Isolated cortices were microdissected using number 10 scalpels and gently triturated with fire-polished Pasteur pipettes of diminishing tip diameter. The cell suspension was passed through a 70 µm cell strainer (BD Biosciences) and cells were subsequently resuspended in a 1:1 mixture of HBSS and plating medium containing Neurobasal

medium (Invitrogen Canada Inc.) and Dulbecco's Modified Eagle Medium Nutrient mix F12 (DMEM/F12; Invitrogen Canada Inc.) at a ratio of 3:2 and supplemented with 10% FBS. To minimize synaptic interactions and ensure accurate morphometric analyses, neurons were plated at low density ($\sim 1 \times 10^5$ cells cm^{-2}) on poly-D-lysine/laminin-coated 12 mm coverslips (BD Biosciences) and maintained for 72 h at 37°C under a 5% CO₂ atmosphere. The plating medium was replaced with serum-free growth medium containing Neurobasal medium and DMEM/F12 at a ratio of 3:2 containing penicillin/streptomycin and 2% B27 supplements (Invitrogen Canada Inc.) 2 hours after plating. The culture medium was subsequently half-changed every 24 h with fresh medium.

2.1.3.2 NHE1^{-/-} neurons

Mice which harbor a spontaneous mutation in the *Nhe1* allele were obtained from The Jackson Laboratory (B6.SJL, *+/*swe**; Bar Harbor, MA; see [134]) and were housed under conditions of controlled temperature (20°C-22°C) and lighting (lights on 0600-1900). Food (Lab Diet, PMI Feeds Inc., St. Louis, MO) and water were available *ad libitum*.

2.1.3.2.1 Breeding

To maintain our colony, NHE1^{+/-} male mice were mated with WT C57BL/6 female mice, thereby generating litters of WT and NHE1^{+/-} mice. The adult mice were kept in the same cage until a litter was born, at which time the male was removed to a new cage and the female was left to tend to the newborn pups. When the pups were 3-4 weeks of age, ear punches were taken to genotype (see section 1.3.2.2) and identify NHE1^{+/-} mice which could be mated to generate the NHE1^{-/-} mice for experiments.

For NHE1^{-/-} mice, a NHE1^{+/-} male and two NHE1^{+/-} females were placed in the same cage and were left to mate for 5 days before removing the females and placing them into a new cage. Cages were checked twice daily and newborn pups were removed and sacrificed immediately by decapitation. Neocortical neuron cultures (hereafter termed postnatal day 0.5 (P0.5) neurons) were isolated according to the protocol listed below (section 1.3.2.3).

2.1.3.2.2 Genotyping

To determine the genotype of the mice, either ear punches (pups for breeding) or brain tissue samples (pups for the preparation of cultured neurons) were placed in proteinase K buffer (see [175], Table 1) and digested with Proteinase K (Invitrogen Canada Inc.) at 58⁰C for 16 h. Following the digestion the samples were heated to 100⁰C for 15 min to neutralize the enzyme and diluted with 250 μ L (ear punches) or 630 μ L (brain samples) dH₂O and stored at -20⁰C until genotyping. For genotyping, the samples were amplified by polymerase chain reaction (PCR) as described [176] using the following primers: sense, 5'-CACTCTCTGCATCCCTCCTC-3' and antisense, 5'-AAGTCATGCGGCAAGCTAGT-3', corresponding to base pairs 47312-47331 and 47956-47977 of the intronic region of mouse NHE1 cDNA sequence (accession number: BC052708). The PCR reaction mixture contained 28 μ L PCR master mix (Table 2) to which 2 μ L of sample was added and the reaction was carried out using an Eppendorf Mastercycler ep (Eppendorf Canada, Mississauga, ON) with the following program: 10 min at 95⁰C followed by 30 cycles of 1.5 min at 94⁰C, 1 min at 62⁰C and finally 1.5 min at 72⁰C. This was followed by an additional 10 min at 72⁰C and then held at 4⁰C until removal from the machine.

Following amplification using PCR, samples were subjected to restriction enzyme digestion using FastDigest SpeI (Fermentas Life Sciences, Burlington, ON). The mutation in

NHE1^{-/-} mice introduces a restriction enzyme digest site into the DNA which is recognized by the SpeI restriction enzyme (see [177]). Samples were digested by adding 0.4 mL SpeI enzyme, 4.0 mL FastDigest buffer (Fermentas Life Sciences) and 5.6 mL dH₂O to the amplified PCR products and incubated at 37⁰C for 2 h. Samples were then loaded onto a 2% Agarose (EMD Chemicals Inc., San Diego, CA) DNA gel made up in Tris-Acetate-EDTA buffer (TAE) which was made up as a 50x stock containing (in M unless otherwise noted): Tris 2, EDTA 0.1, glacial acetic acid 0.05 % (pH 8.5). To visualize the DNA, 10 μL SYBRsafe fluorescent DNA stain (Invitrogen Canada Inc.) was added to 100 mL of gel. The gel was run at a constant voltage of 100 V for 30 min and was imaged using an AlphaImager 3400 MultiImage Light Cabinet (Alpha Innotech Co., San Leandro, CA). NHE1^{+/+} mice had a single band at 666 bp, NHE1^{-/-} mice had two bands (278 bp and 388 bp) and NHE1^{+/-} mice had 3 bands (666 bp, 388 bp, 278 bp). As a control, samples already confirmed as either NHE1^{+/+} or NHE1^{-/-} were amplified and loaded onto each gel to ensure that there were no problems with the PCR and that there was complete digestion with the restriction enzyme.

2.1.3.2.3 Primary culture of P0.5 neocortical neurons

Neocortical neurons from NHE1^{-/-} mice were cultured in exactly the same way as that described above for E16 neurons (see section 1.3.1). The only exception was that tissue from individual P0.5 pups was kept separate to ensure no cross-contamination of different genotypes in the cultures.

2.2 Transient transfection

2.2.1 DNA constructs

The constructs used in these studies were based on the previously described expression vectors pCMV and pCMV-NHE1-HA ([121, 178]). NHE1 mutants that either lack ion translocation activity (E266I; [121]) or exhibit impaired ERM binding and disrupted cytoskeletal anchoring (KR/A; [121]) were generously provided by Dr. D.L. Barber (University of California, San Francisco). Samples of a second NHE1 mutant with disrupted ERM binding (NHE1- Δ 556-564) were prepared using the Quick Change Site-Directed Mutagenesis Kit (Stratagene, La Jolla, CA) using rat pCMV-NHE1-HA as the template and the following primers: sense 5'-CACTGGAAGGACAAGCTCAACTGTCTAATAGCTGGAGAGCGCTCC-3' and antisense 5'-GGAGCGCTCTCCAGCTATTAGACAGTTGAGCTTGTCCCTTCCAGTG-3'. All cDNAs were verified by DNA sequencing and the Na⁺/H⁺ exchange activity of each mutant was assessed in NHE-deficient PS120 fibroblasts ([164]) co-transfected with EGFP (see below). All of the cDNAs used in this study were tagged with hemmagglutinin (HA).

2.2.2 Transfection protocols

2.2.2.1 PS120 cells

PS120 cells were transfected with full-length NHE1, NHE1-E266I, NHE1-KR/A or NHE1- Δ 556-564 cDNA in conjunction with EGFP cDNA to identify the cells that had been transfected. In addition, a cDNA encoding a puromycin resistance (puro^R) gene was transfected into the cells in order to generate stably transfected cells for the functional characterization experiments outlined below. PS120 cells were plated in 60 mm culture dishes as outlined above (section 1.1) in high-glucose DMEM with GlutaMAX. Cells were allowed to seed to the plates for 6 h before

being transfected with Lipofectamine 2000 (Invitrogen Canada Inc.) according to the manufacturers instructions. Ten μL Lipofectamine was initially diluted in 250 μL serum-free OptiMEM (Invitrogen Canada Inc.) medium and let sit at room temperature for 5 min. cDNA was added to the Lipofectamine/OptiMEM solution to a final Lipofectamine:cDNA ratio of 5 μL :2 μg . Cotransfection of NHE1 constructs and EGFP was empirically determined to be optimal when transfected at a 1:1 ratio and therefore 1 μg NHE1 construct and 1 μg EGFP were added to the Lipofectamine mixture in addition to 0.4 μg puro^R cDNA to achieve puromycin resistance in the transfected cells. The transfection mixtures were incubated at room temperature for 15 min. The entire mixture was then added to a 60 mm plate and the cells were left in the incubator for 48 h before selection.

To select cells which had been transfected, the culture medium was changed to a selection medium consisting of high-glucose DMEM with GlutaMAX supplemented with 10% FBS and containing 4 $\mu\text{g mL}^{-1}$ puromycin. Cells were subsequently grown in the selection medium until the cells were plated on glass coverslips for experiments, at which point they were plated in puromycin-free medium for up to 48 h preceding the experiment. Analysis of the selected cells showed that >80% of the cells selected in this manner were indeed co-transfected with EGFP and an NHE1 construct (data not shown). In addition, cells which were highly expressing EGFP were consistently found to also have high levels of expression for the NHE1-construct, as assessed by staining for the HA tag on the construct (data not shown).

2.2.2.2 PC12 cells

PC12 cells were plated on collagen-coated glass coverslips as described above (section 1.2) and allowed to grow for 24 h, in the absence of NGF, before transfection. Cells were transfected

with plasmid cDNA encoding either full-length NHE1 or one of the mutant NHE1 constructs using the Fugene 6 transfection reagent (Roche Diagnostics, Laval, QC). According to the manufacturer's instructions, the ratio between Fugene 6 and cDNA was arrived at empirically to achieve the best transfection efficiency. For the NHE1, NHE1-KR/A and NHE1- Δ 556-564 constructs a Fugene 6:cDNA ratio of 6 μ L:1 μ g was used; for NHE1-E266I the ratio was 3 μ L:1 μ g. According to the required ratio, Fugene 6 was added to serum-free high-glucose DMEM with GlutaMAX to a final volume of 100 μ L for each coverslip (e.g. 6 μ L Fugene 6, 94 μ L DMEM with GlutaMAX) used and let sit for 5 min at room temperature. The required amount of cDNA was then added to the mixture and left to incubate for an additional 15 min at room temperature. During this time, the culture medium for the PC12 cells was changed to the NGF-containing medium described above (see section 1.2) followed by the addition of 100 μ L of the transfection mixture to each coverslip/well. The cells were then allowed to grow for an additional 72 h in the continued presence of NGF and either DMSO or 1 μ M cariporide with the culture medium changed every 24 h with fresh culture medium.

2.2.2.3 Primary neurons

Primary neurons were plated at 5×10^5 cells mL^{-1} and allowed to seed to the coverslips for 6 h before transfecting the cells with the construct of interest. Transfection of the cells was done using the same protocol as that outlined above for PC12 cells with the exception that the medium in which the Fugene 6 was initially diluted was serum-free Neurobasal medium rather than high-glucose DMEM with GlutaMAX.

2.3 Immunocytochemistry and morphometric analysis

2.3.1 Fixing

Cells were fixed with a 4% paraformaldehyde (PFA) solution made up in PBS. The cells were not washed with PBS before fixation as it was found that this occasionally resulted in the loss of typical growth cone morphology. The PFA-containing solution was left on the cells for 20 min at room temperature and the cells were subsequently washed with 2 volumes of PBS. Cells were either probed immediately or stored at 4⁰C for up to a week before use. There was no loss in signal intensity seen with an extended storage at 4⁰C when compared to cells which were probed immediately.

2.3.2 Staining

Depending on the experiment, cells were probed with a variety of antibodies and/or phalloidin to visualize protein expression and/or the actin cytoskeleton, respectively. The antibodies and their corresponding concentrations used in this study are listed in Table 3. Primary antibodies were diluted in 1% bovine serum albumin (BSA; Sigma-Aldrich Canada Ltd.) made up in PBS. In order to stain intracellular proteins, cells were first permeabilized with a 0.2% Triton X (Thermo Fisher Scientific) solution made up in PBS and applied directly onto the cells for 2 min. Triton-X was subsequently removed and the cells were washed with 1 volume of PBS.

To prevent nonspecific antibody interactions the cells were blocked with 2% BSA made up in PBS. The BSA solution was applied for 20 min before being washed-off with at least 2 volumes of PBS. Fifty µL of the primary antibody solution was then added to the surface of each 12 mm coverslip and left overnight at 4⁰C. Following the overnight incubation, the cells were washed with 3 volumes of PBS for 5 min each to ensure removal of the primary antibody.

Secondary antibody, which was also diluted in 1% BSA, was then added to the cells which were then incubated for 1 h at room temperature before being washed with 3 volumes of PBS for 10 min each. Coverslips were then mounted on glass microscope slides (Thermo Fisher Scientific) using Prolong Gold Antifade reagent with DAPI (Invitrogen Canada Inc.) and let sit at room temperature for 30 min before being stored at -20°C .

For cells that were stained with phalloidin in conjunction with another antibody, phalloidin was applied to the cells following removal of the secondary antibody, and when added independent of other antibodies it was applied to the cells immediately following permeabilization with no prior blocking. Phalloidin, diluted in PBS, was applied for 25 min at room temperature before being washed-off with 3 volumes of PBS for 10 min each prior to mounting.

2.3.3 Morphometric analyses

2.3.3.1 Wide field microscopy

2.3.3.1.1 Equipment and image acquisition

Images of individual cells were captured using a Zeiss Axioplan 2 Imaging Microscope (Carl Zeiss Canada Ltd., Don Mills ON) with a Zeiss 40x EC-Plan Neo-Fluor objective (N.A. 1.3 oil) for neurite outgrowth assays or a Zeiss 100x Plan-Apochromat objective (N.A. 1.4 oil) for growth cone analyses and protein expression determinations. Images were obtained blinded to treatment group and subsequently analyzed using Zeiss AxioVision software (version 4.5) to trace the individual neurites.

2.3.3.1.2 Criteria for inclusion

PC12 cells were included for analysis if they possessed at least one primary neurite (i.e. a neurite that extended directly from the cell body) $\geq 10 \mu\text{m}$ in length, which was determined to be the average cell body diameter of PC12 cells differentiated with NGF for 72 h (data not shown). Branched neurites were neurites which extended off either a primary neurite or another branch and had to be $\geq 8 \mu\text{m}$ in length to be included in the analyses. Measurements were performed on at least 3 separate batches of PC12 cells under each experimental condition, n values indicating the number of cells analyzed for each treatment group (or the number of growth cones analyzed in the case of the filopodia assay).

For mouse neocortical neurons, analysis was restricted to neurons at the stage 2/3 transition (i.e. prior to polarization and the formation of a distinct axon). Neurons were included for analysis if they possessed at least one primary neurite $\geq 10 \mu\text{m}$ in length. For neurons, branches $\geq 3 \mu\text{m}$ in length were included for analysis, reflecting the large number of shorter neurites observed in neurons compared to PC12 cells. Again, measurements were performed on a minimum of 3 separate neuronal cultures under each experimental condition and the n values reflect the number of individual neurons analyzed under each experimental condition.

The parameters measured were the number and lengths of primary neurites per cell and the number and lengths of the branched neurites per cell. In addition the total number and lengths of the neurites (primary and branched) per cell were calculated to give an overall comparison between the various treatment groups. Data are presented as the mean \pm s.e.m for each treatment group. The significance ($P < 0.05$) of mean differences between treatment groups was assessed using SigmaStat software (v. 2.03; Systat Software Inc., Chicago, IL) running

either one-way analysis of variance (ANOVA) followed by either the Student-Newman-Keuls or Dunn's post-hoc analysis, or by Student's two-tailed t -test.

2.4 Live cell imaging

2.4.1 Microspectrofluorimetry

To determine pH_i , the dual-excitation ratiometric technique was employed using the fluorescent hydrogen ion indicator 2',7'-bis-(2-carboxyethyl)-5(6)-carboxyfluorescein (BCECF; Molecular Probes Inc., Eugene, OR; [179, 180]). The acetoxymethyl ester of BCECF (BCECF-AM) is hydrophobic and uncharged which allows it to permeate through the plasma membrane; however, upon entry into the cell, BCECF-AM is hydrolyzed by intracellular esterases to produce hydrophilic, polyanionic BCECF free acid which becomes trapped within the cell.

The dual-excitation ratio method for estimating pH_i with BCECF is based upon the relationship between pH and the ratio of emitted fluorescence intensities at alternating wavelengths of excitation at 495 nm and 440 nm (*i.e.* I_{495}/I_{440}) for the PC12 cell experiments and 488 nm and 452 nm (I_{488}/I_{452}) for the PS120 cell experiments. The intensity of the fluorescence emission during excitation at 495 nm (or 488 nm) is pH-sensitive whereas emission during excitation at 440 nm (or 452 nm) is relatively pH-insensitive. Since the intensities of fluorescence emissions at both excitation wavelengths are from the same cell volume, the ratio of the intensity of light emitted at the two different excitation wavelengths is, in principle, not susceptible to artifacts caused by variations in optical path length, local probe concentrations, illumination intensity or photobleaching [181-183]. Based on a study by Bevensee *et al* (1995, [184]), which monitored the rates of BCECF loss in relation to morphological deterioration of

the cell membrane, cells with a rate of change of I_{452} (or I_{440}) greater than $5\% \text{ min}^{-1}$ were excluded from analysis.

2.4.1.1 Experimental solutions

The live-cell imaging experiments in PC12 cells utilized a $\text{HCO}_3^-/\text{CO}_2$ buffered medium (Table 4) that was maintained at a constant temperature (32°C) and pH (7.35 following equilibration with 5% CO_2) (see [185]). For experiments in which cariporide was applied to the cells, the $\text{HCO}_3^-/\text{CO}_2$ -buffered solution was supplemented with $5 \mu\text{M}$ cariporide (unless otherwise noted).

The experiments to measure NHE1 activity following an imposed internal acid load in PS120 cells utilized a standard HEPES-buffered medium (Table 4) at a constant pH of 7.35 and temperature of 37°C (see [186]). Internal acid loads were imposed by the NH_4^+ prepulse technique. Cells were exposed to a solution containing 20 mM NH_4Cl (Table 4) which causes an increase in pH_i and, upon return to NH_4Cl -free media, pH_i rapidly decreases to a value below the initial steady-state pH_i . From this acidified pH_i cells utilize acid-extrusion mechanisms to recover the pH_i to the normal resting level ([187, 188]). The use of nominally HCO_3^- free solutions results in inactivation of HCO_3^- -dependent pH_i regulatory mechanisms and therefore the measured rate of recovery of pH_i following the intracellular acid-load is dependent on Na^+/H^+ exchange activity.

For all experiments, media were continuously superfused onto the cells at a rate of 1 mL min^{-1} and were maintained at 32°C (37°C for PS120 cells) by passing the solution through an in-line heater immediately prior to entering the chamber. In experiments utilizing PC12 cells 5% CO_2 was applied to the chamber, to ensure a constant pH, by fitting a silicone gasket around the objective which covered the recording chamber during data acquisition.

2.4.1.2 Imaging equipment

The live-cell imaging equipment used for the PC12 experiments consisted of a Zeiss Axioskop 2 FS Plus microscope (Carl Zeiss Canada Ltd.) in conjunction with an Intelligent Imaging Innovations (Denver, CO) digital imaging workstation running Slidebook software (v. 4.2.10). Excitation light was generated using a 175 W xenon short arc bulb (Lambda DG-5 Fast Wavelength Filter Changer; Sutter Instrument Company, Novato, CA), passed through an interference filter centered at either 495 nm or 440 nm, and was subsequently reflected by a dichroic mirror into the water-dipping objective (Zeiss Achroplan, 100x, N.A. 1.0 W Ph3) before exciting the BCECF loaded in the PC12 cells. Fluorescence emitted from the cells was collected at 520 nm and measured by a cooled charge-coupled device (CCD) camera (QImaging Retiga EXi, Surrey, BC). To generate DIC images, light was generated by a 100 W halogen bulb and subsequently passed through a computer-controlled high speed brightfield shutter (Uniblitz Electronics, Rochester, NY) which permitted light to pass through the cells only when DIC images were being acquired.

For experiments utilizing PS120 cells, the imaging equipment consisted of a Zeiss Axiovert 10 inverted microscope (Carl Zeiss Canada Ltd.) in conjunction with an Attofluor Digital Fluorescence Ratio Imaging System (Atto Instruments Inc., Rockville, MD). Excitation light was emitted by a 100 W mercury short arc lamp, alternately passed through one of two interference filters (the first centered at 488 nm and the second centered at 452 nm), and subsequently reflected by a dichroic mirror into the objective (Zeiss LD Achroplan, N.A. 0.60, 40x) to excite the cells loaded with BCECF. Emitted light was again collected at 520 nm and measured by an intensified CCD camera.

For all experiments, camera gains at each excitation wavelength were set to maximize image intensity while at the same time reducing the possibility of camera saturation and were held constant throughout an experiment. Additionally, for the PC12 cells, a bin factor of 4x4 was set to digitally increase the image intensity, with minimal losses to image resolution. In order to reduce photobleaching and UV light-induced toxicity, neutral density filters were placed in the light path and a computer actuated high-speed shutter restricted the exposure of the cells to the UV light to periods when emitted fluorescence intensities were being measured. Typically, ratio pairs were collected once every 1 to 30 seconds throughout the course of an experiment. DIC images were obtained during experiments utilizing PC12 cells following the acquisition of 5 ratio pairs.

2.4.1.3 Dye loading conditions

PC12 cells were loaded with BCECF in the same high-glucose DMEM supplemented with 1% FBS that the cells were differentiated in. The cells were placed in a loading medium containing 0.3 μ M BCECF for 30 min at room temperature. To maintain the pH of the DMEM during the loading procedure, the medium was saturated with 10% CO₂ which kept the pH at 7.30. To ensure complete de-esterification of the acetoxymethylester of BCECF, after loading the cells were washed in DMEM which was free of BCECF for 15 min at room temperature. Coverslips with attached cells were then placed into a temperature-controlled recording chamber (RC27; Warner Instruments, Hamden, CT).

For the PS120 cell experiments, cells were transfected with the NHE1 construct being evaluated as well as with EGFP in order to identify transfected cells. Since EGFP emits fluorescence during excitation at the same wavelengths as BCECF, coverslips with cells attached

were initially superfused with HEPES-buffered medium and those cells expressing EGFP were identified as regions of interest (ROIs). Superfusion was then interrupted and BCECF-AM (2.5 μ M) was added directly to the recording chamber for 10 min, followed by a 15 min wash with BCECF-AM-free medium. Under the conditions employed, BCECF-derived fluorescence emissions at each excitation wavelength (488 and 452 nm) were >20 times greater than the respective signals derived from EGFP and no changes in I_{488}/I_{452} ratio values were observed in response to internal acid loads imposed on cells transfected with EGFP but not loaded with BCECF.

2.4.1.4 Image analysis

PC12 cells were first analyzed to determine if the growth cones were actively extending during the course of the experiment. The DIC images were isolated and a time-lapse movie was generated to evaluate the growth of the neurites. The intensities of fluorescence emissions at both of the excitation wavelengths were measured and the ratio I_{495}/I_{440} was determined. In addition, background readings of autofluorescence at each excitation wavelength were measured by placing a ROI in a region devoid of cellular material. Respective background intensities were subtracted from the raw emission intensities at each excitation wavelength from each ROI throughout the experiment to yield background-corrected ratios of emission intensities (BI_{495}/BI_{440}).

2.4.1.5 Calibration and calculation of pH_i

For *in situ* calibration experiments (Fig. 5), PC12 cells were loaded with BCECF-AM as described above and placed in the recording chamber at room temperature. Cells were

superfused with a series of high- K^+ HEPES-buffered solutions titrated to pH values ranging from pH 5.5 – 8.5 in 0.5 pH increments using 10 M KOH or 1 M HCl. Each of the solutions contained 10 μ M nigericin, a K^+/H^+ ionophore, a charged electron carrier that balances cytoplasmic and extracellular $[K^+]$ and, in so doing, equilibrates pH_o to pH_i ([189, 190]). The average background-subtracted ratios (BI_{495}/BI_{440}) at the growth cone as well as at the cell body were separately normalized to the average background-subtracted ratios at pH 7.00 and a pH titration curve was produced (Fig. 5B). From the curve the maximum ($R_{n(max)}$) and the minimum ($R_{n(min)}$) obtainable normalized ratios as well as the pK_a of BCECF were determined. By normalizing the ratios to pH 7.00 it allowed for a one-point calibration to pH 7.00 for each set of experiments conducted. The calibration parameters were not dependent on temperature of the perfusate or the age of the cells and were re-assessed whenever the xenon arc bulb was changed or there was any change in the optical setup of the microscope.

At the end of each day of experiments a one-point calibration was performed by superfusing the cells with a high- K^+ HEPES-buffered medium containing 10 μ M nigericin and titrated to pH 7.00. To measure the pH_i of the growth cone and the cell body, the experimentally-derived background-corrected ratios (BI_{495}/BI_{440}) were divided by the ratio corresponding to pH 7.00. Normalized ratios were converted to pH_i using equation 1, which is based on the Henderson-Hasselbalch equation for the dissociation of a weak acid:

$$pH_i = \log[(R_n - R_{n(min)}) / (R_{n(max)} - R_n)] + pK_a \quad (\text{Equation 1})$$

where R_n denotes the background-corrected ratio normalized to pH 7.00, $R_{n(max)}$ and $R_{n(min)}$ represent the maximum and minimum obtainable normalized ratios (respectively) and pK_a is the $-\log$ of the dissociation constant of BCECF (for the derivation, see [185]). For all of the

experiments here the $R_{n(\max)}$, $R_{n(\min)}$ and pK_a values obtained at the cell body were 1.84 ± 0.07 , 0.32 ± 0.04 and 7.02 ± 0.01 respectively and at the growth cone the $R_{n(\max)}$, $R_{n(\min)}$ and pK_a values were 1.90 ± 0.06 , 0.31 ± 0.03 and 7.12 ± 0.01 respectively.

2.4.2 Time-lapse DIC microscopy

To generate time-lapse movies of neurite outgrowth independent of pH_i measurements, DIC images were acquired every 30 sec to assess the growth of neurites in response to application of cariporide. The cells were placed in the recording chamber directly from the incubator and were superfused with the HCO_3^-/CO_2 -buffered solution at $32^{\circ}C$ and pH 7.35 for the duration of the experiment. Cariporide was applied to the cells by switching the perfusate to HCO_3^-/CO_2 buffered media supplemented with 5 μM cariporide and increasing the flow rate to 10 mL min^{-1} for 30 sec. The cariporide was left on the cells for the indicated period of time followed by the return to the cariporide-free medium. After the experiment, images were assessed frame by frame to determine the effect on the rate of growth of the neurite and to investigate if there were any morphological changes.

2.5 Protein extraction and Western blot analysis

2.5.1 Protein isolation

To test for the presence of NHE1 protein in PC12 cells in addition to tissue from wild-type and NHE1^{-/-} mice, protein was isolated for Western Blot analysis. To assess the protein expression in the PC12 cells, protein was isolated from cultured cells before and after a 72 h treatment with 50 ng mL^{-1} NGF. Protein expression in the tissue from mice was assessed using protein isolated from brain samples obtained during the culturing of the neurons.

2.5.1.1 Whole brain lysate

Brain samples were isolated during the culturing process and stored at -80°C until proteins were isolated. To isolate the proteins, the brain tissue was first solubilized in 500 μL of a modified ice-cold extraction buffer (0.1% SDS, 1% IGEPAL, 0.5% Sarkosyl, 150 mM NaCl, 50 mM Tris-HCl; pH 8.0; all constituents obtained from Sigma-Aldrich Canada Ltd.) supplemented with CompleteMINI protease inhibitor (made up as a 7x stock; Roche Diagnostics) and phosphatase inhibitors (Sigma-Aldrich Canada Ltd.) at a concentration of 1 mL/100 mL of the buffer. Samples were let sit on ice for 10 min to complete the digestion followed by passing the suspension through a 21 G needle ten times to shear the DNA. The suspension was centrifuged at 10,000 g for 15 min at 4°C and the supernatant was decanted to a fresh tube. Protein concentration was determined using the Pierce BCA protein assay kit (Pierce Biotechnology, Inc., Rockford, IL) as per the manufacturer's instructions. If necessary samples were diluted in ice-cold extraction buffer (final concentration of 1 μg protein/5 μL of buffer) before the addition of 5x sample loading buffer (Table 5) and were stored at -20°C until performing the Western Blot analysis.

2.5.1.2 PC12 cells

NHE1 expression was evaluated in both undifferentiated as well as NGF-differentiated PC12 cells. To differentiate the PC12 cells, 60 mm culture dishes were coated with 10 $\mu\text{g cm}^{-2}$ collagen diluted in PBS in the same fashion as described above for the coverslips. Cells were obtained from a separate dish which had reached confluency and the cells were removed from the plate and resuspended in fresh media as described above with the exception that the cells

were resuspended at a 3:1 media to cell ratio. Cells were plated on the collagen coated plates and were subsequently grown for 72 h in the continued presence of 50 ng mL⁻¹ NGF.

For both the differentiated as well as the undifferentiated cells, cells were initially washed three times with 1 mL ice-cold PBS to completely remove the growth media. An additional 500 mL ice-cold PBS was added to the cells and the cells were removed from the plates using a cell scraper (Thermo Fisher Scientific). The cell suspension was centrifuged at 10,000g for 15 min at 4^oC. The supernatant was removed and the cell pellet was stored at -80^oC. Proteins were extracted from the cell pellet as described above for the brain samples.

2.5.2 Western blot analysis

Proteins were separated using SDS-polyacrylamide gel electrophoresis (SDS-PAGE) according to a method developed by Laemmli [191] on a Bio-Rad Mini Protean apparatus (Bio-Rad Laboratories, Richmond, CA). Samples were thawed and heated to 95^oC for 2 min to denature the proteins. Samples were separated with an 8% separating gel (Table 6) run at a constant voltage of 120 mV. Protein size was estimated with the use of PrecisionPLUS protein markers (Bio-Rad Laboratories) and the gels were run until the 25 kDa marker reached the bottom of the gel at which time the gels were placed in transfer buffer (Table 6).

Proteins were transferred from the gel to Millipore immobilon-P polyvinylidene Fluoride (PVDF; Millipore Canada Ltd., Etobicoke, ON) membranes which were initially moistened with 100% methanol for 15 sec and subsequently equilibrated for a minimum of 5 min with transfer buffer. Proteins were transferred to the PVDF membrane using the Bio-Rad semi-dry transfer apparatus (Bio-Rad Laboratories) according to the manufacturer's instructions at a constant voltage of 15 mV for 35 min. After the transfer, membranes were washed with Tris buffered

saline (TBS, Table 5) supplemented with 0.1% Tween-20 (TBST) at which point the membranes could be stored at 4⁰C for up to 2 months.

The membranes were blotted by first blocking with 5% skim milk powder in TBST for 1 h at room temperature and were then washed with TBST for 5 min. Monoclonal NHE1 antibody was diluted in 1% skim milk powder in TBST to a concentration of 1:500 antibody:1% milk and the membranes were incubated with the antibody solution at 4⁰C overnight. Membranes were washed with TBST 3x10min followed by incubation with secondary horseradish peroxidase (HRP)-conjugated antibodies raised in goats against mice (1:4000 in 1% skim milk in TBST) for 1 h at room temperature. Following incubation with secondary antibody, membranes were washed 3x10min with TBST followed by a 3x5 min wash with TBS to ensure complete removal of the detergent. Membranes were incubated for 5 min in a chemiluminescent working solution from Pierce (SuperSignal West Pico; Pierce Biotechnology Inc.) as per the manufacturer's instructions and the membranes were exposed to Bioflex Econo Film (Clonex Co., Markham, ON). To ensure equal loading of proteins in all of the lanes, membranes were stripped using Restore Stripping Buffer (Pierce Biotechnology Inc.) for 2 min followed by washing in TBST. The membrane was then incubated with GAPDH antibody, which serves as a control of protein loading, as per the protocol above.

Table 1 Proteinase K digestion buffers

	Brain Samples	Ear Punches
Tris-Base	100	100
EDTA	-	5
SDS	-	0.20%
NaCl	-	200
MgCl ₂	20	-
NP-40	0.45%	-
Tween 20	0.45%	-
Gelatin	0.1 mg mL ⁻¹	-
KCl	50	-

Unless otherwise noted concentrations expressed as mM

All reagents were obtained from Sigma-Aldrich Canada Ltd.

Abbreviations used: EDTA, 2-[2-(Bis(carboxymethyl)amino)ethyl-(carboxymethyl)amino]acetic acid; SDS, sodium dodecyl sulfate; NaCl, sodium chloride; MgCl₂, magnesium chloride; NP-40, Nonidet P-40; KCl, potassium chloride.

Table 2 PCR reaction Master Mix

	PCR Master Mix
10x PCR Reagent	3
50 mM MgCl ₂	0.9
10 mM dNTP	0.6
20 mM 3' Primer	0.6
20 mM 5' Primer	0.6
Platinum Taq	0.6
dH ₂ O	21.7

Values expressed as μL used per sample

All reagents were obtained from Invitrogen Canada Inc.

Table 3 Antibodies used in the experiments

Antibody	Concentration	Conjugate	Source	Supplier
Anti-NHE1	ICC: 1:25 Western: 1:500	-	Mouse	BD Biosciences
Anti-HA	ICC: 1:1000	-	Mouse	Covance
Anti-MAP2	ICC: 1:500	-	Mouse	Sigma
Anti-NF200	ICC: 1:200	-	Rabbit	Sigma
Anti-mouse 2°	Western: 1:4000	HRP	Goat	Cedarlane
Anti-rabbit 2°	Western: 1:4000	HRP	Goat	Cedarlane
Anti-mouse 2°	ICC: 1:500	Alexa- Fluor 488 or 568	Goat	Invitrogen
Anti-rabbit 2°	ICC: 1:500	Alexa- Fluor 488 or 568	Goat	Invitrogen
Phalloidin	ICC: 1:40	Alexa- Fluor 488 or 568	N/A	Invitrogen
Anti- Vinculin	ICC: 1:50	-	Rabbit	Sigma

Abbreviations used: HRP, Horseradish peroxidase; ICC, immunocytochemistry; HA, hemmagglutinin; MAP2, microtubule associated protein 2; NF200, neurofilament 200.

Table 4 Compositions of experimental solutions for live-cell imaging

	HCO ₃ ⁻ /CO ₂ -buffered	HEPES - buffered media	NH ₄ Cl-containing	High-K ⁺
NaCl	125.0	136.5	116.5	-
NaHCO ₃	21.5	-	-	-
KCl	3.0	3.0	3.0	-
CaCl ₂	2.0	2.0	2.0	2.0
NaH ₂ PO ₄	1.5	1.5	1.5	1.5
MgSO ₄	1.5	1.5	1.5	1.5
D-Glucose	10.0	10.0	10	10.0
HEPES	-	10.0	10	10.0
NH ₄ Cl	-	-	20	-
Na Glu	-	-	-	10.0
K Glu	-	-	-	130.5
Final pH	7.35 @ 32 ⁰ C	7.35 @ 37 ⁰ C	7.35 @ 37 ⁰ C	
Titrated with	5% CO ₂	10 M NaOH	10 M NaOH	10 M KOH

All concentrations in mM

All reagents were obtained from Sigma-Aldrich Canada Ltd.

Abbreviations used: Na Glu, sodium gluconate; K Glu, potassium gluconate

Table 5 Composition of solutions used during Western Blot analysis

	Running Buffer 10x Stock	Transfer Buffer	Tris Buffered Saline (TBS) 10x Stock	Sample Loading Buffer (5x Stock)
Tris-Base (pH 6.8)	0.5	0.048	0.2	0.312
Glycine	4	0.039	-	-
NaCl	-	-	1.4	-
SDS	0.069	-	-	2.50%
Methanol	-	10%	-	-
Glycerol	-	-	-	50%
Bromophenol Blue	-	-	-	0.006%
β -Mercaptoethanol	-	-	-	50 μ L mL ⁻¹

Unless otherwise noted concentrations are in M

Tris-base, glycine, and NaCl were obtained from Sigma-Aldrich Canada Ltd.

Methanol, Glycerol, and β -mercaptoethanol were obtained from Thermo Fisher Scientific

SDS and Bromophenol Blue were obtained from Bio-Rad Laboratories

Table 6 Composition of the SDS-PAGE gels used to separate proteins

	Stacking Gel	8% Separating Gel
Glycerol	8%	8%
Acrylamide	5%	8%
Tris-Base (pH 6.8)	0.126	0.188
SDS	0.1	0.1
APS	0.1	0.1
TEMED	0.0008%	0.0004%

Unless otherwise noted concentrations in M

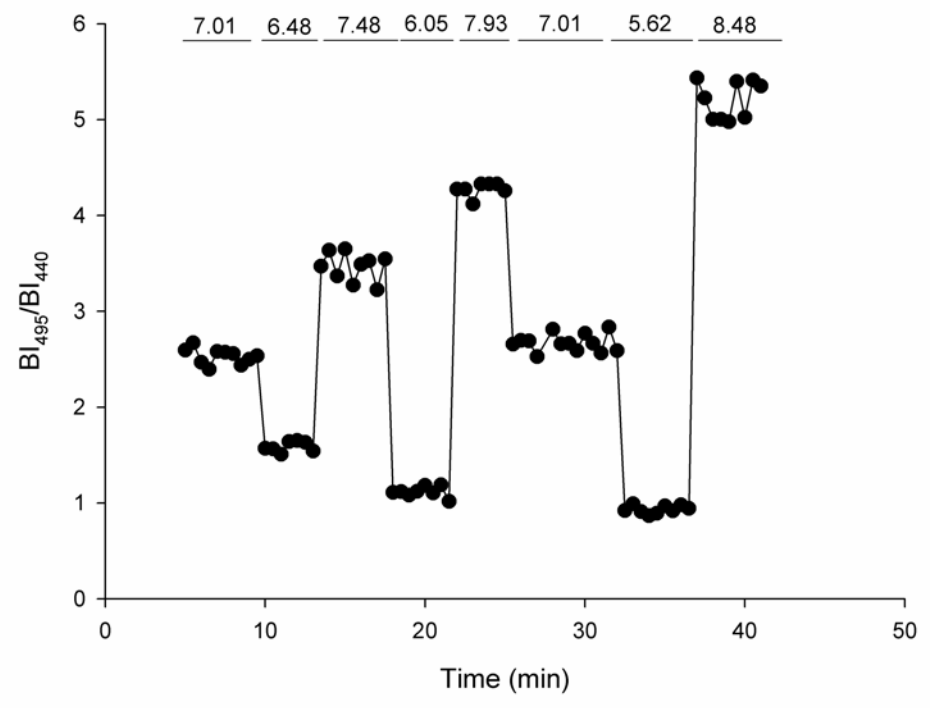
All reagents were obtained from Sigma-Aldrich Canada Ltd. with the exception of Glycerol which was obtained from Thermo Fisher Scientific

Abbreviations used: APS, Ammonium persulfate; TEMED, N,N,N',N'-tetramethylethane-1,2-diamine

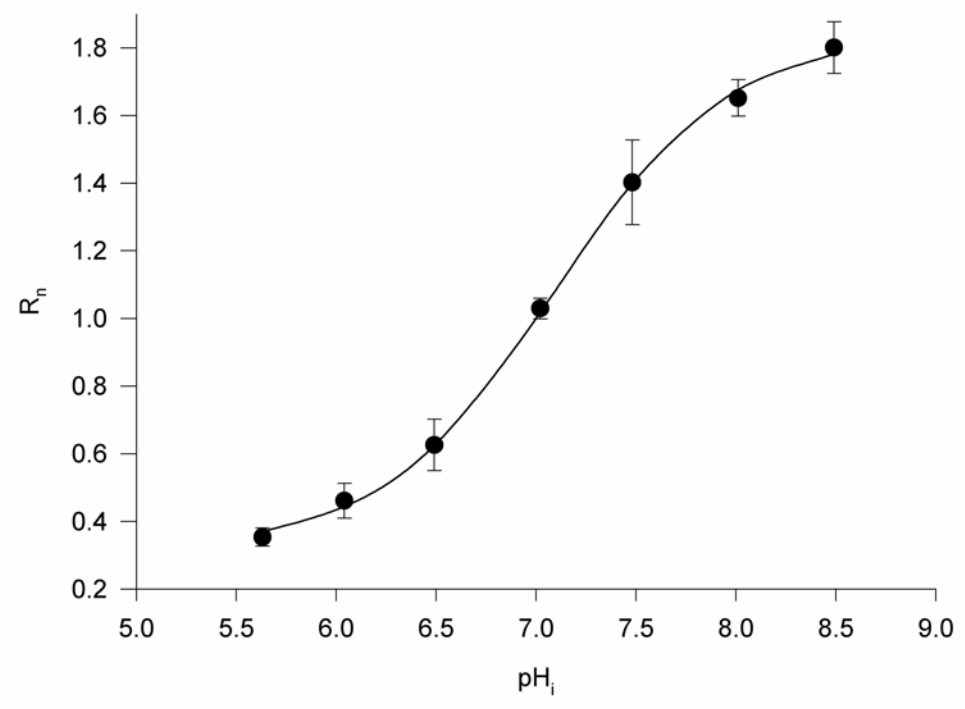
Figure 5 Sample calibration plot for BCECF

(A) Cells were exposed to $\text{HCO}_3^-/\text{CO}_2$ -free, high- K^+ HEPES-buffered solutions containing 10 μM nigericin at pH_o (and therefore pH_i) 5.62, 6.05, 6.48, 7.01, 7.48, 7.93 and 8.48. The duration of each exposure is indicated by the bars above the trace, which is the mean of data obtained from the growth cones of 3 separate PC12 cells recorded on the same coverslip. (B) Plot of pH_i against the resulting ratio normalized to pH 7.00 (R_n). Standard error bars are indicated ($n=4$ coverslips). Where absent, error bars lie within the symbol area. The curve is a result of a non-linear regression fit to equation 1. For this particular calibration, the values of $R_{n(\text{max})}$, $R_{n(\text{min})}$ and pK_a were 1.8974, 0.3126, and 7.1158 respectively.

A



B



3.0 Results

3.1 Role of NHE1 in NGF-induced neurite outgrowth in PC12 Cells.

3.1.1 Endogenous NHE1 is expressed in PC12 growth cones

PC12 cells, a well-defined model system widely employed in studies of neuritogenesis [170], were initially used to assess the involvement of NHE1 in neurite outgrowth and elaboration. In the absence of published data, endogenous NHE1 expression in undifferentiated PC12 cells and PC12 cells which had been differentiated with 50 ng mL⁻¹ NGF for 72 h was first confirmed by Western Blot analysis (Fig. 6A). When compared to undifferentiated PC12 cells, differentiated cells had similar levels of expression suggesting that NHE1 expression is not influenced by NGF differentiation of PC12 cells.

NHE1 expression in PC12 cell growth cones was assessed by differentiating PC12 cells with NGF for 72 h prior to fixing the cells and immunolabelling for NHE1 (Fig. 6B). Cells were co-stained with Alexa-Fluor 568 phalloidin to visualize the actin cytoskeleton and to identify the neurites and corresponding growth cones in individual cells. Endogenous NHE1 was observed as punctate staining at the soma (not shown), along developing neurites and also at terminal growth cones and within the filopodia seen at the growth cone (Fig. 6B). NHE1 expression in PC12 growth cones could lead to localized NHE1 activity creating a permissive environment for the cytoskeletal rearrangements which are essential for neurite outgrowth and branching (see [2, 41, 192]).

3.1.2 Application of cariporide at an NHE1-selective concentration reduces neurite outgrowth

I then examined the effects of inhibiting the activity of NHE1 on neurite outgrowth and elaboration using the Na^+/H^+ exchange inhibitor, cariporide, applied at an NHE1-selective concentration (1 μM ; [193-195]). Cariporide was co-applied with NGF for 72 h. Vehicle treated cells had an average of 4.07 ± 0.06 primary neurites which had an average length of 190.3 ± 3.4 μm and had an average of 2.34 ± 0.10 branched neurites with an average length of 36.9 ± 4.5 μm (Fig. 7). Cariporide (1 μM) reduced the average number of primary neurites to 3.11 ± 0.05 per cell and the average length of these neurites to 79.9 ± 1.9 μm ($P < 0.001$; Fig. 7) and reduced the average number of branched neurites to 0.65 ± 0.05 per cell with an average length of 6.5 ± 1.1 μm ($P < 0.001$; Fig. 7). Representative PC12 cells show that treatment with 1 μM cariporide results in visible reductions in neurite outgrowth when compared to vehicle-treated cells (Fig. 8).

3.1.2.1 Application of cariporide at a concentration to inhibit all known plasmalemmal NHE isoforms has no additional effect on neurite outgrowth

Cariporide is a potent Na^+/H^+ inhibitor that, when applied at 1 μM , is selective for NHE1 (see above). However, when applied at 100 μM , cariporide inhibits the activities of all known plasmalemmal NHE isoforms (see [195]). To investigate the possible role that other NHE isoforms may be playing in modulating neurite outgrowth, 100 μM cariporide was applied to PC12 cells in the continuous presence of 50 ng mL^{-1} NGF for 72 h. When compared to 1 μM cariporide, 100 μM failed to exert additional inhibitory effects (Figs. 7 and 8). The lack of an additional effect on neurite outgrowth in the presence of 100 μM cariporide suggests that the

effects of 1 μM cariporide to reduce neurite outgrowth and branching in PC12 cells were consequent upon the inhibition of NHE1.

3.1.2.2 Inhibition of neurite outgrowth by 100 μM cariporide is reversible

I then determined if the effect that cariporide had on neurite outgrowth was a result of a toxic effect that it may have been having on the cells. To this end the reversibility of the inhibition of neurite outgrowth as seen with 100 μM cariporide was evaluated. A timecourse of neurite outgrowth in response to NGF showed that PC12 cells fixed and stained after 24, 48 or 72 h treatment with NGF in the presence of 0.1% DMSO exhibited time-dependent increases in neurite lengths and branching (Fig. 9). The number of primary neurites per cell increased from 2.9 ± 0.1 after 24 h, to 3.5 ± 0.1 after 48 h and finally to 4.0 ± 0.3 after 72 h. Similarly the average length of the primary neurites increased from $61 \pm 4 \mu\text{m}$ after 24 h to $153 \pm 6 \mu\text{m}$ after 48 h and to a final average length of $221 \pm 9 \mu\text{m}$ after 72 h. There was also an increase in the number and lengths of the branched neurites (Fig. 9).

To test the reversibility of cariporide, additional batches of PC12 cells were treated with 100 μM cariporide for 24 h, starting 24 h after the addition of NGF. In one case, cells were fixed 24 h after the addition of cariporide whereas, in a second case, cariporide-containing medium was washed off and cells were incubated for a further 24 h in cariporide-free medium before fixation (a total of 72 h in culture). Consistent with my initial observations, a 24 h exposure to 100 μM cariporide significantly inhibited the increase in growth expected between the 24 and 48 h time-points in vehicle-treated PC12 cells (Fig. 9). Cells that had been fixed immediately after the 24 h exposure to cariporide had an average of 3.1 ± 0.1 primary neurites per cell with an average length of $78 \pm 4 \mu\text{m}$ and had an average of 0.6 ± 0.1 branched neurites per cell with an

average length of $12 \pm 1 \mu\text{m}$ (Fig. 9). However, cells that had been maintained in cariporide-free medium for a further 24 h exhibited a return to normal rates of growth with an average of 3.8 ± 0.2 primary neurites per cell (with an average length of $145 \pm 5 \mu\text{m}$) and an average of 1.7 ± 0.3 branched neurites per cell (with an average length of $21 \pm 5 \mu\text{m}$) (Fig. 9). These results suggest that the reduction of neurite outgrowth seen with the application of cariporide is a result of inhibiting NHE1 activity rather than through a toxic effect on the cells.

3.1.3 Transient transfection of either full-length NHE1 or mutant NHE1 constructs modulates neurite outgrowth

In non-neuronal cell types, NHE1 regulates growth and directional motility, effects which require both the ion translocating and actin cytoskeletal anchoring functions of the protein at the leading edge [120, 121, 157]. To assess whether these functions contribute to the modulation of neurite outgrowth and elaboration by NHE1, PC12 cells were transiently transfected with cDNAs encoding HA-tagged wild-type (WT) NHE1 or mutant NHE1s with either defective ion translocation (NHE1-E266I) or impaired ERM binding and cytoskeletal anchoring (NHE1-KR/A and NHE1- Δ 556-564) ([120, 121]).

3.1.3.1 Functional characterization of the full-length and mutant NHE1 constructs

To determine the ion translocation activity of the constructs, PS120 cells, which do not possess any functional NHE activity [164], were co-transfected with EGFP and one of the NHE1 constructs (WT NHE1, NHE1-E266I, NHE1-KR/A or NHE1- Δ 556-564). PS120 cells were loaded with the fluorescent pH indicator BCECF and the recovery of pH_i from NH_4^+ -induced internal acid loads was examined to determine NHE1 activity.

PS120 fibroblasts transfected with WT NHE1 exhibited cariporide-sensitive, pH_i -dependent recoveries of pH_i from imposed internal acid loads (Fig. 10A). PS120 cells that were transfected with either of the cytoskeletal anchoring deficient mutants (NHE1-KR/A or NHE1- Δ 556-564) exhibited reduced but still measureable cariporide-sensitive recoveries of pH_i (Fig. 10C, D). In contrast, untransfected cells as well as cells expressing NHE1-E266I were unable to recover from the imposed internal acid load suggesting that NHE1-E266I is indeed deficient in ion translocation ability (Fig. 10B; see also [121]).

3.1.3.2 Transient transfection of full-length NHE1 enhances neurite outgrowth

After functionally characterizing the NHE1 constructs, I then examined what effect they had on neurite outgrowth in NGF-differentiated PC12 cells. Compared to untransfected control cells, which had an average of 3.59 ± 0.09 primary neurites with an average length of $189 \pm 5 \mu\text{m}$ and an average of 2.4 ± 0.1 branched neurites with an average length of $39 \pm 5 \mu\text{m}$, PC12 cells which had been transiently transfected with full-length NHE1 exhibited an increase to an average of 3.8 ± 0.1 primary neurites which had an average length of $215 \pm 6 \mu\text{m}$ ($P < 0.05$ and $P < 0.001$ respectively compared to untransfected PC12 cells; Fig. 11). In contrast, compared to untransfected cells the number of branches was not significantly increased in NHE1-transfected cells which had an average of 2.6 ± 0.2 branched neurites ($P > 0.05$; Fig. 11), although the average length of the branches was significantly increased to $74 \pm 6 \mu\text{m}$ ($P < 0.001$; Fig. 11). When NHE1-overexpressing PC12 cells were treated with $1 \mu\text{M}$ cariporide, the numbers and lengths of both primary and branched neurites were reduced to levels comparable to those observed in untransfected cariporide-treated PC12 cells. Figure 12 shows representative examples of untransfected as well as NHE1-overexpressing cells, showing a visible increase in

neurite outgrowth in the transfected cells. These data suggest that an increase in NHE1 expression is able to enhance neurite outgrowth and elaboration of NGF-differentiated PC12 cells. However, these results do not shed any light on whether the ion translocating or actin cytoskeletal anchoring functions of NHE1 are necessary for this enhancement of growth.

3.1.3.3 Transient transfection of mutant NHE1 constructs reduces neurite outgrowth in NGF-differentiated PC12 cells

In order to determine which function of NHE1 was important in modulating neurite outgrowth, I transfected PC12 cells with the mutant NHE1 constructs deficient in either ion translocation activity or cytoskeletal anchoring ability mentioned above. Cells transfected with NHE1-E266I had an average of 2.55 ± 0.08 primary neurites which had an average length of $75 \pm 3 \mu\text{m}$ and an average of 0.53 ± 0.06 branched neurites with an average length of $10 \pm 3 \mu\text{m}$ ($P < 0.001$ in all cases, compared to untransfected cells; Fig. 11). These results suggest that the ion translocation activity of NHE1 is important for modulating neurite outgrowth in NGF-differentiated PC12 cells.

Compared to vehicle-treated untransfected cells, NHE1-KRA transfected vehicle-treated cells had a reduced average number and length of both primary as well as branched neurites (Fig. 11). When treated with $1 \mu\text{M}$ cariporide for 72 h the average number and lengths of primary neurites in NHE1-KR/A transfected cells were further reduced as were the average number and lengths of branches (Fig. 11). The sensitivity to cariporide of the limited neurite outgrowth observed in NHE1-KR/A over-expressing PC12 cells likely reflects the fact that these cells support cariporide-sensitive acid efflux (see Fig. 10).

Cells that were transfected with NHE1- Δ 556-564 followed by treatment with vehicle for 72 h also had reductions in both the average number and lengths of the primary neurites as well as a reduction in the average number and lengths of the branched neurites (Fig. 11). When cells transfected with NHE1- Δ 556-564 were treated with 1 μ M cariporide for 72 h, no further decreases in the number or lengths of primary neurites or the number or lengths of the branched neurites were observed (Fig. 11). Figure 12 shows representative examples of untransfected PC12 cells as well as PC12 cells transfected with full-length NHE1 and each of the NHE1-mutant constructs. Taken together, these results indicate that both ion translocation and cytoskeletal anchoring contribute to the regulation of neurite outgrowth and elaboration by NHE1.

3.1.4 pH_i measured in the growth cones of PC12 cells

The above results indicate that the ion translocation function of NHE1 is important for the NHE1-dependent modulation of NGF-induced neurite outgrowth in PC12 cells. To investigate whether pH_i in the growth cones of actively extending neurites is higher than in non-extending neurites, live-cell pH_i measurements in conjunction with concurrent DIC microscopy to monitor growth cone morphology and neurite outgrowth were conducted.

3.1.4.1 pH_i in actively extending neurites is higher than that found at the cell body

In order to determine the pH_i in the growth cones of PC12 cells, cells which had been treated with 50 ng mL⁻¹ NGF for 48 h were loaded with the fluorescent pH indicator BCECF. DIC images were captured during the course of each experiment to identify the growth cones of neurites which were actively extending. By this method I found that the pH_i in the growth cones

of actively-extending neurites (7.36 ± 0.02) was significantly ($P < 0.01$, $n = 10$) elevated compared to pH_i measured simultaneously in more proximal regions (7.23 ± 0.03 ; Fig. 13A). In contrast, pH_i in growth cones which did not extend during the 30 min time course of a given experiment (7.22 ± 0.03) was not significantly different ($P = 0.58$, $n = 10$) from that measured simultaneously at the soma and/or in proximal regions of primary neurites (7.20 ± 0.02 ; Fig. 13B). These findings provide evidence that NHE1 may be creating an elevated pH_i microenvironment in the spatially restricted growth cone which in turn could promote the actin cytoskeletal rearrangements that are necessary for neurite outgrowth and elaboration. However, since all of these experiments were conducted in the presence of HCO_3^- , the above results do not exclude the possibility that the elevated pH_i may be a result of HCO_3^- -dependent pH_i regulatory mechanisms rather than ion translocation activity mediated by NHE1 activity. To address this, the effect of cariporide on the pH_i at the growth cone of actively extending neurites was evaluated.

3.1.4.2 Application of 5 μM cariporide reduces pH_i in the growth cones of actively extending neurites

As with the experiments described above, PC12 cells were grown for 48 h in the continual presence of 50 ng mL^{-1} NGF before being loaded with BCECF to measure the pH_i at the cell body and at the growth cone. Once loaded with BCECF, PC12 cells were placed into the recording chamber and were perfused with cariporide-free medium for up to 10 min in order to establish if the neurites were extending and to establish the baseline pH_i . Prior to cariporide application, pH_i at the growth cones of actively extending neurites ($\text{pH} = 7.38 \pm 0.05$) was significantly higher ($P < 0.05$, $n = 6$) than that found at the cell body (7.25 ± 0.03 ; Fig. 14). A 5

- 10 min application of 5 μM cariporide reduced the pH_i at the growth cone to 7.12 ± 0.04 and the pH_i at the cell body to 7.10 ± 0.04 ($P > 0.05$; Fig. 14). After the 5 - 10 min application of 5 μM cariporide, cells were returned to cariporide-free medium to allow them to recover from the inhibitor. The pH_i at the growth cone returned to near resting levels (7.36 ± 0.05) and again became significantly higher ($P < 0.05$) than the pH_i at the cell body (Fig. 14). These results suggest that the elevated pH_i found at the growth cones of actively extending neurites is most likely a result of NHE1 activity in the spatially-restricted region of the growth cone.

3.1.4.2.1 Application of cariporide results in a transient cessation of neurite outgrowth

If an elevated pH_i is indeed important for promoting the cytoskeletal dynamics required for neurite outgrowth, it would follow that cariporide-induced reductions in growth cone pH_i should be associated with a transient cessation of neurite outgrowth. To this end, PC12 cells were grown for 48 h in the presence of 50 ng mL^{-1} NGF before imaging. For these experiments, the cells were not loaded with BCECF and DIC time-lapse images were taken for up to 90 min. As can be seen in the still images in Fig. 15, before cariporide was applied to the cell the growth cone was actively extending. A five to ten min application of 2 μM cariporide resulted in a rapid cessation of neurite outgrowth. During the application of cariporide, I also noticed that, in addition to halting neurite outgrowth, cariporide resulted in a reduction in the number of filopodia at the growth cone. When cariporide was washed off the neurite eventually resumed growth and the number of filopodia at the growth cone increased (Fig. 15). These findings suggest that the elevated pH_i , as a result of NHE1 activity, at the growth cone might be providing the necessary environment to promote neurite outgrowth.

3.1.5 NHE1 is involved in the organization of the actin cytoskeleton at the growth cones of NGF-differentiated PC12 cells

The studies described above provide evidence that both functional domains of NHE1 (ion translocation as well as actin cytoskeletal anchoring) are important for modulating neurite outgrowth in NGF-differentiated PC12 cells. The pH_i measurements provided further evidence that the ion translocation activity of NHE1 is involved in modulating neurite outgrowth and the cariporide-induced reduction in the number of growth cone filopodia observed in the live cell imaging experiments suggested that NHE1 activity might facilitate neurite outgrowth by modulating the actin cytoskeleton. Therefore, I examined if NHE1 was involved in the organization of the actin cytoskeleton at the growth cones of PC12 cells.

3.1.5.1 Cariporide reduces the total but not the mean length of filopodia at the growth cone

PC12 cells were grown in the presence of either vehicle (0.1 % DMSO) or 1 μM cariporide in the continual presence of 50 ng mL^{-1} NGF for 72 h. Cells were fixed and stained with Alexa-Fluor-488 phalloidin to stain the actin cytoskeleton in order to visualize actin at the growth cone (Fig. 16). I found that 1 μM cariporide reduced the total but not the mean length of filopodia at the growth cone (Figs. 16 and 17A). The fact that there was no significant difference between the mean lengths of growth cone filopodia in control versus cariporide-treated cells suggested that the difference between the total lengths of filopodia observed under the two conditions is a result of a reduction in filopodial number.

3.1.5.2 Filopodia number is affected by modulating NHE1 activity

To investigate whether NHE1 might be affecting the number of filopodia at the growth cone, the number of growth cone filopodia was determined in PC12 cells that were vehicle-treated, treated with 1 μM cariporide and also in cells that had been transfected with full-length NHE1 (in the presence and absence of 1 μM cariporide), NHE1-E266I or NHE1-KR/A.

3.1.5.2.1 Cariporide reduces the number of filopodia at the growth cone

As expected, application of 1 μM cariporide for 72 h in the presence of 50 ng mL⁻¹ NGF reduced the number of growth cone filopodia (Figs. 16 and 17B). Untransfected cells which had been vehicle-treated had an average of 5.0 ± 0.3 filopodia per growth cone (Fig. 17B). However, when untransfected cells were exposed to 1 μM cariporide for 72 h the number of filopodia at the growth cone was reduced to 3.1 ± 0.3 ($P < 0.001$; Figs. 16 and 17B). These results suggest that NHE1 plays a role in promoting the actin cytoskeletal reorganization which is important for neurite outgrowth.

3.1.5.2.2 Transient transfection of full-length NHE1 increases the number of filopodia at the growth cone in a cariporide-sensitive manner

Inhibition of NHE1 activity with cariporide resulted in a reduction in filopodia number at the growth cones of NGF-differentiated PC12 cells. I then examined if filopodia number could be increased by the transient overexpression of full-length NHE1. PC12 cells were transfected with full-length NHE1 prior to being differentiated with 50 ng mL⁻¹ NGF for 72 h in the presence of either vehicle or 1 μM cariporide before being stained with an antibody towards the HA tag to determine cells which had been transfected as well as Alexa-Fluor-488 phalloidin to visualize

the actin cytoskeleton. When compared to untransfected cells on the same coverslip (i.e. mock-transfected cells), cells overexpressing full-length NHE1 had an increase in the number of filopodia at the growth cone, which in turn was sensitive to the application of 1 μ M cariporide (Fig. 16). Mock-transfected cells had an average of 5.6 ± 0.4 filopodia per growth cone which was reduced to 4.0 ± 0.4 in the presence of 1 μ M cariporide ($P < 0.01$; Fig. 17B). In contrast, cells which were transfected with full-length NHE1 exhibited an increase to an average of 8.3 ± 0.4 filopodia per growth cone which was reduced to 4.0 ± 0.5 after treatment with cariporide ($P < 0.001$; Figs. 16 and 17B). The cariporide-sensitive increase in filopodia number observed following the overexpression of full-length NHE1 suggests that NHE1 is likely playing a role in creating an environment within the growth cone to promote cytoskeletal rearrangements.

3.1.5.2.3 Transient transfection of NHE1-E266I or NHE1-KR/A does not lead to an increase in the number of filopodia at the growth cone

PC12 cells were transfected with either NHE1-E266I or NHE1-KR/A prior to exposure to 50 ng mL⁻¹ NGF for 72 h. Cells were subsequently fixed and transfected cells were identified by probing with anti-HA antibody and the filopodia were visualized with the aid of Alexa-Fluor-488 phalloidin to stain the actin cytoskeleton. When compared to mock-transfected cells on the same coverslips, which had an average of 4.5 ± 0.4 filopodia per growth cone, cells transfected with NHE1-E266I did not exhibit an increase in the number of filopodia, 5.0 ± 0.5 per growth cone ($P > 0.05$; Fig. 17C). Similarly, cells transfected with NHE1-KR/A had an average of 5.0 ± 0.6 filopodia per growth cone, not significantly different to the average of 5.1 ± 0.4 filopodia per growth cone found in mock-transfected cells ($P > 0.05$; Fig. 17C). These results suggest that the

NHE1-dependent alterations in growth cone filopodia number described above require both the ion translocation and actin cytoskeletal anchoring functions of the protein.

3.2 Role of NHE1 in non-stimulated neurite outgrowth in mouse neocortical neurons

Following the findings that NHE1 plays a role in regulating NGF-induced neurite outgrowth in PC12 cells, I then examined if NHE1 was playing a similar role in regulating neurite outgrowth in primary neurons. To do this I used mouse neocortical neurons obtained from both wild-type C57BL/6 mice at 16 days of gestation (E16) and from NHE1^{-/-} mice and their NHE1^{+/+} and NHE1^{+/-} littermates at postnatal day 0.5 (P0.5).

3.2.1 Neurite outgrowth in wild-type E16 neocortical neurons

Neocortical neurons were isolated from wild type C57BL/6 embryonic mice at 16 days of gestation. The neurons were subsequently maintained in primary culture for 72 h prior to fixation and morphometric analysis to evaluate neurite outgrowth.

3.2.1.1 Endogenous NHE1 is expressed in the growth cones of E16 neurons

To confirm that NHE1 is expressed in the growth cones of E16 neocortical neurons, neurons were fixed and stained with monoclonal NHE1 antibody in addition to either Alexa-Fluor-568 phalloidin or polyclonal anti-vinculin in order to visualize the growth cones. Consistent with findings in PC12 cells, NHE1 was found to be expressed in the growth cones of mouse neocortical neurons, and was again found to be expressed in the filopodia (Fig. 18). Again, the presence of NHE1 in growth cones suggests that it may be playing a role in creating a

microenvironment in the spatially-restricted region of the growth cone to promote the cytoskeletal reorganization necessary for neurite outgrowth.

3.2.1.2 E16 neurons treated with NHE1 inhibitors exhibit reduced neurite outgrowth

The expression of NHE1 within the growth cones of E16 mouse neocortical neurons suggests that NHE1 activity may be an important modulator of neurite outgrowth in these cells as well as PC12 cells. Therefore, neurite outgrowth and branching were evaluated in E16 mouse neocortical neurons that had been treated with vehicle, cariporide (at 1 and 100 μM) and also ethylisopropyl amiloride (EIPA), another Na^+/H^+ exchange inhibitor with a high potency but reduced isoform-specific selectivity [196]. Vehicle-treated neurons had an average of 4.9 ± 0.2 primary neurites with an average length of $194 \pm 7 \mu\text{m}$ and an average of 5.2 ± 0.3 branched neurites with an average length of $46 \pm 4 \mu\text{m}$ (Fig. 19). Consistent with findings in PC12 cells, 1 μM cariporide reduced the number and lengths of primary neurites as well as the number and lengths of branched neurites (Fig. 19). In addition neurons treated with 100 μM cariporide exhibited reductions in the average number and lengths of primary neurites and branches which were not significantly different to those found in neurons treated with 1 μM cariporide (Fig. 19). As in PC12 cells, the failure of 100 μM cariporide to exert an additional inhibitory effect on neurite outgrowth suggests that the reductions in neurite outgrowth observed with 1 μM cariporide are a consequence of inhibition of NHE1 activity.

Neurons treated with 1 μM EIPA had a reduced average number of 4.0 ± 0.2 primary neurites per cell ($P < 0.05$; Fig 19) with an average length of $182 \pm 8 \mu\text{m}$, which was not significantly different from the lengths of the primary neurites found in the vehicle-treated

neurons ($194 \pm 7 \mu\text{m}$, $P > 0.05$; Fig. 19). In contrast, the number of branches per cell (2.9 ± 0.4) as well as the lengths of the branches ($27 \pm 3 \mu\text{m}$) were reduced in neurons treated with $1 \mu\text{M}$ EIPA when compared to the vehicle-treated neurons (Fig. 19). Representative examples of WT E16 mouse neocortical neurons as well as neurons treated with $1 \mu\text{M}$ cariporide or $1 \mu\text{M}$ EIPA are shown in Fig. 20.

These findings suggest that NHE1 may be playing a similar role in modulating neurite outgrowth in WT E16 mouse neocortical neurons as in PC12 cells. To further examine this possibility, next I examined whether overexpression of NHE1 in WT E16 neocortical neurons had an effect on neurite outgrowth.

3.2.1.3 Transient overexpression of full-length NHE1 enhances neurite outgrowth in a cariporide-sensitive manner

Wild-type E16 neurons were transiently transfected with full-length NHE1 and the cells were maintained for 72 h in the continual presence of either cariporide vehicle or $1 \mu\text{M}$ cariporide. Neurons were stained with Alexa-Fluor-488 phalloidin in addition to antibodies against the HA-tag that was attached to the NHE1 construct in order to identify neurons which had been successfully transfected. Neurons which transiently overexpressed full-length NHE1 exhibited a significant, cariporide-sensitive, increase in the number and lengths of both primary and branched neurites (Fig. 21).

Untransfected neurons had an average of 5.9 ± 0.2 primary neurites with an average length of $169 \pm 4 \mu\text{m}$ and had an average of 5.2 ± 0.5 branched neurites which had an average length of $50 \pm 4 \mu\text{m}$ (Fig. 22). While neurons that transiently overexpressed NHE1 did not exhibit a significant increase in the number of primary neurites (6.4 ± 0.3 ; $P > 0.05$; Fig. 22),

there was an increase in the average length of the primary neurites ($188 \pm 8 \mu\text{m}$; $P < 0.05$; Fig. 22) in addition to an increase in both the number and lengths of the branched neurites to 9 ± 1 and $86 \pm 6 \mu\text{m}$ respectively ($P < 0.05$; Fig. 22). NHE1-overexpressing neurons which were treated with $1 \mu\text{M}$ cariporide exhibited a subsequent reduction in the number and lengths of both primary and branched neurites, consistent with experiments in PC12 cells (Fig. 22).

3.2.2 Neurite outgrowth in NHE1^{-/-} P0.5 mouse neocortical neurons

The above findings suggest that NHE1 participates in the regulation of early neurite outgrowth and elaboration in NGF-differentiated PC12 cells and E16 WT mouse neocortical neurons in primary culture. To confirm and extend these findings, which were obtained using a predominantly pharmacological approach, I examined neurite outgrowth in cultured (3 D.I.V.) neocortical neurons obtained from P0.5 *Nhe1* homozygous mutant (NHE1^{-/-}) mice and compared it to that in their WT (NHE1^{+/+}) and heterozygous (NHE1^{+/-}) littermates.

3.2.2.1 NHE1^{-/-} neurons do not express endogenous NHE1

In light of previous reports [197-199], I first confirmed that neurons from NHE1^{-/-} P0.5 mice did in fact not express endogenous NHE1. Compared to brain tissue isolated from NHE1^{+/+} littermates, brain tissue isolated from NHE1^{-/-} mice showed an absence of NHE1 protein by Western analysis using an anti-NHE1 antibody raised against the C-terminus of NHE1 (Fig. 23A). In addition, neocortical neurons isolated from both NHE1^{-/-} mice as well as NHE1^{+/+} littermates were maintained for 72 h in primary culture before fixing and staining with the anti-NHE1 antibody in conjunction with Alexa-Fluor-488 phalloidin to visualize the growth cones

(Fig. 23B). While neurons obtained from NHE1^{+/+} littermates expressed NHE1 in their growth cones, neurons from NHE1^{-/-} mice did not (Fig. 23B).

3.2.2.2 Neurite outgrowth is reduced in neurons obtained from NHE1^{+/-} mice and to a greater extent in neurons obtained from NHE1^{-/-} mice

When compared to NHE1^{+/+} neurons, neurons obtained from NHE1^{-/-} mice exhibited significant reductions in the number and lengths of both primary and branched neurites, values which were not further reduced by 1 μ M cariporide (Fig. 24). NHE1^{+/-} neurons exhibited an intermediate level of neurite outgrowth when compared to NHE1^{+/+} and NHE1^{-/-} neurons (Fig. 24). Additionally, neurite outgrowth in NHE1^{+/-} neurons appeared to have an intermediate sensitivity to application of 1 μ M cariporide (Fig. 24). Taken together, these findings suggest strongly that a lack of NHE1 protein underlies the attenuated neurite elongation and branching observed in NHE1^{-/-} neurons. Together with the findings that inhibition of NHE1 activity reduces neurite outgrowth in both NGF-differentiated PC12 cells as well as neocortical neurons obtained from WT E16 and NHE1^{+/+} P0.5 mice, these results further support the possibility that NHE1 regulates neurite outgrowth.

3.2.2.3 Transient overexpression of full-length NHE1 rescues neurite outgrowth in neurons obtained from NHE1^{-/-} mice in a cariporide-sensitive manner

Neurons isolated from NHE1^{-/-} mice were transiently transfected with full-length NHE1 and maintained for 72 h in the presence or absence of 1 μ M cariporide. Compared to untransfected NHE1^{-/-} neurons, neurons transfected with full-length NHE1 exhibited an increase in both the number and the lengths of primary neurites as well as an increase in the number and lengths of

branched neurites (Fig. 25). Application of 1 μ M cariporide to NHE1-overexpressing NHE1^{-/-} neurons reduced the average number of primary neurites per cell to 3.8 ± 0.2 with an average length of 134 ± 8 μ m and reduced the number of branches per cell to 6.5 ± 0.6 with a reduced average length of 79 ± 10 μ m ($P < 0.05$ in both cases; Fig. 25). Representative examples of neurons from each condition can be seen in Fig. 26.

3.2.2.4 Transient overexpression of either NHE1-E266I or NHE1-KR/A fails to rescue neurite outgrowth in NHE1^{-/-} neurons

I next examined if transient transfection of either NHE1-E266I or NHE1-KR/A was able to rescue neurite outgrowth in neurons obtained from NHE1^{-/-} mice. Neurons from NHE1^{-/-} mice were transiently transfected with either NHE1-E266I or NHE1-KR/A for 72 h in the presence and absence of 1 μ M cariporide. Neurons transiently overexpressing NHE1-E266I had an average number of 3.5 ± 0.3 primary neurites (average length of 141 ± 14 μ m) and an average of 6 ± 1 branches (average length of 72 ± 16 μ m), values which were not significantly different to those obtained in NHE1^{-/-} neurons ($P > 0.05$ in all cases; Fig. 25). In addition, NHE1-E266I-overexpressing neurons treated with 1 μ M cariporide did not exhibit a further reduction in the number or lengths of either the primary or branched neurites (Fig. 25).

NHE1^{-/-} neurons overexpressing NHE1-KR/A had an average number of 4.1 ± 0.1 primary neurites with an average length of 152 ± 9 μ m and an average number of 6.6 ± 0.8 branched neurites which had an average length of 81 ± 13 μ m, values which, as in the case of NHE1-E266I overexpressing neurons, were not significantly different to those observed in untransfected NHE1^{-/-} neurons ($P > 0.05$ in all cases; Fig. 25). Additionally, NHE1^{-/-} neurons

overexpressing NHE1-KR/A and treated with 1 μ M cariporide did not exhibit further reductions in either the number or lengths of primary or branched neurites (Fig. 25). Representative examples of neurons from each treatment are shown in Fig. 26.

The above results indicate that NHE1 is a novel modulator of neurite outgrowth in both NGF-differentiated PC12 cells and non-stimulated mouse neocortical neurons in primary culture. In addition, both the ion translocation and actin cytoskeletal anchoring functions of NHE1 appear to be necessary for NHE1-mediated modulation of neurite outgrowth in both cell types.

3.3 NHE1 is involved in stimulated neurite outgrowth in mouse neocortical neurons

The findings above indicate that NHE1 is involved in early neurite outgrowth and branching in non-stimulated neocortical neurons maintained for 72 h in primary culture. I then determined if NHE1 was also playing a role in regulating the growth-promoting effects of a number of extracellular factors which are known to promote neurite outgrowth and/or branching in mammalian central neurons. The extracellular factors used were netrin-1, BDNF and IGF-1 which are all known to enhance neurite outgrowth and elaboration in mammalian central neurons.

3.3.1 1 μ M cariporide abolishes netrin-1 enhanced neurite outgrowth but not outgrowth stimulated by BDNF or IGF-1

The role NHE1 plays in mediating the growth-promoting effects of extracellular factors known to enhance neurite outgrowth were evaluated in neurons obtained from NHE1^{+/+} P0.5 mice and subsequently treated with 200 ng mL⁻¹ netrin-1, 50 ng mL⁻¹ BDNF or 50 ng mL⁻¹ IGF-1 for 72 h in the presence or absence of 1 μ M cariporide.

NHE1^{+/+} neurons treated with 200 ng mL⁻¹ netrin-1 exhibited increases in the number and lengths of branched neurites which were markedly reduced by 1 μ M cariporide (Fig. 27). While there were no significant increases in the lengths or the number of primary neurites in response to netrin-1, application of 1 μ M cariporide resulted in reductions in both (Fig. 27). While neurons obtained from NHE1^{+/+} mice and treated with 50 ng mL⁻¹ BDNF exhibited an increase in the number and lengths of both primary and branched neurites, 1 μ M cariporide only modestly reduced the number and lengths of branched neurites while having no effect on the number or lengths of primary neurites (Fig. 27). Similar to BDNF, treatment of neurons obtained from NHE1^{+/+} mice with 50 ng mL⁻¹ IGF-1 increased the number and lengths of both primary and branched neurites (Fig. 27). Application of 1 μ M cariporide to IGF-1-treated NHE1^{+/+} neurons only modestly reduced the number and lengths of branched neurites, while only reducing the lengths but not the number of primary neurites (Fig. 27). Figure 28 shows representative examples of NHE1^{+/+} neurons treated with netrin-1, BDNF and IGF-1 in the presence and absence of 1 μ M cariporide.

The above results suggest that NHE1 may be playing a role in mediating the promotion of neurite outgrowth elicited by netrin-1, IGF-1 and BDNF. However, whereas cariporide had only modest effects on the increases in neurite outgrowth elicited by BDNF and IGF-1, it effectively abolished the neurite outgrowth promoting effects of netrin-1.

3.3.2 Netrin-1 fails to stimulate neurite outgrowth in NHE1^{-/-} neurons while BDNF and IGF-1 enhance outgrowth

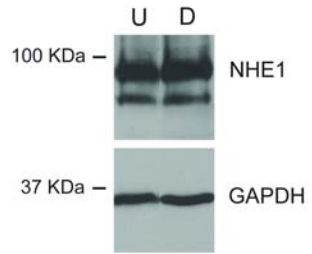
The ability of the above growth factors to enhance neurite outgrowth in the absence of NHE1 expression was examined by treating neurons obtained from NHE1^{-/-} mice with netrin-1, BDNF

or IGF-1 for 72 h in the presence or absence of 1 μM cariporide. Neurons isolated from $\text{NHE1}^{-/-}$ mice and treated with 200 ng mL^{-1} netrin-1 exhibited no significant increases in the number or lengths of primary or branched neurites when compared to untreated $\text{NHE1}^{-/-}$ neurons suggesting that netrin-1 stimulated neurite outgrowth is NHE1-dependent (Fig. 29). In contrast, $\text{NHE1}^{-/-}$ neurons treated with either 50 ng mL^{-1} BDNF or 50 ng mL^{-1} IGF-1 exhibited increases in the average number and lengths of primary as well as branched neurites (Fig. 29). Application of 1 μM cariporide had no effect on neurite outgrowth in the $\text{NHE1}^{-/-}$ neurons treated with netrin-1, BDNF or IGF-1 (Fig. 29). Representative examples of $\text{NHE1}^{-/-}$ neurons treated with netrin-1, BDNF or IGF-1 in the presence or absence of 1 μM cariporide are shown in Figure 30.

Figure 6. Endogenous expression of NHE1 in PC12 cells

(A) Endogenous expression of NHE1 in PC12 cells was assessed by Western analysis with anti-NHE1 antibody. Comparison between undifferentiated (U) PC12 cells and cells that were differentiated (D) with 50 ng mL⁻¹ NGF for 72 h showed that there is no increase in NHE1 expression with differentiation. GAPDH was used as a loading control. (B) To assess endogenous NHE1 expression in the growth cones of PC12 cells, cells were differentiated with 50 ng mL⁻¹ NGF for 72 h and immunostained with anti-NHE1 antibody and Alexa Fluor 568-conjugated phalloidin. Scale bar, 10 μm.

A



B

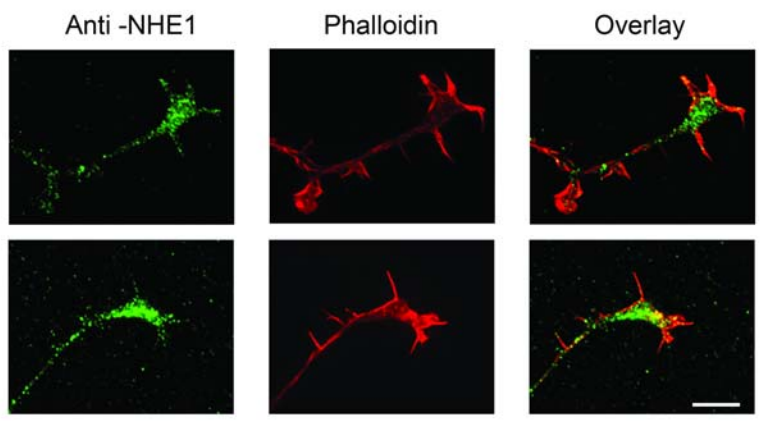


Figure 7. Inhibition of NHE1 with cariporide reduces NGF-induced neurite outgrowth in PC12 cells

Compared to cells cultured in the presence of 0.1% DMSO (Con; open bars), PC12 cells treated with 1 μ M cariporide (grey bars) had a reduction in the number and lengths of both primary and branched neurites per cell. In addition, while application of 100 μ M cariporide (grey hatched bars) reduced neurite outgrowth compared to vehicle-treated cells, there was no further reduction when compared to PC12 cells treated with 1 μ M cariporide. For all parameters measured, there was no significant difference ($P > 0.05$) between PC12 cells cultured in the absence *vs.* presence of 0.1% DMSO (data not shown). The experiments were conducted in parallel, all measured parameters are per cell, error bars represent s.e.m. and n values are in the columns. ***, $P < 0.001$, and n.s, not significant ($P > 0.05$) by Kruskal-Wallis one-way ANOVA followed by Student-Newman-Keuls post-hoc test.

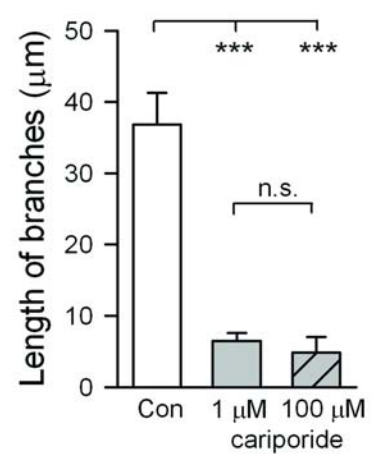
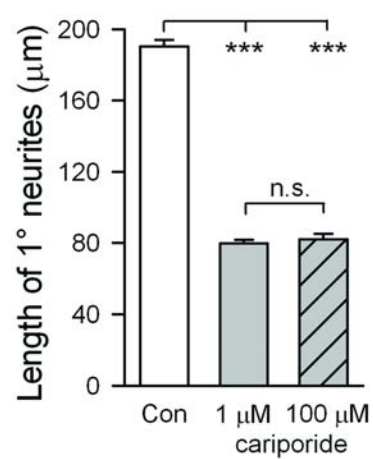
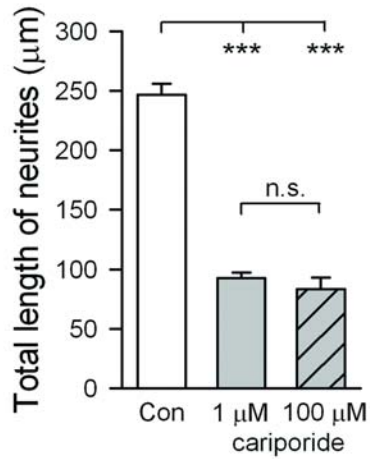
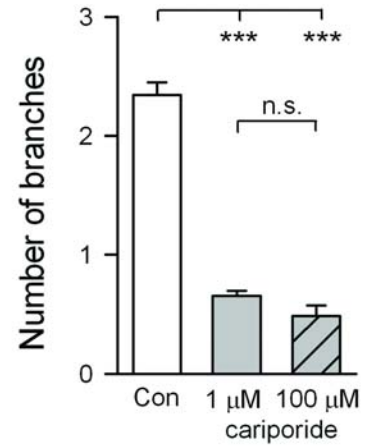
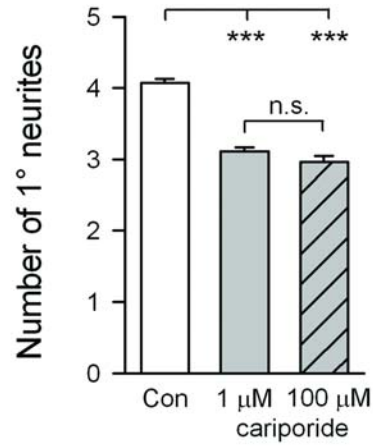
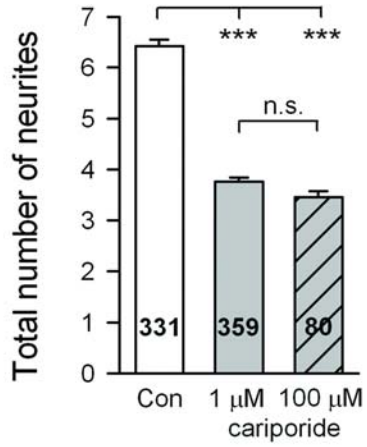


Figure 8. Representative PC12 cells showing reduced neurite outgrowth in response to cariporide treatment

Representative examples of PC12 cells differentiated with 50 ng mL⁻¹ NGF for 72 h in the continuous presence of cariporide vehicle (Con; 0.1% DMSO) as well as cariporide at an NHE1 selective concentration (1 μM) or at a concentration to inhibit all known plasmalemmal isoforms (100 μM). 1 μM cariporide caused a visible reduction in neurite outgrowth, however application of 100 μM did not result in a further reduction suggesting a dominant role for NHE1 activity in modulating neurite outgrowth. Cells were stained with Alexa Fluor 488-conjugated phalloidin to visualize F-actin. Scale bar, 20 μm.

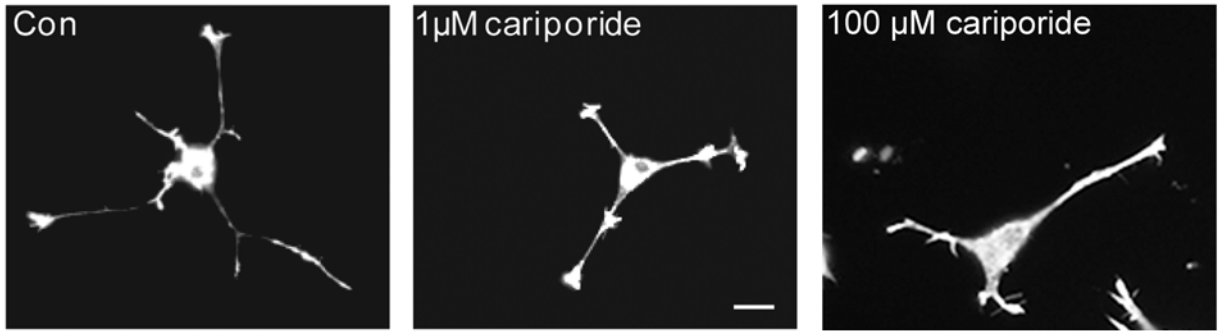


Figure 9. The effects of 100 μ M cariporide on neurite outgrowth are reversible

PC12 cells were differentiated with NGF for 24 (column 1), 48 (column 2) or 72 (column 3) h in the presence of cariporide vehicle (0.1% DMSO). Data in columns 4 and 5 are from parallel experiments in which 100 μ M cariporide was applied from 24 - 48 h and cells were fixed at 48 h and 72 h, respectively. Quantitatively similar results were obtained with 1 μ M cariporide (data not shown). The experiments were conducted in parallel, all measured values are per cell, error bars represent s.e.m. and n values are shown in the columns. n.s., not significant ($P > 0.05$) by Kruskal-Wallis one-way ANOVA followed by Student-Newman-Keuls post-hoc test.

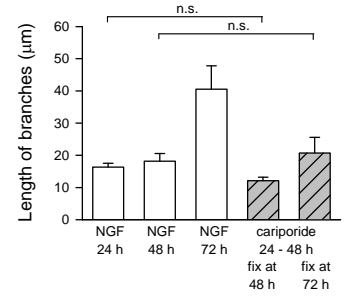
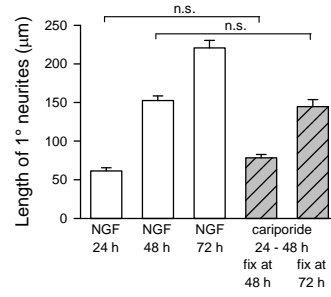
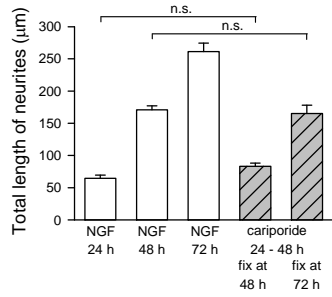
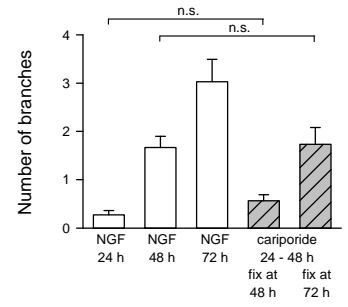
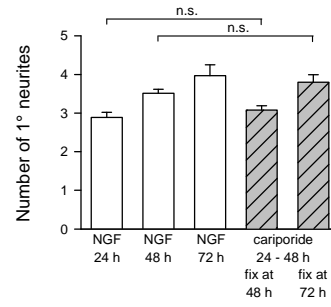
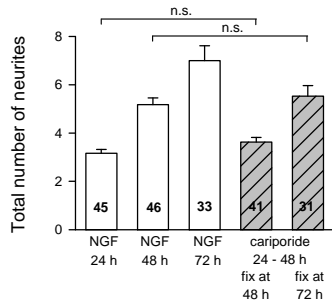


Figure 10. Functional characterization of full-length and mutant NHE1 constructs expressed in NHE-deficient PS120 cells

Sub-confluent PS120 cells were co-transfected with EGFP and plasmids containing cDNA encoding either WT NHE1, NHE1-KR/A, NHE1-E266I or NHE1- Δ -556-564 at a ratio of 1:1. Shown are pH_i recoveries (expressed as BI_{488}/BI_{452} ratio values) from 20 mM NH_4^+ -induced internal acid loads recorded simultaneously from EGFP-expressing cells (green traces) and from adjacent non-EGFP-expressing cells (red traces) loaded with BCECF. Cells co-transfected with EGFP and WT NHE1 (**A**), NHE1- Δ 556-564 (**C**) or NHE1-KR/A (**D**) exhibited cariporide-sensitive recoveries of pH_i from imposed internal acid loads, whereas cells expressing NHE1-E266I (**B**) and untransfected cells under all conditions did not. Records are representative of 3 - 4 independent experiments for each treatment group. Under the conditions employed, BCECF-derived fluorescence emissions at each excitation wavelength (488 and 452 nm) were >20 times greater than the respective signals derived from EGFP and no changes in BI_{488}/BI_{452} ratio values were observed in response to internal acid loads imposed on cells transfected with EGFP but not loaded with BCECF.

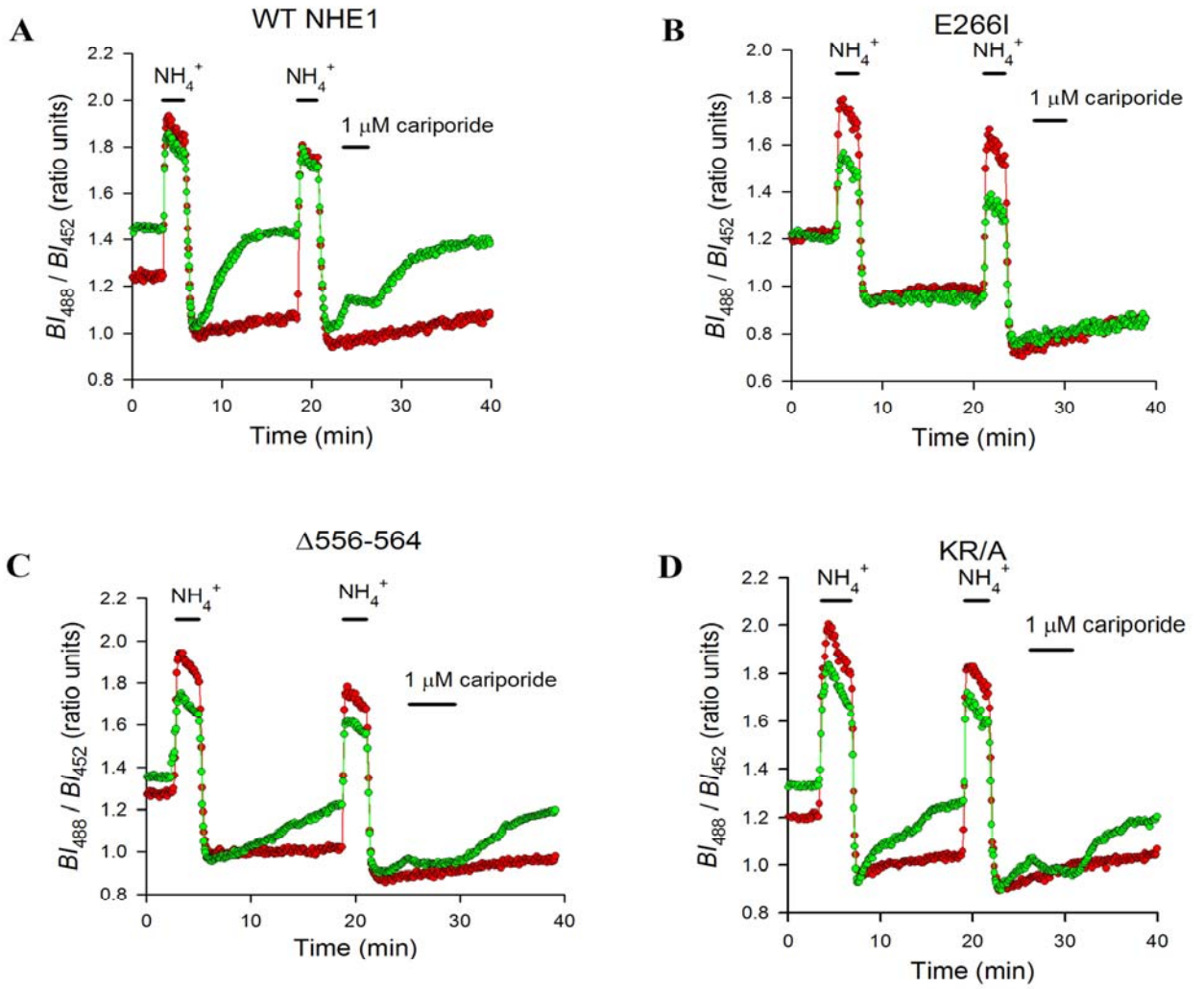


Figure 11. Quantification of the effects of overexpressing full-length or mutant NHE1 constructs on neurite outgrowth

Untransfected PC12 cells (Con) or PC12 cells transiently transfected with WT NHE1, NHE1-E266I, NHE1-KR/A or NHE1- Δ 556-564, in either the absence (open bars) or continuous presence (grey bars) of 1 μ M cariporide were differentiated with 50 ng mL⁻¹ NGF for 72 h. When compared to control cells, PC12 cells transfected with full-length NHE1 exhibited cariporide-sensitive increases in the number and lengths of primary neurites while only increasing the lengths but not the number of branched neurites. In contrast, cells transfected with NHE1-E266I, NHE1-KR/A or NHE1- Δ 556-564 all exhibited reductions in the number and lengths of branched as well as primary neurites. The reductions seen in NHE1-KR/A-overexpressing cells were further reduced by the application of 1 μ M cariporide while cells transfected with NHE1-E266I and NHE1- Δ 556-564 were insensitive to cariporide application. Experiments were conducted in parallel, all measured values are per cell, error bars represent s.e.m. and *n* values are shown in the columns. *, *P* < 0.05; **, *P* < 0.01, ***, *P* < 0.001 and n.s., not significant (*P* > 0.05) by Kruskal-Wallis one-way ANOVA followed by Student-Newman-Keuls post-hoc test.

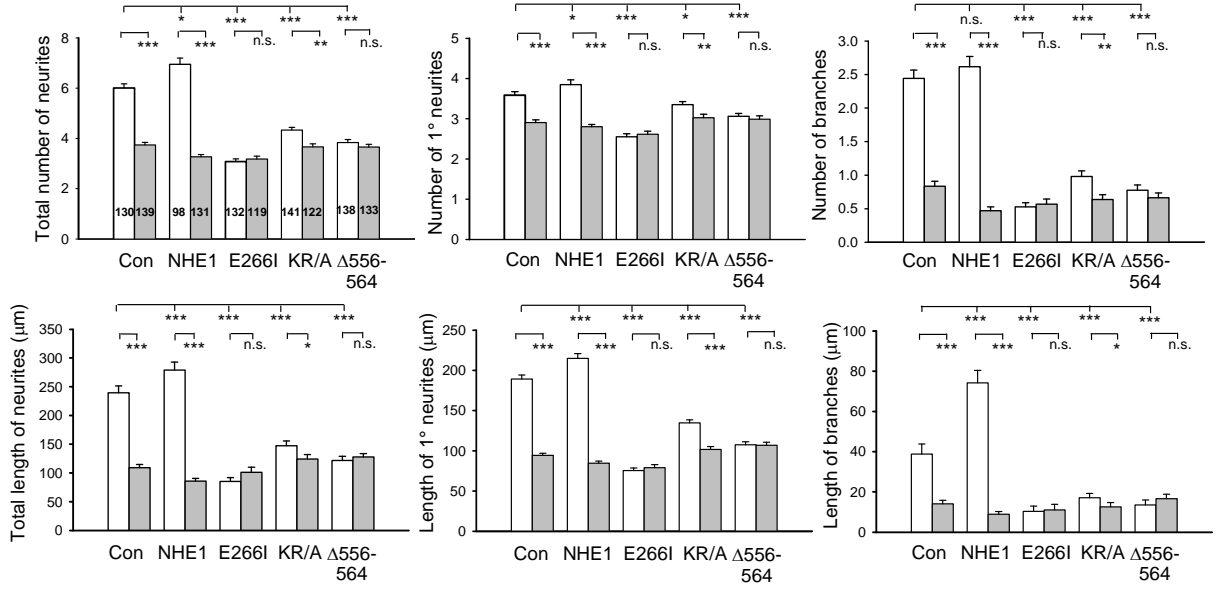


Figure 12. Representative PC12 cells showing the effects of overexpressing WT or mutant NHE1s on neurite outgrowth in NGF-differentiated PC12 cells

Representative cells were either untransfected (Con) or transiently transfected with WT NHE1 (NHE1), NHE1 lacking ion transport (E266I) or NHE1 mutants lacking cytoskeletal anchoring (KR/A or NHE1- Δ 556-564). The cells were subsequently differentiated for 72 h in the presence of 50 ng mL⁻¹ NGF. Cells transfected with full-length NHE1 displayed a visible increase in neurite outgrowth when compared to control, however cells transfected with any one of the mutants displayed a visible reduction in neurite outgrowth. Untransfected and transfected cells were labeled with Alexa Fluor 488-conjugated phalloidin and anti-HA antibody, respectively. Scale bar, 20 μ m.

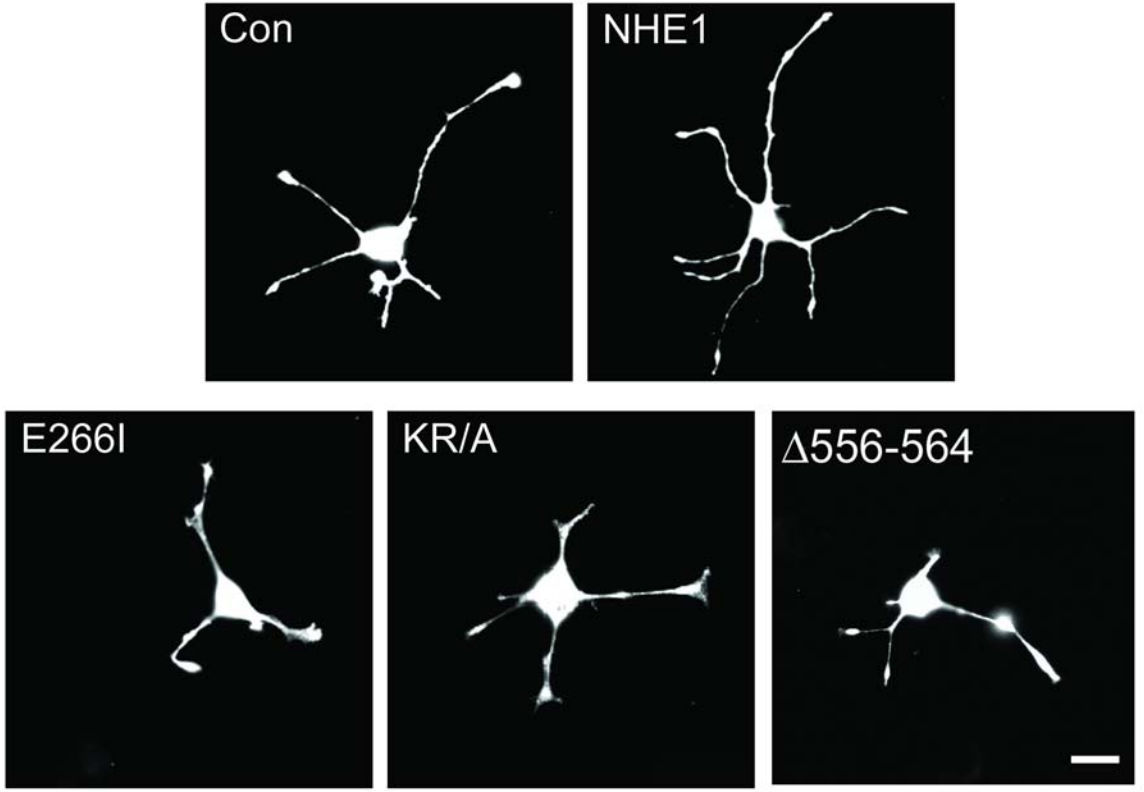


Figure 13. pH_i in actively extending neurites is elevated compared to that found at the cell body.

(A) and (B) Superimposed records of pH_i measured simultaneously at the growth cones (open circles) and somata and/or proximal regions of primary neurites (black squares) in PC12 cells differentiated with 50 ng mL^{-1} NGF for 72 h. (A) pH_i at the growth cones of actively extending neurites (7.36 ± 0.02) was consistently higher than in more proximal regions (7.23 ± 0.03 ; $P < 0.01$). (B) In contrast, pH_i in growth cones of stalled neurites (7.22 ± 0.03) was not significantly different to that measured in more proximal regions (7.20 ± 0.02 ; $P = 0.58$). Open triangles indicate time points at which DIC images were captured to identify actively extending neurites. In both (A) and (B) measurements were obtained from 10 separate cells. Significance measured by Students *t*-test.

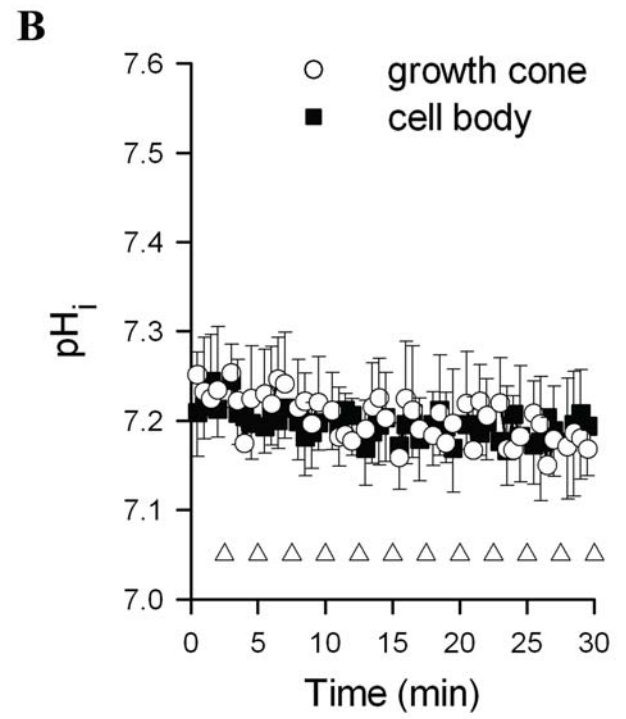
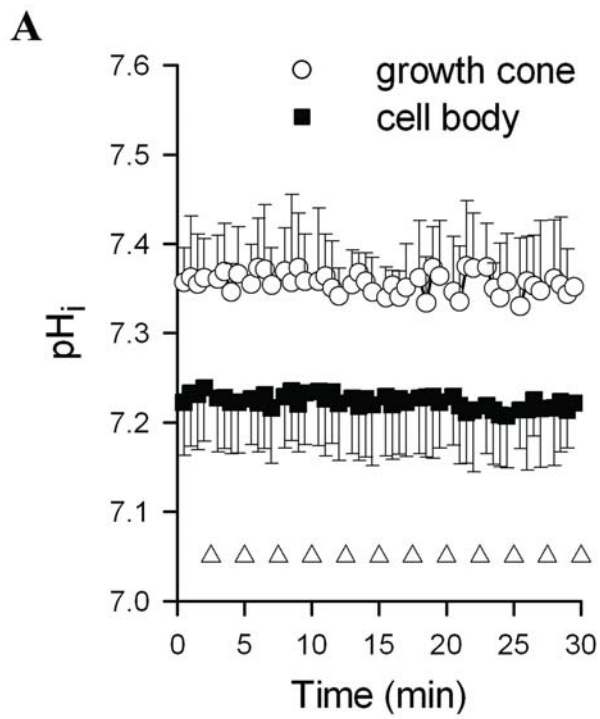


Figure 14. Cariporide (5 μM) caused reversible reductions in pH_i measured simultaneously at the cell body and in the growth cones of actively extending neurites

Superimposed records of pH_i measured simultaneously at the growth cones (open circles) and somata and/or proximal regions of primary neurites (black squares) in PC12 cells differentiated with 50 ng mL^{-1} NGF for 72 h. Records are the means of data obtained from six PC12 cells on different coverslips; error bars are s.e.m. pH_i values in growth cones prior to (7.38 ± 0.05) and after recovery from cariporide (7.36 ± 0.05) were significantly ($P < 0.05$ in both cases by Student's t test) higher than those measured simultaneously at the cell body (7.25 ± 0.03 and 7.28 ± 0.05 , respectively). In contrast, at the end of the 6 min application of cariporide, pH_i at the growth cone (7.12 ± 0.04) was not significantly different from pH_i at the cell body (7.10 ± 0.04).

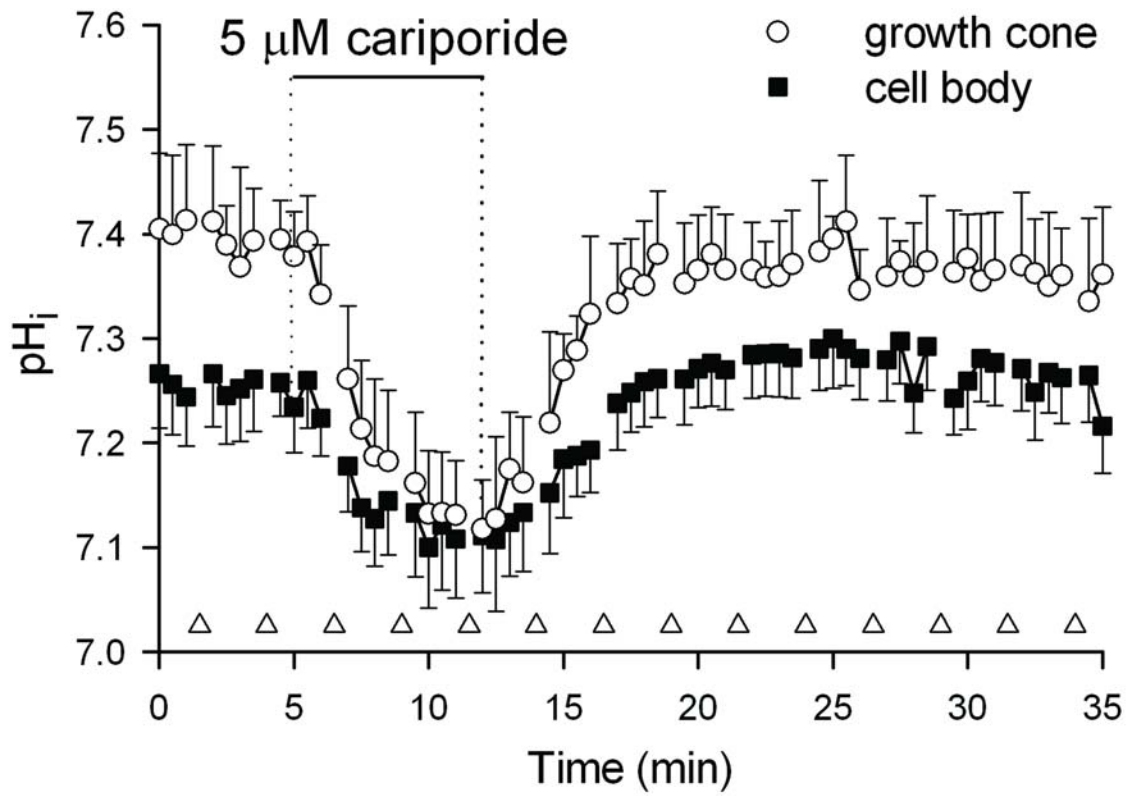


Figure 15. Cariporide treatment halts neurite outgrowth and results in the loss of filopodia at the growth cone

DIC time-lapse images show that the application of cariporide (2 μM for 6 min, starting at 13 min) was temporally associated with a reversible reduction in filopodial number (and motility; not shown) and a reversible cessation of neurite outgrowth. Between the start of the experiment (0 min) and immediately before application of cariporide (at 12 min), the growth cone can be seen to have advanced. Two min after the application of cariporide (15 min), the growth cone has not advanced beyond the 12 min time point and following washout of cariporide the growth cone was seen to resume growth as can be seen at the final time point (75 min). Scale bar, 5 μm .

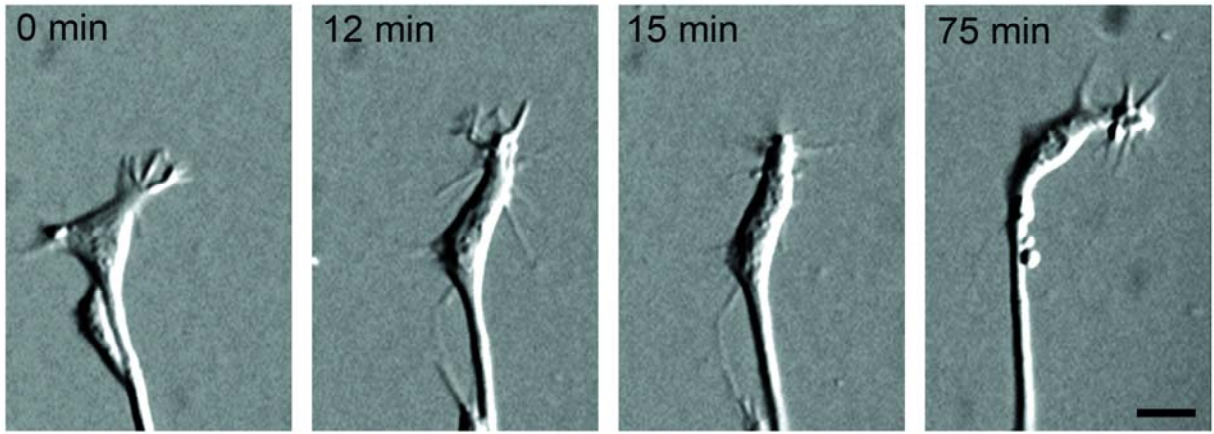


Figure 16. NHE1 regulates filopodia number in PC12 cell growth cones

PC12 cells were differentiated with 50 ng mL⁻¹ NGF for 72 h and labeled with phalloidin under the conditions shown on the figure. Overexpression of full-length NHE1 resulted in an increase in the number of filopodia at the growth cone when compared to both control cells in addition to mock transfected cells on the same coverslip. One μ M cariporide reduced the number of filopodia at the growth cone in untransfected, mock-transfected and NHE1-transfected PC12 cells. Cells were labeled with phalloidin to visualize the growth cone filopodia and transfected cells were also labeled with anti-HA antibody to identify transfected cells (not shown). Scale bar, 10 μ m.

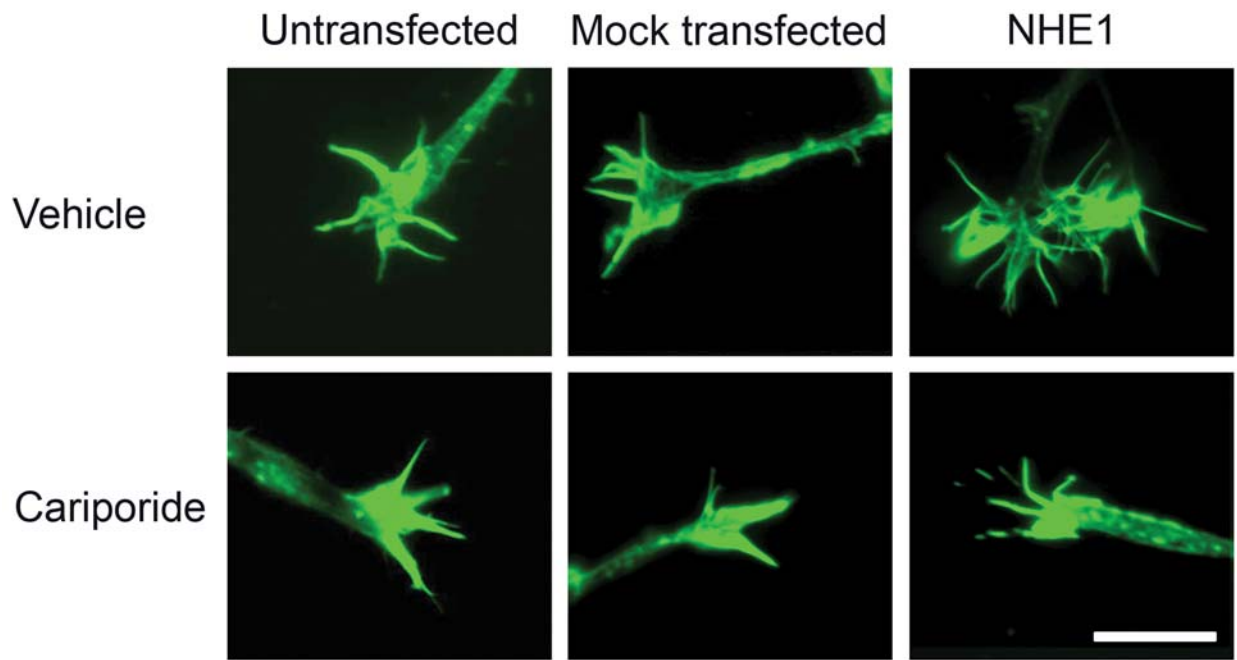
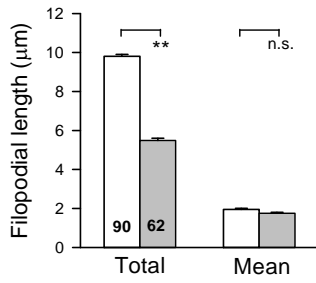


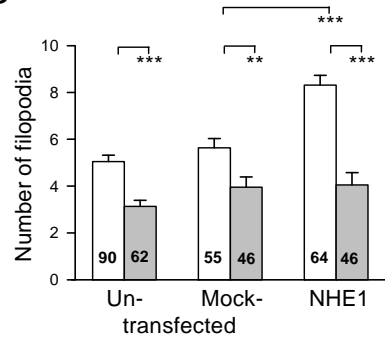
Figure 17. Quantification of the effects of modulating NHE1 activity and expression on growth cone filopodia

PC12 cells were differentiated with 50 ng mL⁻¹ NGF for 72 h and labeled with Alexa-Fluor-488 phalloidin. **(A)** Compared to control (open bars; 0.1% DMSO), the total length of filopodia per growth cone was reduced in the presence of 1 μM cariporide (grey bars) while the mean filopodial length was unaffected. **(B)** Compared to untransfected and mock-transfected cells cultured in the presence of cariporide vehicle (0.1% DMSO; open bars), 1 μM cariporide (grey bars) reduced the number of filopodia per growth cone. Overexpression of WT NHE1 (NHE1) increased the number of growth cone filopodia in a cariporide-sensitive manner. **(C)** When compared to mock-transfected cells (open bars), cells transfected with either NHE1-E266I or NHE1-KR/A (hatched bars) failed to exhibit an increase in the number of filopodia at the growth cone, in contrast to the effect of full-length NHE1. For all graphs, error bars represent s.e.m. and *n* values are shown in the columns. *, *P* < 0.05 ** , *P* < 0.01, ***, *P* < 0.001 and n.s., not significant (*P* > 0.05) by Student's *t* test.

A



B



C

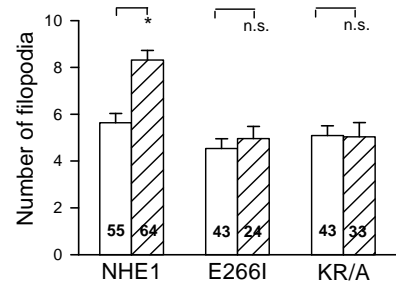


Figure 18. NHE1 is endogenously expressed at the growth cones of WT E16 mouse neocortical neurons

Endogenous expression of NHE1 was evaluated at the growth cones of two different WT E16 mouse neocortical neurons. The neurons were fixed at 3 D.I.V. and immunostained with monoclonal anti-NHE1 antibody (green) and either Alexa-Fluor-568 phalloidin (red, left cell) or polyclonal anti-vinculin antibody (red, right cell). In both cells NHE1 expression is seen in the growth cone and extends out to the filopodia. Scale bars, 5 μm .

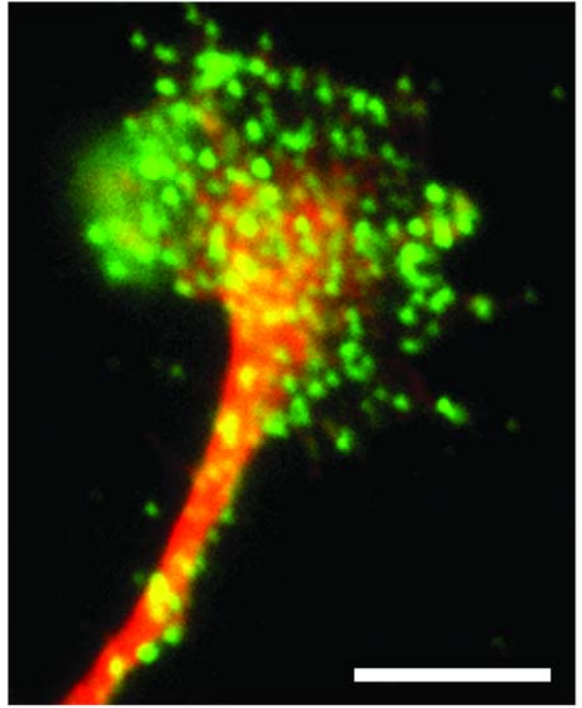
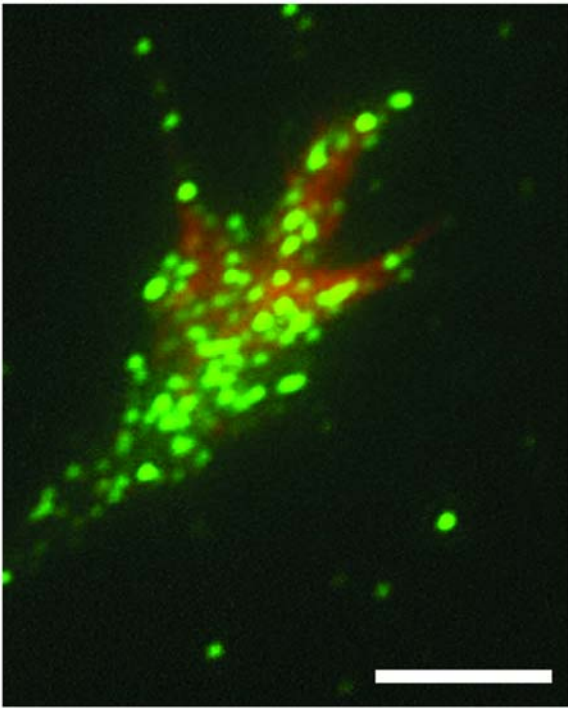


Figure 19. Quantification of the effects of cariporide and EIPA on neurite outgrowth in WT E16 mouse neocortical neurons

Compared to neurons cultured under control conditions (Con; 0.1% DMSO), neurons cultured for 72 h in the presence of 1 μ M cariporide, 100 μ M cariporide or 1 μ M EIPA had reduced levels of neurite outgrowth. All experiments were conducted in parallel, all measured values are per cell, error bars represent s.e.m. and *n* values are shown in the columns. *, $P < 0.05$, **, $P < 0.01$ and n.s., not significant ($P > 0.05$) by Kruskal-Wallis one-way ANOVA on ranks followed by Dunn's method for pair-wise comparison.

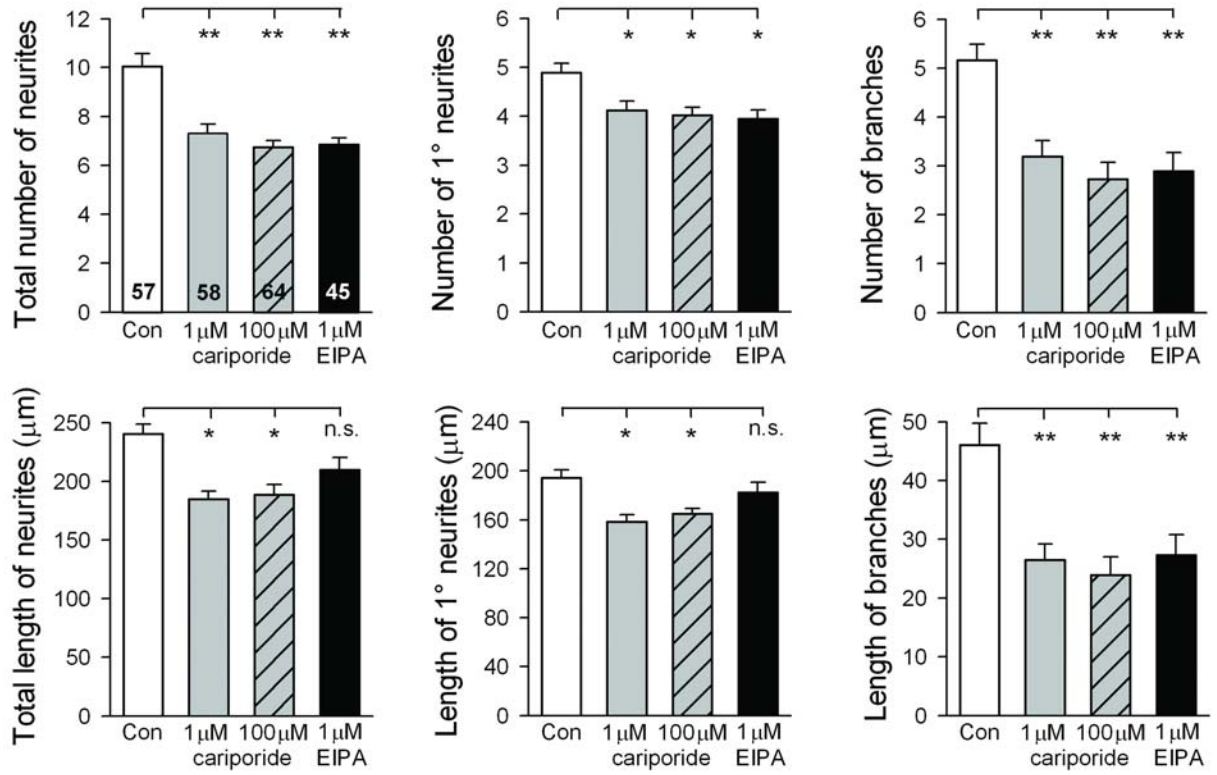


Figure 20. Representative WT E16 neocortical neurons show reduced neurite outgrowth in response to NHE1 inhibitors

WT E16 mouse neocortical neurons were cultured for 72 h in the continuous presence of 0.1% DMSO (Con), 1 μ M cariporide or 1 μ M EIPA. Both of the NHE1 inhibitors resulted in visible reductions in the number and lengths of the neurites with the most prominent effect seen in the reduction of the lengths and number of branched neurites. Neurons were fixed at 3 D.I.V. and control cells were labeled with monoclonal anti-MAP2 antibody in conjunction with polyclonal anti-neurofilament 200 antibody. Scale bar, 10 μ m.

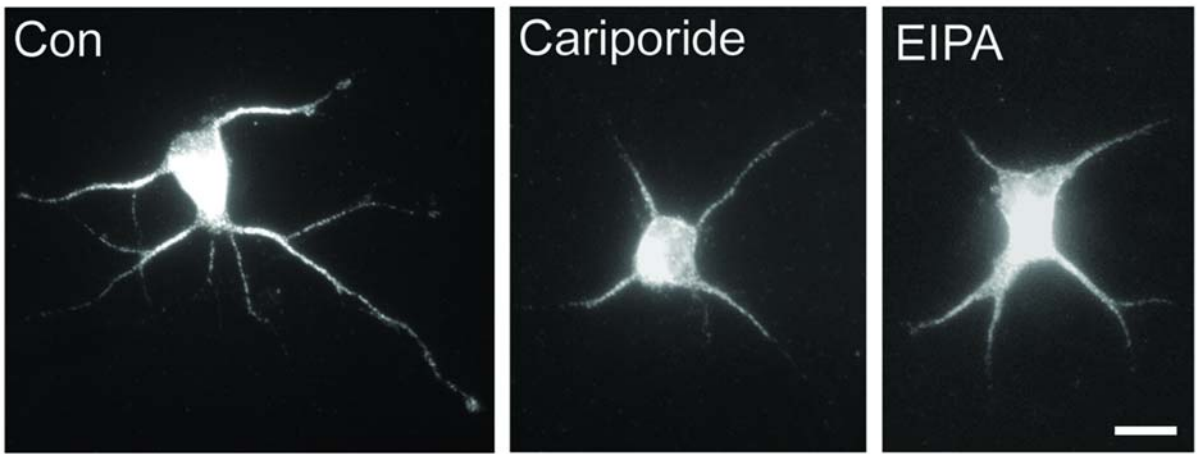


Figure 21. Overexpression of full-length NHE1 in WT E16 mouse neocortical neurons enhances neurite outgrowth

Compared to untransfected neurons (Con; 0.1% DMSO), the overexpression of full-length NHE1 visibly enhanced neurite outgrowth in E16 WT mouse neocortical neurons. This enhancement of neurite outgrowth was sensitive to the application of 1 μ M cariporide. Neurons were fixed at 3 D.I.V. and control cells were labeled with monoclonal anti-MAP2 antibody in conjunction with polyclonal anti-neurofilament 200 antibody while transfected cells were labeled with anti-HA antibody. Scale bar, 10 μ m.

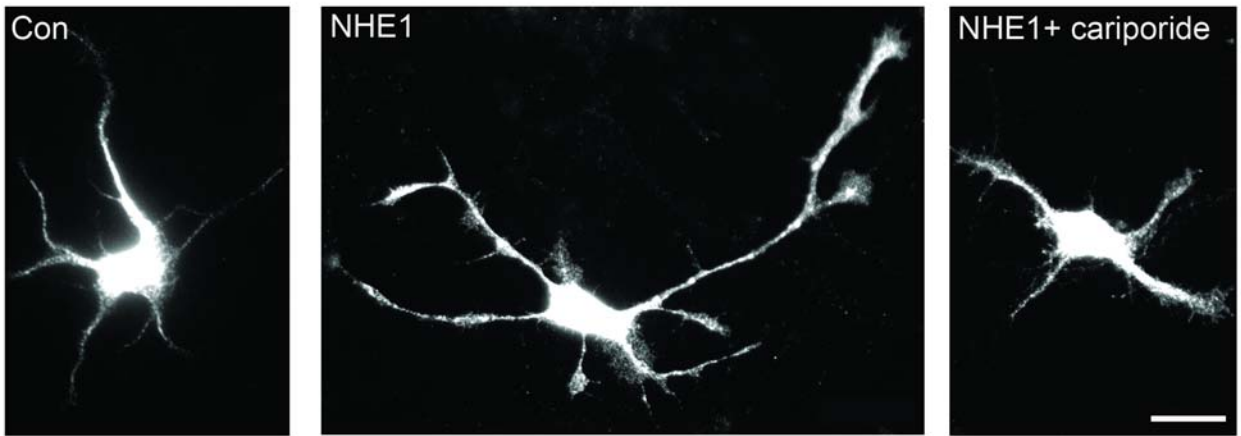


Figure 22. Quantification of the effects of overexpressing NHE1 in WT E16 mouse neocortical neurons

Compared to untransfected neurons (Con; open bars), neurons overexpressing full-length NHE1 (NHE1; open hatched bars) exhibited enhanced neurite outgrowth which was sensitive to the application of 1 μ M cariporide (grey hatched bars). Experiments were conducted in parallel, all measured values are per cell, error bars represent s.e.m. and *n* values are shown in the columns. *, $P < 0.05$; **, $P < 0.01$, ***, $P < 0.001$ and n.s., not significant ($P > 0.05$) by Kruskal-Wallis one-way ANOVA on ranks followed by Dunn's method for pair-wise comparison.

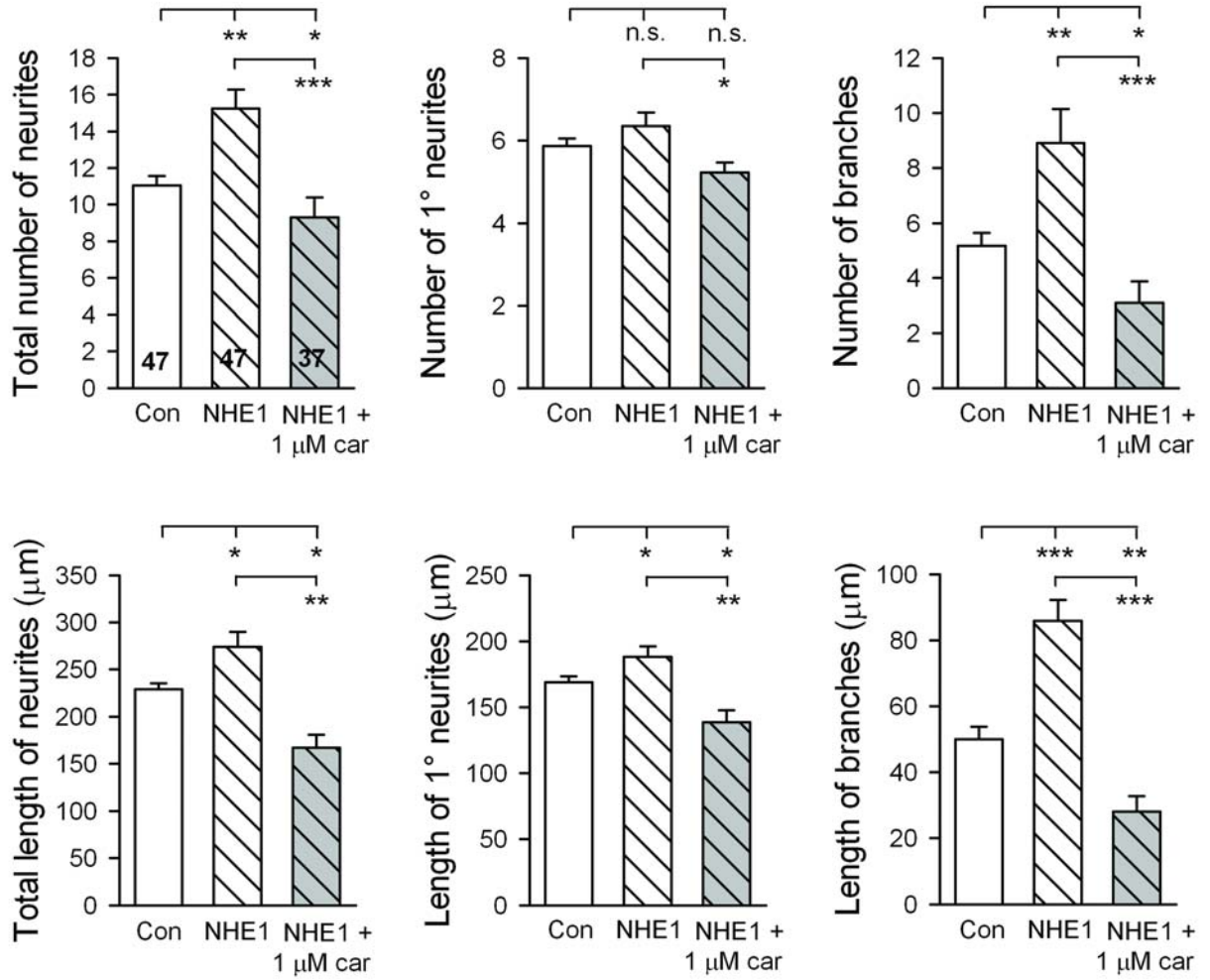


Figure 23. NHE1^{-/-} neurons do not express endogenous NHE1

(A) Expression of endogenous NHE1 in brain tissue from NHE1^{+/+} and NHE1^{-/-} mice, assessed by Western analysis with anti-NHE1 antibody. GAPDH was used as a loading control. (B) Expression of endogenous NHE1 in growth cones of NHE1^{+/+} and NHE1^{-/-} neocortical neurons. Neurons were fixed at 3 D.I.V. and co-labeled with monoclonal anti-NHE1 antibody and Alexa-Fluor-568 phalloidin to visualize the growth cone. Scale bar, 5 μ m.

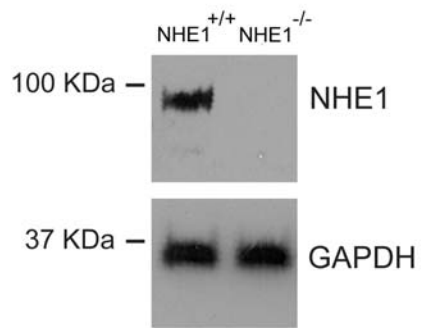
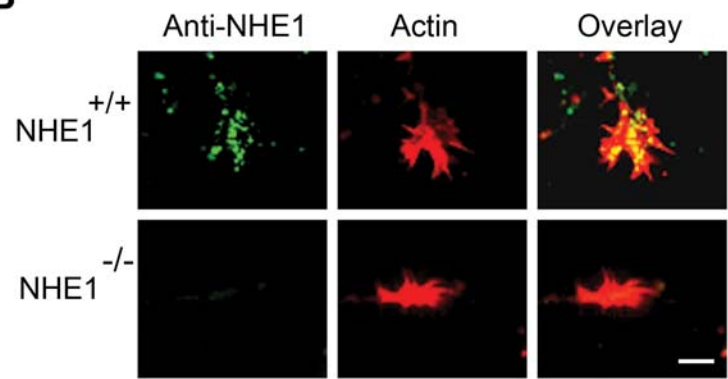
A**B**

Figure 24. NHE1^{+/-} neurons have intermediate neurite outgrowth and sensitivity to 1 μ M cariporide compared to NHE1^{+/+} and NHE1^{-/-} neurons

Compared to vehicle-treated (open bars) NHE1^{+/+} neurons, vehicle-treated neurons obtained from both NHE1^{+/-} and NHE1^{-/-} mice exhibited reductions in the number and/or lengths of both primary and branched neurites, with the most pronounced reductions seen in NHE1^{-/-} neurons. While application of 1 μ M cariporide (grey bars) reduced neurite outgrowth in NHE1^{+/+} neurons, only a limited effect on neurite outgrowth was seen in neurons from NHE1^{+/-} mice and no effect in neurons obtained from NHE1^{-/-} mice. Experiments were conducted in parallel, all measured values are per cell, error bars represent s.e.m. and *n* values are shown in the columns. *, *P* < 0.05; and n.s., not significant (*P* > 0.05) by Kruskal-Wallis one-way ANOVA on ranks followed by Dunn's method for pair-wise comparison.

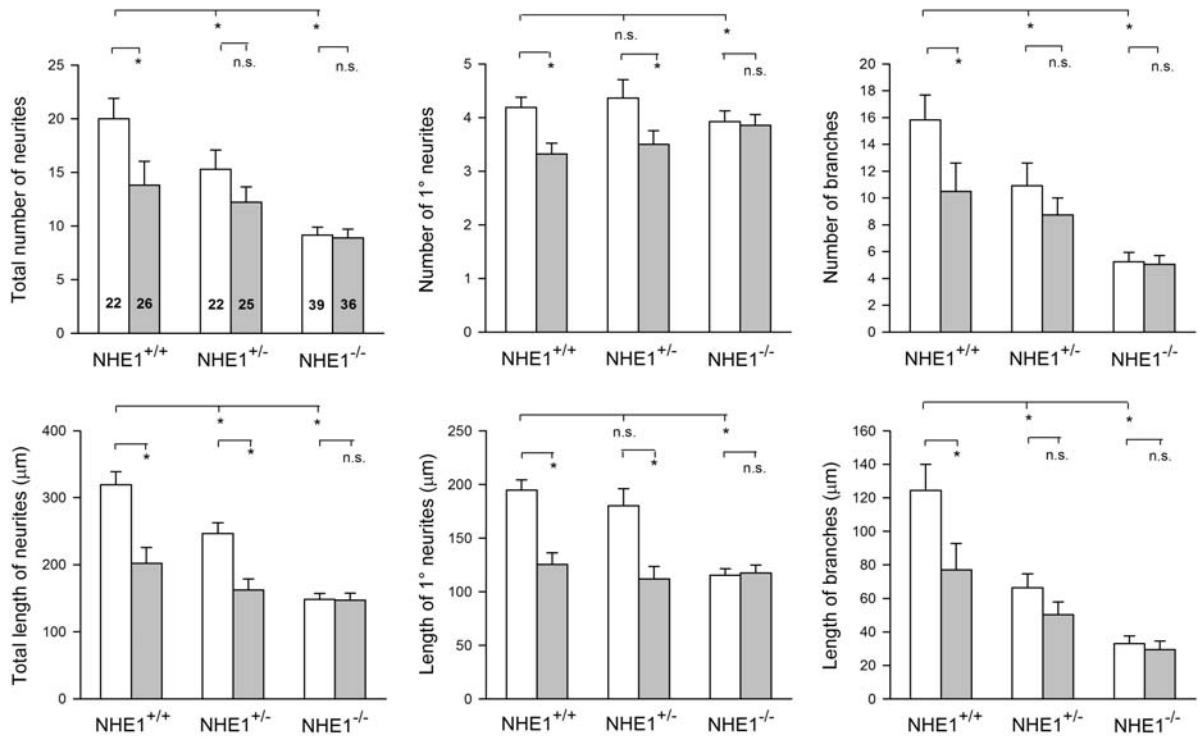


Figure 25. Quantification of neurite outgrowth in NHE1^{-/-} neurons transiently overexpressing full-length NHE1 or one of the NHE1 mutant constructs

Compared to untransfected NHE1^{-/-} neurons cultured in the absence of cariporide (Con; open bars), NHE1^{-/-} neurons overexpressing full-length NHE1 exhibited increases in the number and lengths of primary and branched neurites, which were sensitive to the application of 1 μ M cariporide (grey bars). In contrast NHE1^{-/-} neurons transfected with NHE1-E266I or NHE1-KR/A did not exhibit an increase in neurite growth compared to untransfected NHE1^{-/-} cells and had no further reduction in outgrowth in response to 1 μ M cariporide. Experiments were conducted in parallel, all measured values are per cell, error bars represent s.e.m. and *n* values are shown in the columns. *, $P < 0.05$; **, $P < 0.01$; ***, $P < 0.001$ and n.s., not significant ($P > 0.05$) by Kruskal-Wallis one-way ANOVA on ranks and then Dunn's method for pair-wise comparison.

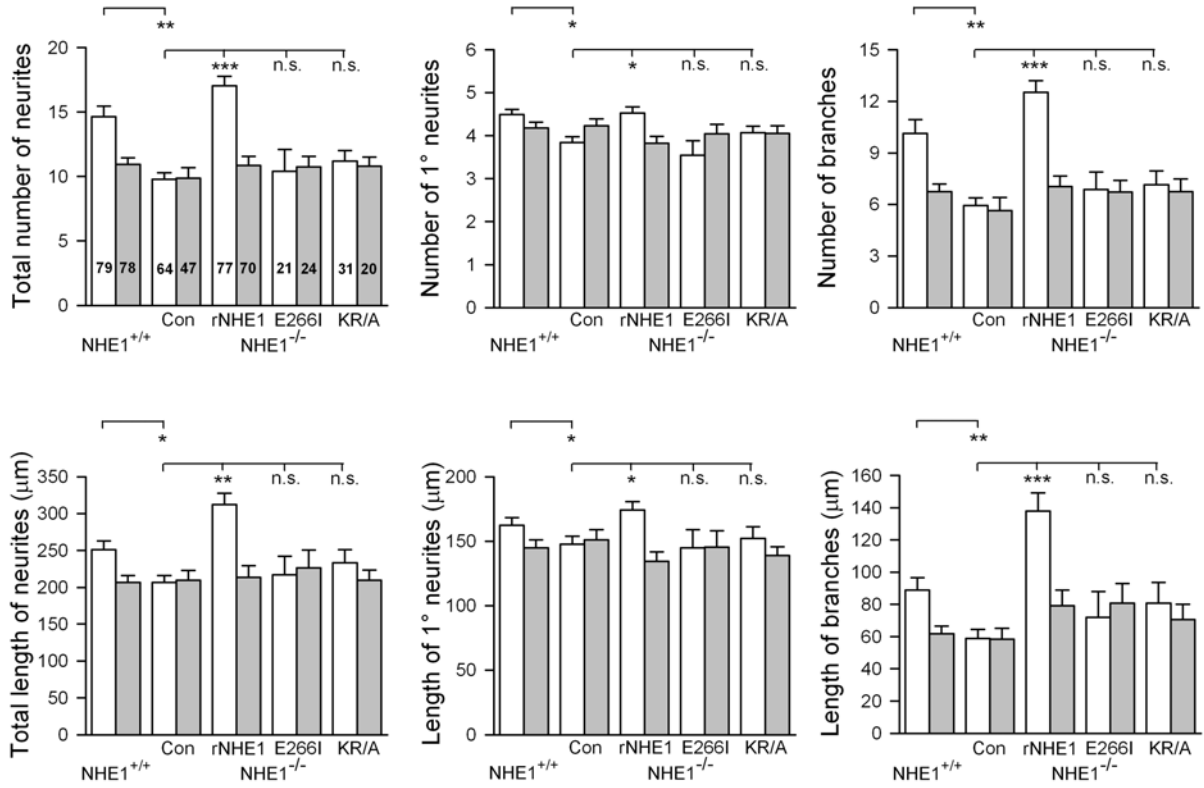


Figure 26. Reduced neurite outgrowth in NHE1^{-/-} neurons can be rescued by transient overexpression of WT NHE1 but not by overexpression of NHE1 mutant constructs

Representative examples of NHE1^{+/+} neurons, NHE1^{-/-} neurons and NHE1^{-/-} neurons transfected with full-length recombinant NHE1 (NHE1^{-/-} + rNHE1) or one of the NHE1 mutant constructs (NHE1-E266I or NHE1-KR/A), in the absence and presence of 1 μ M cariporide. NHE1^{-/-} neurons overexpressing full-length NHE1 display a visible enhancement of neurite outgrowth which is sensitive to the application of cariporide while NHE1^{-/-} neurons overexpressing either NHE1-E266I or NHE1-KR/A did not. Experiments were performed in parallel in neuronal cultures prepared from NHE1^{+/+} and NHE1^{-/-} littermates. Scale bar, 20 μ m.

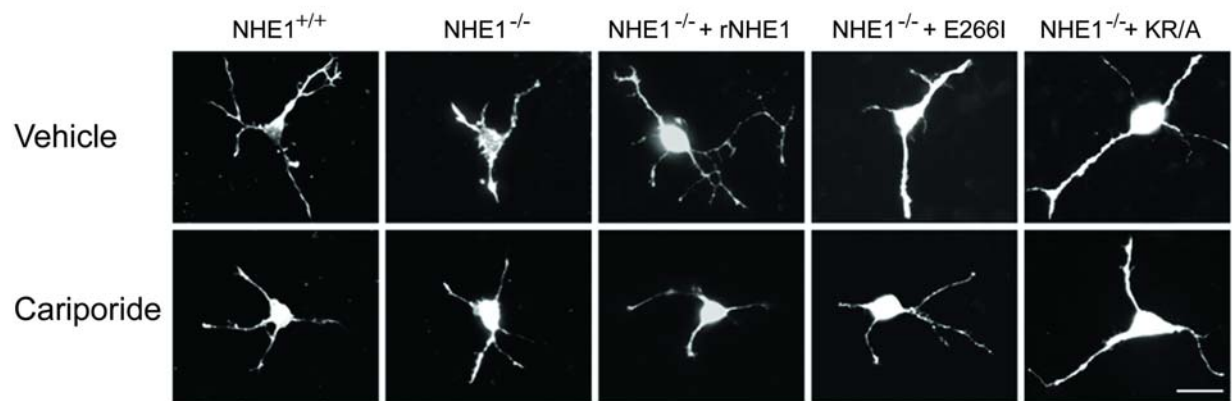


Figure 27. Quantification of the effect of 1 μ M cariporide on netrin-1, BDNF and IGF-1 enhanced neurite outgrowth in NHE1^{+/+} P0.5 mouse neocortical neurons

NHE1^{+/+} neurons treated with netrin-1 in the absence of cariporide (open bars) exhibited increases in the number and lengths of branched neurites. Application of 1 μ M cariporide (grey bars) to NHE1^{+/+} neurons treated with 200 ng mL⁻¹ netrin-1 reduced the average number and lengths of both the primary and branched neurites. In contrast, while NHE1^{+/+} neurons treated with 50 ng mL⁻¹ BDNF or 50 ng mL⁻¹ IGF-1 exhibited increased neurite outgrowth, treatment with 1 μ M cariporide caused only moderate (if any) reductions in neurite outgrowth in these cells. Experiments were conducted in parallel, all measured values are per cell, error bars represent s.e.m. and *n* values are shown in the columns. *, *P* < 0.05; **, *P* < 0.01 and n.s., not significant (*P* > 0.05) by Kruskal-Wallis one-way ANOVA on ranks and then Dunn's method for pair-wise comparison.

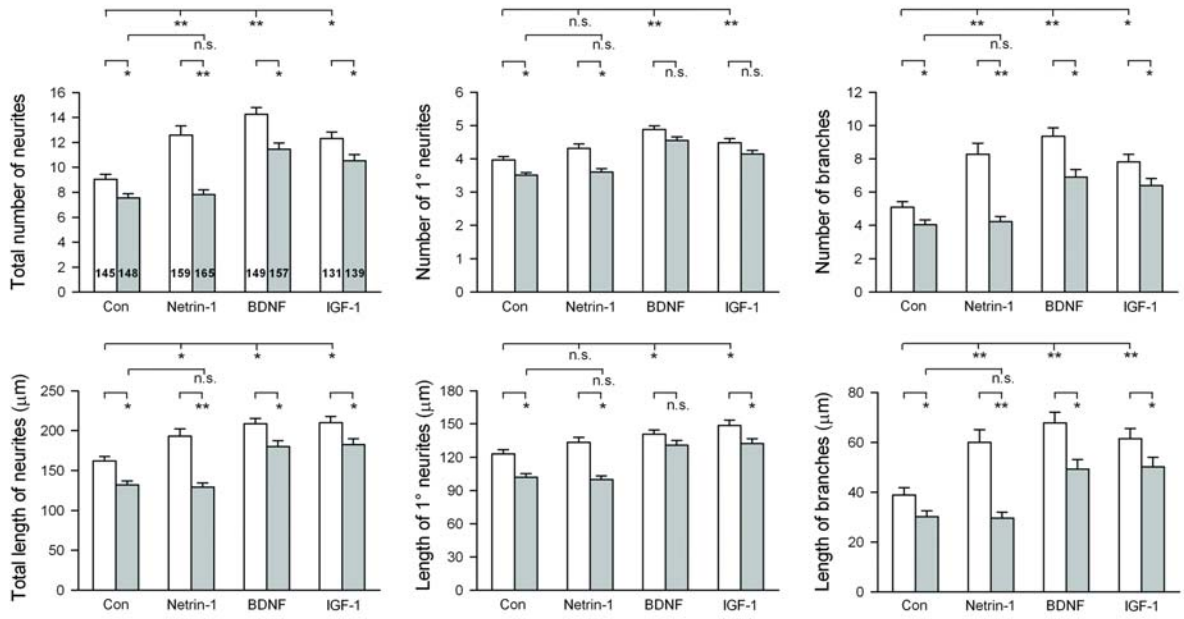


Figure 28. Effects of cariporide on increases in neurite outgrowth induced by netrin-1, BDNF and IGF-1 in NHE1^{+/+} P0.5 mouse neocortical neurons.

Compared to control (Con), NHE1^{+/+} neurons cultured in the presence of 200 ng mL⁻¹ netrin-1, 50 ng mL⁻¹ BDNF or 50 ng mL⁻¹ IGF-1 exhibited increases in neurite outgrowth. When cultured in the presence of 1 μM cariporide, only control neurons and neurons treated with netrin-1 exhibited reductions in neurite outgrowth while neurons treated with either BDNF or IGF-1 did not appear to be affected. Neurons were fixed at 3 D.I.V. and labeled with Alexa-Fluor-568 phalloidin. Scale bar, 20 μm.

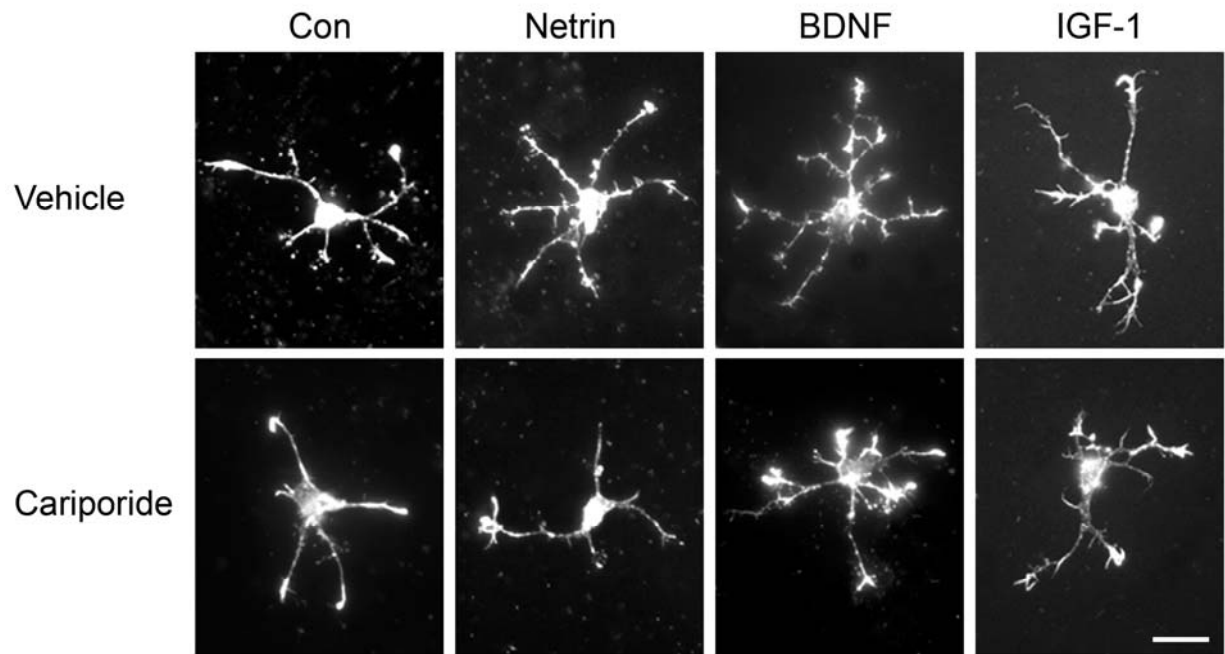


Figure 29. Quantification of neurite outgrowth in NHE1^{-/-} P0.5 mouse neocortical neurons treated with netrin-1, BDNF or IGF-1

NHE1^{-/-} neurons cultured in the presence of 200 ng mL⁻¹ netrin-1 failed to exhibit enhanced neurite outgrowth (open bars) and there was no further reduction in neurite outgrowth with application of cariporide (gray bars). In contrast, NHE1^{-/-} neurons treated with 50 ng mL⁻¹ BDNF or 50 ng mL⁻¹ IGF-1 both exhibited increases in neurite outgrowth which were insensitive to the application of 1 μM cariporide (grey bars). Experiments were conducted in parallel, all measured values are per cell, error bars represent s.e.m. and *n* values are shown in the columns. *, *P* < 0.05; **, *P* < 0.01 and n.s., not significant (*P* > 0.05) by Kruskal-Wallis one-way ANOVA on ranks and then Dunn's method for pair-wise comparison.

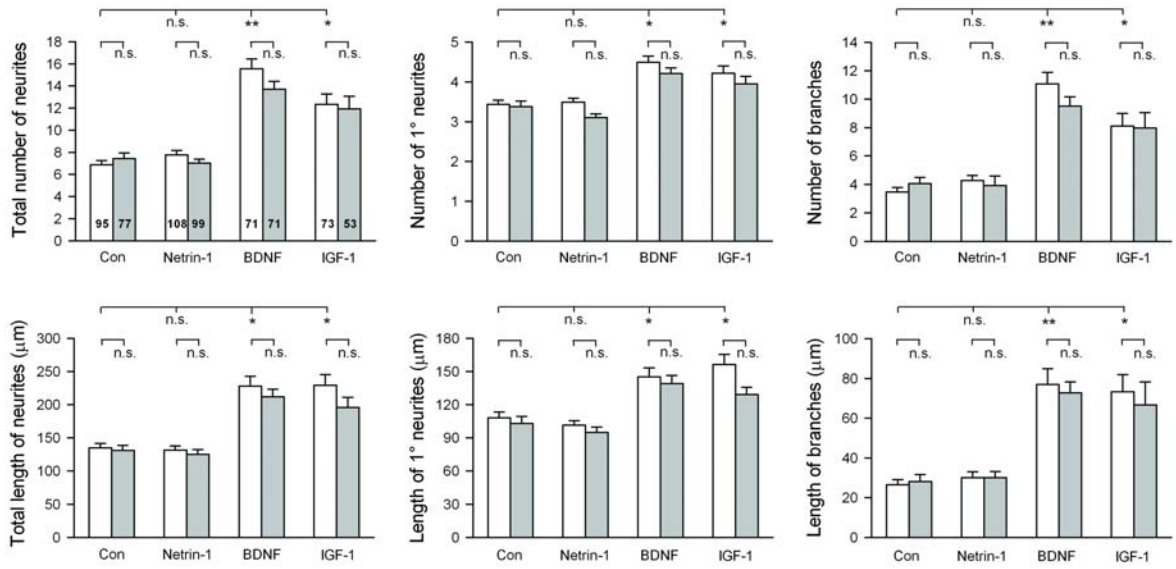
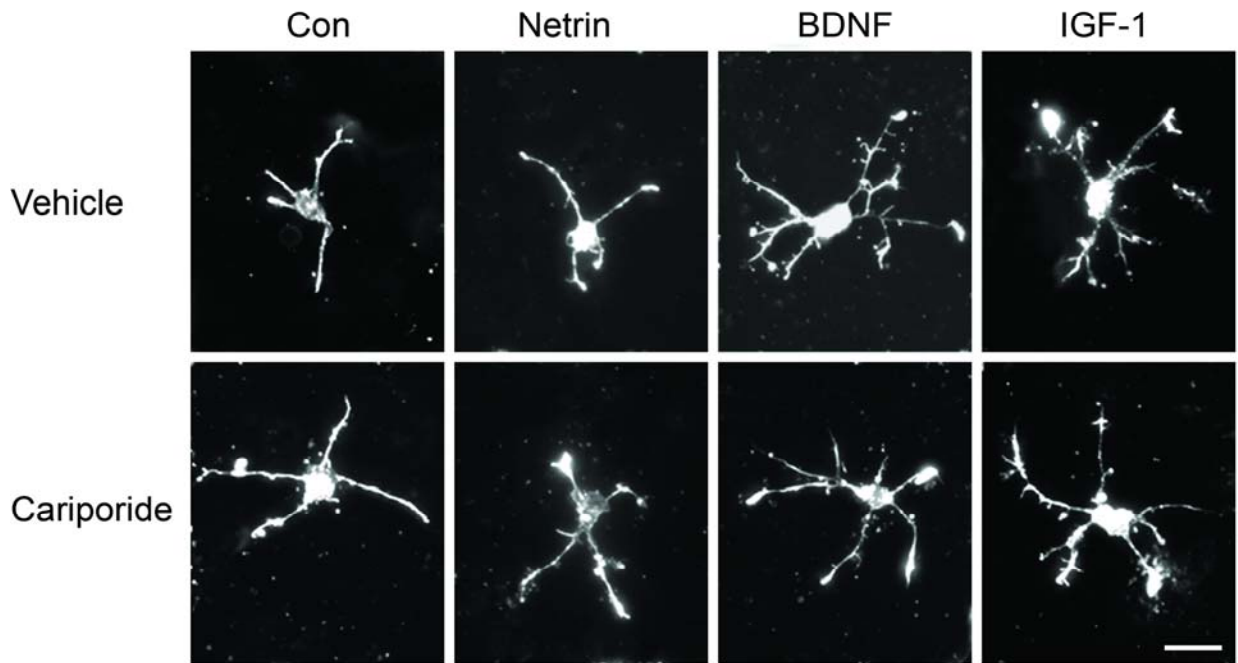


Figure 30. Netrin-1 fails to enhance neurite outgrowth in NHE1^{-/-} P0.5 mouse neocortical neurons

Compared to control NHE1^{-/-} neurons (Con), neurons cultured in the presence of 200 ng mL⁻¹ netrin-1 failed to exhibit increases in neurite outgrowth. In contrast, neurons cultured in the presence of 50 ng mL⁻¹ BDNF or 50 ng mL⁻¹ IGF-1 exhibited increases in neurite outgrowth. Application of 1 μM cariporide did not have any effect on neurite outgrowth under any of the treatments. Neurons were fixed at 3 D.I.V. and labeled with Alexa-Fluor-568 phalloidin. Scale bar, 20 μm.



4.0 Discussion

The results reported in this thesis indicate that NHE1 is an important modulator of early neurite outgrowth *in vitro*. NHE1 has previously been shown to play a permissive role in directed cell migration in fibroblasts [120, 121] as well as in tumor cell growth and metastasis [157], however, the involvement of NHE1 in neurite outgrowth had not previously been reported. The results presented in this thesis indicate that NHE1 is expressed within the growth cones of developing neurites and that the pH_i within the growth cone of an actively extending neurite is elevated compared to that found in non-extending neurites or at the cell body. Additionally, pharmacological inhibition of NHE1 results in a reduction in growth cone pH_i and neurite outgrowth in NGF-differentiated PC12 cells and a reduction in neurite outgrowth in WT neocortical neurons, an effect which was also observed in neocortical neurons isolated from NHE1^{-/-} mice. In accordance with previous studies in migrating fibroblasts [120, 121], both ion translocation activity as well as actin cytoskeleton anchoring by NHE1 are involved in the regulation of neurite outgrowth by NHE1.

The findings that neurite formation, growth and elaboration proceed, albeit to a reduced extent, in PC12 cells and WT mouse neocortical neurons treated with cariporide as well as in NHE1^{-/-} neurons suggest that NHE1 is playing a permissive rather than a deterministic role in regulating neurite outgrowth. In agreement with these observations, a recent report by Hayashi *et al.* [200] showed that, while NHE1 was required for maximally efficient cell migration in non-neuronal cells, it is not essential for the initiation of migration. Evidence for NHE1 playing a permissive rather than a deterministic role in regulating neurite outgrowth is also provided by the fact that NHE1^{-/-} mice, while exhibiting severe neurological disorders, do not display any gross neurodevelopmental abnormalities (see [134, 201]). Although NHE1 does not appear to be

essential for neurite morphogenesis a permissive role in modulating neurite outgrowth is not without potential consequence. As discussed in the Introduction, NHE1 activity is regulated by a number of environmental stimuli which signal through a variety of membrane receptors initiating diverse signal transduction cascades which converge on the C-terminal domain of NHE1 to regulate exchange activity. Several of the mechanisms which are important for regulating the activity of NHE1 are also important modulators of neurite outgrowth. It may therefore be that NHE1 is in a position to act as an integrator of diverse signaling pathways which together regulate neurite outgrowth.

In agreement with NHE1 playing a permissive rather than deterministic role in regulating neurite morphogenesis, NHE1 played only a modest role in neurite outgrowth stimulated by BDNF or IGF-1. While increases in neurite outgrowth were observed in NHE1^{+/+} neurons treated with either BDNF or IGF-1, concurrent application of cariporide resulted in only modest reductions. Additionally, NHE1^{-/-} neurons treated with either BDNF or IGF-1 exhibited increases in neurite outgrowth similar to those observed in NHE1^{+/+} neurons. In striking contrast, NHE1 appears to be an important regulator of netrin-1-stimulated neurite outgrowth. NHE1^{+/+} neurons treated with netrin-1 exhibited increases in neurite outgrowth which were abolished by cariporide and application of netrin-1 to NHE1^{-/-} neurons failed to promote neurite outgrowth and elaboration.

This discussion will focus on the role of NHE1 ion translocation activity in creating [ion]_i microdomains within the growth cone to promote neurite outgrowth and the potential role of the structural functions NHE1 in modulating neurite outgrowth. Additionally I will discuss the role of NHE1 in netrin-1-stimulated neurite outgrowth.

4.1 NHE1 ion translocation and neurite outgrowth

The translocation of ions via NHE1 was found to play an important role in modulating neurite outgrowth and elaboration. In NGF-differentiated PC12 cells transiently overexpressing a translocation dead NHE1-mutant construct (NHE1-E266I) neurite outgrowth was inhibited to a similar extent as in untransfected cells which had been treated with cariporide. In addition, in contrast to NHE1^{-/-} P0.5 neurons overexpressing full-length NHE1, NHE1^{-/-} neurons transiently overexpressing NHE1-E266I failed to exhibit the WT phenotype. Interestingly, the pH_i within the growth cones of actively extending neurites was elevated to that found at the cell body while the pH_i at the growth cones of non-extending neurites was not. Additionally, application of cariporide reversibly reduced growth cone pH_i and caused a reversible cessation of neurite outgrowth and a reversible loss of growth cone filopodia. A role for NHE1-dependent elevations in pH_i in mediating neurite outgrowth is also supported by the fact that pH_i (as well as neurite outgrowth; see Fig. 24) is greater in NHE1^{+/+} neurons when compared to NHE1^{-/-} neurons, with NHE1^{+/-} neurons exhibiting intermediate levels of both neurite outgrowth and NHE1-dependent H⁺ efflux (see Fig. 24 and [198, 202]). NHE1 ion translocation activity within the growth cone may serve to: a) create an [ion]_i microdomain within the growth cone to promote actin dynamics, b) create an acidified extracellular microenvironment to promote the strength of collagen-integrin interactions, and/or c) may function cooperatively with other ion transporters and/or channels to mediate salt and concomitant osmotic water uptake, leading to growth cone swelling and subsequent neurite outgrowth.

4.1.1 NHE1 may be creating an $[\text{ion}]_i$ microdomain within the growth cone to promote actin dynamics

NHE1-mediated proton efflux at the leading edge is known to be important for directed migration in non-neuronal cells. Although increases in pH_i have been difficult to measure in this region (see [203]), recent reports have indicated that pH_i is indeed elevated [204]. Similarly, in the present study I found (in agreement with an early report by Dickens *et al.* [205]) that the pH_i is elevated in growth cones of actively extending neurites but not in the growth cones of stalled neurites. The relative ease with which I was able to measure an elevated pH_i at the growth cones of actively extending neurites could be a result of the restricted geometry of a growth cone combined with the high expression of NHE1 observed within this region. Growth cones have a relatively large surface area to volume ratio which could facilitate the creation of a pH_i microdomain that may not be easily discernable at the leading edge of migrating fibroblasts. The restricted geometry at the growth cone combined with the relatively slow diffusion rate of protons in the cytosol (e.g. see [206, 207]) could allow for the formation of a restricted $[\text{ion}]_i$ microdomain within this region.

An elevated pH_i at the growth cone of actively extending neurites could serve to create an appropriate environment for the activity of actin regulatory proteins to promote actin cytoskeletal dynamics to drive neurite outgrowth. Elevations in pH_i are known to directly increase actin polymerization (see [208]) as well as promote the activities of actin regulatory proteins (e.g. ADF/cofilin and Cdc42; see [209]). A number of reports have indicated that the activation and translocation of ADF/cofilin to the leading edge membrane in migrating fibroblasts is dependent on an elevated pH_i within this region [161, 209-211]. As discussed in the Introduction, activated ADF/cofilin depolymerize F-actin, thus freeing actin monomers for subsequent polymerization

at the leading edge by the Arp2/3 complex (see also [105, 212]). Ion translocation via NHE1 could generate the necessary pH_i microenvironment within the growth cones of neurites to maintain the activation of ADF/cofilin to drive neurite outgrowth. Interestingly, it has recently been reported that the activation of Cdc42 at the leading edge of migrating fibroblasts is dependent on H^+ efflux through NHE1 [213]. Activated Cdc42 signals to its effector, N-WASP, which subsequently activates the Arp2/3 complex promoting actin monomer nucleation and subsequent actin polymerization. It is therefore conceivable that NHE1 could stimulate neurite outgrowth by promoting an elevated pH_i microenvironment to promote the activities of ADF/cofilin and Cdc42 within the growth cone.

In addition to actin filament dynamics, pH_i has also been suggested to play an important role in FA turnover at the leading edge of migrating fibroblasts [119, 120]. Focal adhesion dynamics are integral to directed migration in fibroblasts, with assembly being required at the leading edge to generate traction and disassembly being required at the trailing edge for cell movement. Focal adhesion dynamics are controlled, in part, by the FA-associated protein talin, which binds integrins and F-actin thereby anchoring the actin cytoskeleton to integrin adhesion complexes [209]. Disruptions in the association of talin with F-actin or integrins have been shown to disrupt the formation of FAs as well as disrupting cell spreading, indicating that talin is an important regulator of FA dynamics [214, 215]. Interestingly, it has recently been shown that talin functions as a sensitive pH sensor for FA assembly [209]. Under conditions of reduced pH_i , talin has a decreased affinity for F-actin binding which disrupts the localization of F-actin to the integrin complexes thereby disrupting FA assembly [209]. Talin has also been found expressed in growth cone filopodia where its expression and function has been shown to be important for filopodial motility and axon growth and guidance [216-218]. NHE1 ion

translocation could therefore be raising the pH_i to facilitate the binding of talin to F-actin and subsequently modulate FA remodeling at the growth cone to promote the traction required for outgrowth.

Ion translocation via NHE1 may also be inducing elevations in intracellular calcium within the growth cone, which, as described in the Introduction, is a key regulator of neurite outgrowth and elaboration. Changes in both pH_i and pH_o elicit changes in intracellular calcium concentration by mobilizing intracellular calcium stores as well as by modulating calcium influx via voltage-gated calcium channels within the plasma membrane (e.g. see [205, 219, 220]) For example, Dickens *et al.* [205] showed that increasing pH_i at the tips of neurites resulted in a concomitant increase in calcium within the same region, likely as a result of the mobilization of intracellular calcium stores [205]. Additionally, a recent report by Huang *et al.* [220] showed that extracellular acidification elevated intracellular calcium levels in a human medulloblastoma cell line by activating PLC which led to the activation of IP3 receptors and the subsequent mobilization of calcium from intracellular stores. They also reported that a decreased pH_o could result in the activation of plasma membrane calcium channels to generate inward calcium currents [220]. Calcium, acting via CaM, is known to activate NHE1 in some cell types [145-147] suggesting that there may exist a positive feedback loop between these two systems to cooperatively stimulate neurite outgrowth.

4.1.2 NHE1 may create an acidified extracellular microenvironment to promote the strength of collagen-integrin bonds

There have been a number of reports which have suggested that tumor cell growth and subsequent metastasis require the generation of an acidified extracellular microenvironment

contributed in part by the ion translocation activity of NHE1 (see [160, 221] and references therein). The precise role of an acidified extracellular microenvironment in promoting cell migration is complicated by the fact that decreased pH_o serves to increase the activities of a variety of proteases known to digest the ECM while also increasing the strength of collagen-integrin interactions [160, 221]. Stock *et al.* [221] recently suggested that the extracellular acidification around tumor cells initially aids in the digestion of the ECM to create attachment sites for adhesion receptors while also releasing latent ECM-associated growth and motility factors. Increased ECM digestion ultimately leads to a mesenchymal to amoeboid transition which activates the growth and motility factors and promotes the invasiveness of the cells [221]. NHE1 was shown to be a key mediator for the generation of the acidified extracellular microenvironment and inhibition of NHE1 activity resulted in a reduction in tumor growth and invasiveness [157-160]. By similar mechanisms, NHE1 activity may be creating an acidified extracellular microenvironment for adhesion turnover at the growth cone to ultimately promote neurite outgrowth.

4.1.3 NHE1 may be functioning cooperatively with other ion transporters and/or channels to mediate localized growth cone swelling

It has been suggested that ion transporters, including NHE1, regulate directed cell migration in non-neuronal cell types by regulating osmolyte fluxes with a concomitant osmotic water uptake leading to localized swelling and protrusion of the leading edge membrane [162, 163, 222, 223]. A number of ion transporters (including NHE1, Na^+ -independent $\text{Cl}^-/\text{HCO}_3^-$ exchangers (AE), Na^+ -dependent $\text{Cl}^-/\text{HCO}_3^-$ exchangers (NDCBE), Na^+ - HCO_3^- cotransporters (NBC), K^+/Cl^- cotransporters (KCC) and/or $\text{Na}^+/\text{K}^+/2\text{Cl}^-$ cotransporters (NKCC)) have been proposed to work

in parallel to induce these ion fluxes with the subsequent water uptake into the cell largely regulated by aquaporins [162, 163]. Mechanical stress caused by membrane swelling could activate small Rho-family GTPases [224-226], with subsequent effects on actin cytoskeleton dynamics, or it could result in an increase in cytosolic calcium levels via activation of mechano-sensitive transient receptor potential (TRP) channels thereby promoting cell migration (see [227, 228] for reviews). As all of the experiments reported in this thesis were conducted under physiological (i.e. $\text{HCO}_3^-/\text{CO}_2$ buffered) conditions so as to not skew the results in favor of NHE1, a role for HCO_3^- -dependent pH_i regulatory mechanisms in modulating neurite outgrowth cannot be excluded. The potential involvement of HCO_3^- transporters is, however, tempered by the fact that there is currently no evidence for their expression in neuronal growth cones. However, it has recently been shown that NKCC1 and KCC2 are involved in neurite morphogenesis suggesting that mechanisms involved in neurite outgrowth may be similar to those involved in directed cell migration in non-neuronal cells [229-231]. Indeed, Nakajima *et al.* [229] found that NKCC1 promoted NGF-induced neurite outgrowth, but not neurite formation, in PC12D cells while Pieraut *et al.* [230] showed that NKCC1 modulated peripheral nerve regeneration, an effect which was dependent on NKCC1-mediated $[\text{Cl}^-]_i$ increases and concomitant osmotic swelling at the growth cone. Additionally, Li *et al.* [231] showed that KCC2 promoted dendritic spine morphogenesis, an effect that was dependent on interactions of the transport mechanism with protein 4.1 (which tethers the actin cytoskeleton to integral membrane proteins; see section 1.3.3.1.1 of the Introduction) but independent of transporter activity. It could be that NHE1, signaling cooperatively with these additional transporters within the growth cone, could be mediating localized swelling leading to neurite outgrowth.

4.2 Potential involvement of the structural functions of NHE1 in regulating neurite outgrowth

Actin anchoring to NHE1 was shown to be required for neurite outgrowth in NGF-differentiated PC12 cells as well as in mouse neocortical neurons in primary culture. Transient overexpression of mutant NHE1 constructs which lacked the ability to bind ERM proteins (NHE1-KR/A and NHE1- Δ 556-564) and subsequently anchor the actin cytoskeleton resulted in a reduction of neurite outgrowth in PC12 cells. Additionally, while the transient overexpression of full-length NHE1 in NHE1^{-/-} P0.5 neocortical neurons rescued neurite outgrowth, the transient overexpression of NHE1-KR/A failed to restore the WT phenotype. These results suggest that NHE1 modulation of neurite outgrowth, in accordance with studies in migrating fibroblasts [120, 121], requires anchoring of the actin cytoskeleton to NHE1.

As discussed in the Introduction, NHE1 binds to ERM proteins at the leading edge of migrating fibroblasts and this interaction is essential for directed cell migration in these cells. The recruitment of ERM proteins to the actin cytoskeleton by NHE1 (see [232]) may similarly anchor actin filaments to the growth cone plasma membrane to promote neurite outgrowth. Indeed, Paglini *et al.* [233] showed that suppression of radixin and moesin expression reduced neurite outgrowth and elaboration in hippocampal neurons, indicating the importance of anchoring the actin cytoskeleton within the growth cone. It may be that anchoring of NHE1 to the actin cytoskeleton is required to localize the exchanger within the growth cone where it may contribute to localized pH_i changes to affect the activities of actin regulatory proteins and subsequently actin filament dynamics (see [125, 130]). In NHE1-deficient PS120 cells stably expressing full-length NHE1 or NHE1 mutants, exogenous full-length NHE1 accumulated at the leading edge to promote leading edge membrane protrusion and directional migration [120, 121].

In contrast, NHE1-KR/A mislocalized away from the leading edge, resulting in an impairment of motility [120, 121]. In the present study, I was unable to determine if there was any reduction in NHE1-KR/A or NHE1- Δ 556-564 expression at the growth cone as transient transfection caused their overexpression throughout the cell (unpublished observations).

In migrating fibroblasts, the structural functions of NHE1 also serve to localize F-actin with associated signaling molecules at the leading edge plasma membrane [119, 125, 130]. Importantly, NHE1 binds PIP2 and NIK which are key regulators of actin filament dynamics necessary for both directed cell migration in fibroblasts and neurite outgrowth ([119, 125, 130, 141, 234, 235]; see Fig. 3). Interestingly, Poinat *et al.* [234] showed that in *C. elegans* NIK interactions with integrins were required for proper growth and pathfinding of commissural neurons suggesting that this kinase may be an important modulator of neurite outgrowth. Additionally, Shirai *et al.* [235] found that PKC-induced neurite induction was dependent on PIP2-PKC interactions in neuroblastoma cell lines. This evidence that both NIK and PIP2 appear to be involved in neurite outgrowth combined with evidence that both of these proteins interact with NHE1 suggests that they might be playing a role in NHE1-mediated neurite morphogenesis.

Both NIK and PIP2 aid in the activation of ERM proteins and are therefore important regulators of F-actin anchoring at the leading edge of migrating cells [119, 130, 236, 237]. It has been shown that NIK directly phosphorylates and therefore activates ERM proteins while PIP2 is required for maintaining the proteins in their active conformation [119, 130, 236, 237]. Interestingly, NIK has also been shown to bind, phosphorylate and subsequently activate NHE1 at the leading edge of migrating fibroblasts [128, 140, 141] and it has also been shown that

disruption of NHE1-PIP2 interactions results in an inhibition of NHE1 activity [148] which suggests that there are likely links between NHE1 activation and actin cytoskeletal dynamics.

NIK and PIP2 are known to activate the Arp2/3 complex leading to actin monomer nucleation and subsequent actin filament polymerization [156, 238]. A report by Rohatgi *et al* [156] showed that NIK binds to Nck1 which subsequently activates N-WASP leading to the activation of the Arp2/3 complex, and actin monomer nucleation. NIK was found to work cooperatively with PIP2 to mediate this activation of Arp2/3 [156]. The facts that NHE1 is expressed in the growth cone and that the loss of the ability of NHE1 to anchor the actin cytoskeleton leads to the inhibition of neurite outgrowth suggests that an association of actin filaments and actin regulatory proteins with NHE1 may be required for the promotion of outgrowth. It may be that NHE1 is playing a role in localizing the actin cytoskeleton with necessary actin regulatory proteins within the growth cone to mediate the actin dynamics which are required for neurite outgrowth.

4.3 NHE1 modulates netrin-1- but not BDNF- or IGF-1-enhanced neurite outgrowth

Netrin-1, BDNF and IGF-1 all resulted in enhanced neurite outgrowth when applied to WT mouse neocortical neurons, however, neurons treated with BDNF or IGF-1 exhibited only modest reductions in neurite outgrowth when also treated with cariporide. In contrast, netrin-1-stimulated outgrowth was completely attenuated by cariporide. Additionally, neurons obtained from NHE1^{-/-} mice did not exhibit an enhancement of neurite outgrowth when treated with netrin-1, however both BDNF and IGF-1 increased neurite outgrowth in these neurons. These results indicate that NHE1 is an important regulator of netrin-1 but not BDNF or IGF-1 stimulated neurite outgrowth. Although the basis of the differential role of NHE1 in netrin-1 vs.

BDNF or IGF-1 stimulated neurite outgrowth remains unknown, the results are consistent with the possibility that NHE1 may be an upstream regulator of the signaling cascades that are especially involved in the promotion of neurite morphogenesis by netrin-1.

There are a number of potential mechanisms by which NHE1 could modulate netrin-1-stimulated neurite outgrowth. Preliminary experiments suggest that DCC is expressed in close proximity to NHE1 in the growth cones of NHE1^{+/+} mouse neocortical neurons and that treatment with a DCC function blocking antibody (see [59]) abolishes netrin-1-stimulated cariporide-sensitive neurite outgrowth in these cells (Figs. 31 and 32). Upon netrin-1 binding to DCC a variety of signaling molecules are recruited to the plasma membrane and form a signaling complex with DCC within the growth cone [39, 64-70]. Of note is that DCC has been shown to interact with Nck1, N-WASP, Cdc42, Rac1 and PAK which all have established roles in actin cytoskeletal dynamics involved in neurite outgrowth [70]. As noted above, NHE1 interacts with NIK which leads to the Nck1-dependent activation of N-WASP and thereby promotes actin dynamics through the action of the Arp2/3 complex. Therefore it may be that NHE1 and DCC are working cooperatively to form a signaling complex within the growth cone to promote actin cytoskeletal dynamics necessary for neurite outgrowth.

There is also evidence that, in addition to providing a scaffold for signaling complexes, netrin-1/DCC interactions are important regulators of the activation states of the small Rho-family GTPases. Elevations in the activities of Cdc42 and Rac1 in response to netrin-1 binding to DCC elicit increases in growth cone filopodia, neurite branching and neurite elongation [39, 64-70]. In this regard, the recent finding that H⁺ efflux via NHE1 is required for Cdc42 activation in migrating fibroblasts (see section 1.1 above) provides a plausible explanation for the finding that NHE1 is required for netrin-1-stimulated neurite outgrowth. In addition, there is

also evidence that RhoA activity is decreased in response to netrin-1/DCC interactions and this decreased activity is required for netrin-1-induced DCC plasma membrane trafficking as well as netrin-1-stimulated neurite outgrowth [67, 109]. Interestingly, preliminary experiments have shown that NHE1 appears to signal upstream of RhoA to inhibit its activation (unpublished observations). Indeed NHE1 overexpression failed to rescue reductions in neurite outgrowth in response to lysophosphatidic acid (LPA; unpublished observations) which activates RhoA and leads to neurite retraction (see [239]). Additionally, promotion of neurite outgrowth induced by the ROCK inhibitor Y-27632 was not sensitive to cariporide suggesting that NHE1 acts upstream of RhoA to affect its activation state (unpublished observations). Taken together, these findings suggest that NHE1 may be acting as an upstream regulator of the activation states of Rho-family GTPases to modulate netrin-1-stimulated neurite outgrowth.

As discussed in section 1.1 above, elevations in pH_i mediated by NHE1 have been shown to lead to rises in intracellular calcium and changes in intracellular calcium have been shown to be important regulators of netrin-1-stimulated neurite outgrowth as well as netrin-1-mediated axonal guidance [71, 73, 74]. In a report by Tang and Kalil [73], increases in axonal branching in response to treatment of cortical neurons with netrin-1 coincided with increases in calcium transients through the mobilization of intracellular calcium stores; inhibition of IP3 receptors to inhibit this release led to a complete attenuation of axonal branching in response to netrin-1. In this regard, the role of NHE1 in regulating netrin-1-stimulated neurite outgrowth could involve the activation of IP3 receptors within the growth cone to elicit the necessary mobilization of calcium from intracellular stores (see section 1.1 above).

Additionally, although the precise role that cAMP/PKA plays in netrin-1-stimulated neurite outgrowth is controversial, there have been reports that netrin-1 leads to an increase in

cAMP/PKA signaling in some cell types [77-79]. Indeed, in preliminary experiments I have found that treatment of WT E16 mouse neocortical neurons with netrin-1 increases cAMP levels suggesting that cAMP may be involved in netrin-1-stimulated neurite outgrowth in my system (unpublished observations). Interestingly a rise in PKA activity has been linked to increased trafficking of DCC to the plasma membrane where, as discussed above, it could form a signaling complex with NHE1 and thereby stimulate neurite outgrowth. Interestingly, ion translocation via NHE1 has been shown to elevate cAMP levels by increasing the activities of the calcium/CaM-stimulatable transmembrane adenylyl cyclases (tmACs) AC1 and AC8, which are found in growth cones [240-242]. Elevations in calcium elicited by the elevations in pH_i mediated by NHE1 (see section 1.1 above) could indirectly lead to an increase in the activation of the tmACs thereby leading to an increase in the levels of cAMP necessary for netrin-1-stimulated neurite outgrowth. In addition, the catalytic activities of these tmACs have also been shown to be regulated directly by physiological changes in pH and the reduction of ~0.3 pH units evoked by cariporide in actively growing neurites (see Fig. 14) results in approximately a 3-fold decrease in the activity of AC8 while also dramatically decreasing its sensitivity to calcium [241, 243]. Therefore, it is possible that ion translocation via NHE1 could regulate netrin-1-stimulated neurite outgrowth by promoting elevations in growth cone cAMP. Interestingly, a report by Wu *et al.* [79] indicated that netrin-1-stimulated neurite outgrowth required elevations in cAMP mediated by a soluble adenylyl cyclase (sAC) which itself is regulated not only by intracellular calcium but also intracellular HCO₃⁻ [244, 245]. It has also been reported that this HCO₃⁻-dependence of sAC activity in mammalian spermatozoa is regulated by a sperm-specific Na⁺/H⁺ exchanger (sNHE; [246]) which could provide another potential explanation for the role which NHE1 is playing in modulating netrin-1-stimulated neurite outgrowth.

Finally, netrin-1-stimulated neurite outgrowth has been shown to rely on FA remodeling and dynamics and a number of reports have linked the activation of focal adhesion kinase (FAK) with netrin-1 binding to DCC, with this activation being required for netrin-1-stimulated neurite outgrowth [247-249]. Additionally, a report by Ren *et al.* [247] showed that FAK and DCC appear to be colocalizing within growth cones suggesting that FAK is potentially involved in a signaling complex with DCC. Although NHE1 is not structurally associated with adhesion complexes it has been shown that NHE1 ion translocation is required for the proper assembly of FAs at the leading edge of migrating fibroblasts (see section 1.1 above and also [119]). Therefore it is possible that NHE1 may be regulating netrin-1-stimulated neurite outgrowth by promoting FA remodeling within the growth cone.

4.4 Future directions

The results presented in this thesis provide strong evidence that NHE1 is involved in early neurite morphogenesis *in vitro*, an effect which requires both the ion translocating as well as the actin cytoskeletal anchoring functions of the transporter. Ion translocation via NHE1 may be creating discrete $[ion]_i$ microdomains within the growth cone which may promote the activation of actin regulatory proteins necessary for neurite outgrowth. Elevations in pH_i have previously been shown to increase the activation states of ADF/cofilin as well as Cdc42 in migrating fibroblasts, however to date there is no evidence if this is the case for neurite outgrowth. Therefore it would be interesting to see if ADF/cofilin as well as Cdc42 activation is affected by cariporide treatment or in NHE1^{-/-} neurons. Additionally, there is evidence that elevations in pH_i lead to elevations in intracellular calcium in a variety of cell types, including neurons, and it

would be interesting to see if there is an elevation in calcium coinciding with the rise in pH_i in actively extending neurites and if that rise in calcium is sensitive to cariporide.

As discussed in section 1.3 above, all of the experiments outlined in this thesis were carried out under physiological (i.e. $\text{HCO}_3^-/\text{CO}_2$ buffered) conditions which opens the possibility that HCO_3^- transporters may also be involved in the modulation of neurite outgrowth. Three of the main families HCO_3^- transporters in the brain which may be involved are the AE family, the NDCBE family and the NBC family. Interestingly, Xue *et al.* [176] showed that in neurons obtained from $\text{NHE1}^{-/-}$ mice, expression of the acid-loading $\text{Cl}^-/\text{HCO}_3^-$ exchanger AE3 was decreased, suggesting a compensatory mechanism in these cells to mitigate against the loss of acid extrusion via NHE1. In terms of neurite outgrowth this could mean that, by reducing AE3 expression, the cells are better able to maintain the elevated pH_i microdomain within the growth cone to promote actin remodeling in the absence of NHE1 expression. Additionally, it has been found that the AE isoform found in epithelial cells (AE2) localizes to the leading edge of MDCK-F cells where its activity is required for directed cell migration [250]. Although the expression levels of NBCs and NDCBEs in $\text{NHE1}^{-/-}$ neurons remain to be determined there is some evidence that NBC expression and activity is increased in NHE1-depleted MDCK-F cells and that inhibiting NBC activity in these cells leads to a reduction in directed cell migration [222, 223]. It will be interesting to investigate whether the expression and/or activities of these transporters is modified in $\text{NHE1}^{-/-}$ neurons and also if they are playing a role in regulating neurite outgrowth.

The involvement of NHE1 in regulating netrin-1-stimulated neurite outgrowth is still poorly understood. As discussed in section 3.0 above there a number of speculative possibilities for the role of NHE1 in netrin-1-stimulated neurite outgrowth and each of the possibilities

warrant further study. Preliminary experiments have already suggested that NHE1 and DCC are expressed in close proximity in the growth cones of WT E16 mouse neocortical neurons under basal conditions. It would be interesting to see if there is any disruption of DCC expression in growth cones in response to cariporide or conversely if there is an increase in the association of NHE1 and DCC following treatment with netrin-1. In addition, there is a possibility that netrin-1 may be increasing NHE1 activation and it would be interesting to investigate whether there is an increase in growth cone pH_i in response to netrin-1. Also there is evidence that netrin-1-stimulated neurite outgrowth is dependent on rises in intracellular calcium which may be promoted by NHE1-dependent rises in pH_i . Therefore, it would be interesting to examine whether netrin-1-induced increases in growth cone calcium concentrations are sensitive to the application of cariporide.

The activities of the small Rho-family GTPases are modulated by netrin-1 and there is recent evidence to suggest that NHE1 may be an important upstream regulator of this activation. Therefore, the role of NHE1 in activating Cdc42 and Rac1 and downregulating RhoA following netrin-1 needs to be examined further. To this end we are currently conducting experiments utilizing fluorescence resonance energy transfer (FRET) microscopy to determine if there is any modulation of the activation states of the Rho GTPases in response to cariporide and/or netrin-1. Finally, increases in cAMP appear to be important in netrin-1-stimulated neurite outgrowth in some cell types and it would be interesting to examine if these rises in cAMP are sensitive to the application of cariporide.

Figure 31. DCC and NHE1 are expressed in close proximity in the growth cones of WT E16 mouse neocortical neurons

WT E16 neocortical neurons were grown for 72 h prior to being fixed and probed with a monoclonal anti-NHE1 antibody (BD Bioscience; red) and a polyclonal anti-DCC antibody (Santa Cruz Biotechnology Inc.; green). White arrowheads indicate areas of association of NHE1 with DCC. Confocal images; bar, 2 μm .

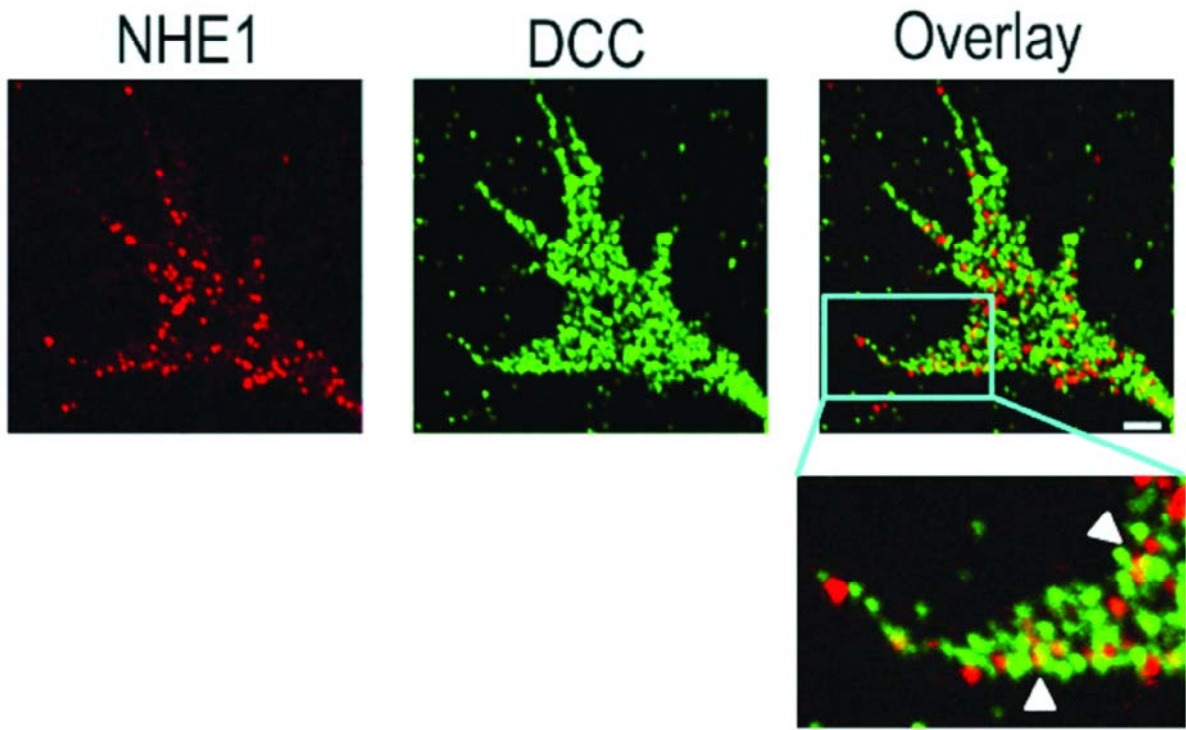
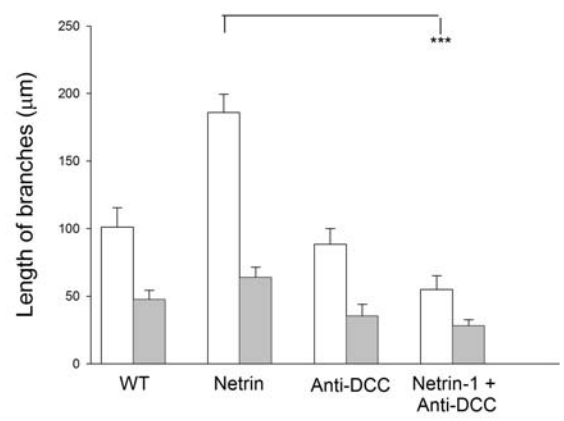
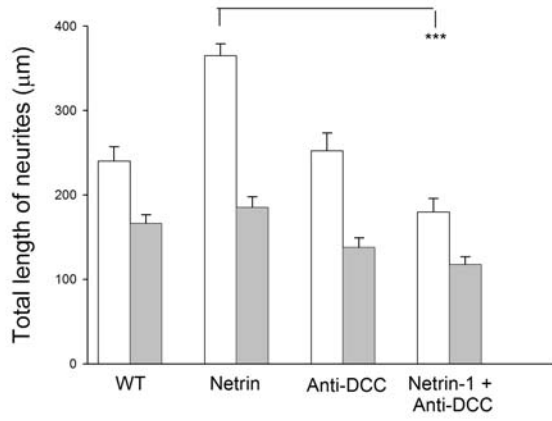
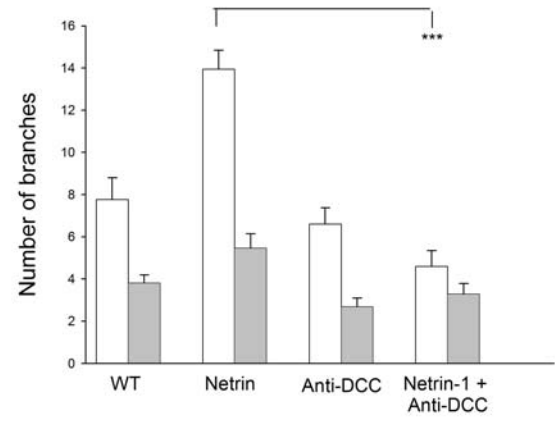
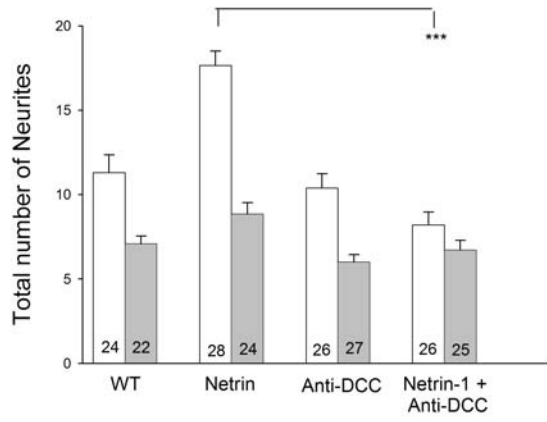


Figure 32. DCC is required for netrin-1-stimulated neurite outgrowth in WT E16 mouse neocortical neurons

Netrin-1 binding to DCC is required for netrin-1-induced cariporide-sensitive neurite outgrowth in E16 WT mouse neocortical neurons (grey bars, cariporide 1 μM). Functional DCC blocking antibody (clone AF5, 10 $\mu\text{g mL}^{-1}$; see [59]) was applied 1 h before the addition of netrin-1. Addition of species-matched immunoglobulin served as a control (not shown). Experiments were conducted in parallel, all measured values are per cell, error bars represent s.e.m. and n values are shown in the columns. ***, $P < 0.001$ by Students t -test



5.0 References

1. da Silva, J, and Dotti, CG, Breaking the neuronal sphere: regulation of the actin cytoskeleton in neuritogenesis. *Nat Rev Neurosci*, 2002. 3: p. 694-704.
2. Luo, L, Actin cytoskeleton regulation in neuronal morphogenesis and structural plasticity. *Annu Rev Cell Dev Biol*, 2002. 18: p. 601-35.
3. Baker, M, and Macagno, ER, In vivo imaging of growth cone and filopodial dynamics: evidence for contact-mediated retraction of filopodia leading to the tiling of sibling processes. *J Comp Neurol*, 2007. 500: p. 850-62.
4. Dent, E, and Gertler, FB, Cytoskeletal dynamics and transport in growth cone motility and axon guidance. *Neuron*, 2003. 40: p. 209-27.
5. Ellis, L, Wallis, I, Abreu, E, and Pfenninger, KH, Nerve growth cones isolated from fetal rat brain. IV. Preparation of a membrane subfraction and identification of a membrane glycoprotein expressed on sprouting neurons. *J Cell Biol*, 1985. 101: p. 1977-89.
6. Grabham, P, Seale, GE, Bennecib, M, Goldberg, DJ, and Vallee, RB, Cytoplasmic dynein and LIS1 are required for microtubule advance during growth cone remodeling and fast axonal outgrowth. *J Neurosci*, 2007. 27: p. 5823-34.
7. Guirland, C, Suzuki, S, Kojima, M, Lu, B, and Zheng, JQ, Lipid rafts mediate chemotropic guidance of nerve growth cones. *Neuron*, 2004. 42: p. 51-62.
8. Gungabissoon, R, and Bamburg, JR, Regulation of growth cone actin dynamics by ADF/cofilin. *J Histochem Cytochem*, 2003. 51: p. 411-20.
9. Maskery, S, and Shinbrot, T, Deterministic and stochastic elements of axonal guidance. *Annu Rev Biomed Eng*, 2005. 7: p. 187-221.
10. Medeiros, N, Burnette, DT, and Forscher, P, Myosin II functions in actin-bundle turnover in neuronal growth cones. *Nat Cell Biol*, 2006. 8: p. 215-26.
11. Dent, E, Tang, F, and Kalil, K, Axon guidance by growth cones and branches: common cytoskeletal and signaling mechanisms. *Neuroscientist*, 2003. 9: p. 343-53.

12. Arimura, N, and Kaibuchi, K, Neuronal polarity: from extracellular signals to intracellular mechanisms. *Nat Rev Neurosci*, 2007. 8: p. 194-205.
13. Higginbotham, H, and Gleeson, JG, The centrosome in neuronal development. *Trends Neurosci*, 2007. 30: p. 276-83.
14. Yoshimura, T, Arimura, N, and Kaibuchi, K, Signaling networks in neuronal polarization. *J Neurosci*, 2006. 26: p. 10626-30.
15. Yoshimura, T, Arimura, N, Kawano, Y, Kawabata, S, Wang, S, and Kaibuchi, K, Ras regulates neuronal polarity via the PI3-kinase/Akt/GSK-3beta/CRMP-2 pathway. *Biochem Biophys Res Commun*, 2006. 340: p. 62-8.
16. Grzywa, E, Lee, AC, Lee, GU, and Suter, DM, High-resolution analysis of neuronal growth cone morphology by comparative atomic force and optical microscopy. *J Neurobiol*, 2006. 66: p. 1529-43.
17. Dent, E, and Kalil, K, Dynamic imaging of neuronal cytoskeleton. *Methods Enzymol*, 2003. 361: p. 390-407.
18. Mattila, P, and Lappalainen, P, Filopodia: molecular architecture and cellular functions. *Nat Rev Mol Cell Biol*, 2008. 9: p. 446-54.
19. Chhabra, E, and Higgs, HN, The many faces of actin: matching assembly factors with cellular structures. *Nat Cell Biol*, 2007. 9: p. 1110-21.
20. Aspenstrom, P, Effectors for the Rho GTPases. *Curr Opin Cell Biol*, 1999. 11: p. 95-102.
21. Aspenstrom, P, The Rho GTPases have multiple effects on the actin cytoskeleton. *Exp Cell Res*, 1999. 246: p. 20-5.
22. Koh, C, Rho GTPases and their regulators in neuronal functions and development. *Neurosignals*, 2006. 15: p. 228-37.
23. Endo, M, Ohashi, K, and Mizuno, K, LIM kinase and slingshot are critical for neurite extension. *J Biol Chem*, 2007. 282: p. 13692-702.

24. Korobova, F, and Svitkina, T, Arp2/3 complex is important for filopodia formation, growth cone motility, and neuritogenesis in neuronal cells. *Mol Biol Cell*, 2008. 19: p. 1561-74.
25. Wegner, A, Nebhan, CA, Hu, L, Majumdar, D, Meier, KM, Weaver, AM, and Webb, DJ, N-WASP and the Arp2/3 complex are critical regulators of actin in the development of dendritic spines and synapses. *J Biol Chem*, 2008. 283: p. 15912-20.
26. Brittis, P, Lu, Q, and Flanagan, JG, Axonal protein synthesis provides a mechanism for localized regulation at an intermediate target. *Cell*, 2002. 110: p. 223-35.
27. Campbell, D, and Holt, CE, Chemotropic responses of retinal growth cones mediated by rapid local protein synthesis and degradation. *Neuron*, 2001. 32: p. 1013-26.
28. Ming, G, Wong, ST, Henley, J, Yuan, XB, Song, HJ, Spitzer, NC, and Poo, MM, Adaptation in the chemotactic guidance of nerve growth cones. *Nature*, 2002. 417: p. 411-8.
29. Twiss, J, and van Minnen, J, New insights into neuronal regeneration: the role of axonal protein synthesis in pathfinding and axonal extension. *J Neurotrauma*, 2006. 23: p. 295-308.
30. Engert, F, and Bonhoeffer, T, Dendritic spine changes associated with hippocampal long-term synaptic plasticity. *Nature*, 1999. 399: p. 66-70.
31. Katz, L, and Shatz, CJ, Synaptic activity and the construction of cortical circuits. *Science*, 1996. 274: p. 1133-8.
32. Kirkland, R, and Franklin, JL, Rate of neurite outgrowth in sympathetic neurons is highly resistant to suppression of protein synthesis: role of protein degradation/synthesis coupling. *Neurosci Lett*, 2007. 411: p. 52-5.
33. Li, Z, Van Aelst, L, and Cline, HT, Rho GTPases regulate distinct aspects of dendritic arbor growth in *Xenopus* central neurons in vivo. *Nat Neurosci*, 2000. 3: p. 217-25.
34. Li, Z, Aizenman, CD, and Cline, HT, Regulation of rho GTPases by crosstalk and neuronal activity in vivo. *Neuron*, 2002. 33: p. 741-50.

35. Naeve, G, Ramakrishnan, M, Kramer, R, Hevroni, D, Citri, Y, and Theill, LE, *Neuritin: a gene induced by neural activity and neurotrophins that promotes neuritogenesis*. *Proc Natl Acad Sci U S A*, 1997. 94: p. 2648-53.
36. Rajan, I, and Cline, HT, *Glutamate receptor activity is required for normal development of tectal cell dendrites in vivo*. *J Neurosci*, 1998. 18: p. 7836-46.
37. Reichardt, L, *Neurotrophin-regulated signalling pathways*. *Phil Trans R Soc Lond B Biol Sci*, 2006. 361: p. 1545-64.
38. Calabrese, E, *Enhancing and regulating neurite outgrowth*. *Crit Rev Toxicol*, 2008. 38: p. 391-418.
39. Barallobre, M, Pascual, M, Del Rio, JA, and Soriano, E, *The Netrin family of guidance factors: emphasis on Netrin-1 signalling*. *Brain Res Brain Res Rev*, 2005. 49: p. 22-47.
40. Bondy, C, and Cheng, CM, *Signaling by insulin-like growth factor 1 in brain*. *Eur J Pharmacol*, 2004. 490: p. 25-31.
41. Gallo, G, and Letourneau, PC, *Neurotrophins and the dynamic regulation of the neuronal cytoskeleton*. *J Neurobiol*, 2000. 44: p. 159-73.
42. Huang, E, and Reichardt, LF, *Neurotrophins: roles in neuronal development and function*. *Annu Rev Neurosci*, 2001. 24: p. 677-736.
43. McAllister, AK, Katz, LC, and Lo, DC, *Neurotrophins and synaptic plasticity*. *Annu Rev Neurosci*, 1999. 22: p. 295-318.
44. Beck, K, Knusel, B, and Hefti, F, *The nature of the trophic action of brain-derived neurotrophic factor, des(1-3)-insulin-like growth factor-1, and basic fibroblast growth factor on mesencephalic dopaminergic neurons developing in culture*. *Neuroscience*, 1993. 52: p. 855-66.
45. Hanamura, K, Harada, A, Katoh-Semba, R, Murakami, F, and Yamamoto, N, *BDNF and NT-3 promote thalamocortical axon growth with distinct substrate and temporal dependency*. *Eur J Neurosci*, 2004. 19: p. 1485-93.

46. Niblock, M, Brunso-Bechtold, JK, and Riddle, DR, Insulin-like growth factor I stimulates dendritic growth in primary somatosensory cortex. *J Neurosci*, 2000. 20: p. 4165-76.
47. Pillai, A, Brain-derived neurotropic factor/TrkB signaling in the pathogenesis and novel pharmacotherapy of schizophrenia. *Neurosignals*, 2008. 16: p. 183-93.
48. Jacques-Fricke, B, Seow, Y, Gottlieb, PA, Sachs, F, and Gomez, TM, Ca^{2+} influx through mechanosensitive channels inhibits neurite outgrowth in opposition to other influx pathways and release from intracellular stores. *J Neurosci*, 2006. 26: p. 5656-64.
49. Takei, K, Shin, RM, Inoue, T, Kato, K, and Mikoshiba, K, Regulation of nerve growth mediated by inositol 1,4,5-trisphosphate receptors in growth cones. *Science*, 1998. 282: p. 1705-8.
50. D'Ercole, A, Ye, P, Calikoglu, AS, and Gutierrez-Ospina, G, The role of the insulin-like growth factors in the central nervous system. *Mol Neurobiol*, 1996. 13: p. 227-55.
51. Ozdinler, P, and Macklis, JD, IGF-I specifically enhances axon outgrowth of corticospinal motor neurons. *Nat Neurosci*, 2006. 9: p. 1371-81.
52. Rotwein, P, Burgess, SK, Milbrandt, JD, and Krause, JE, Differential expression of insulin-like growth factor genes in rat central nervous system. *Proc Natl Acad Sci U S A*, 1988. 85: p. 265-9.
53. Feldman, E, Sullivan, KA, Kim, B, and Russell, JW, Insulin-like growth factors regulate neuronal differentiation and survival. *Neurobiol Dis*, 1997. 4: p. 201-14.
54. Laurino, L, Wang, XX, de la Houssaye, BA, Sosa, L, Dupraz, S, Caceres, A, Pfenninger, KH, and Quiroga, S, PI3K activation by IGF-1 is essential for the regulation of membrane expansion at the nerve growth cone. *J Cell Sci*, 2005. 118: p. 3653-62.
55. Miller, F, and Kaplan, DR, Signaling mechanisms underlying dendrite formation. *Curr Opin Neurobiol*, 2003. 13: p. 391-8.
56. Kennedy, T, Cellular mechanisms of netrin function: long-range and short-range actions. *Biochem Cell Biol*, 2000. 78: p. 569-75.

57. Manitt, C, and Kennedy, TE, Where the rubber meets the road: netrin expression and function in developing and adult nervous systems. *Prog Brain Res*, 2002. 137: p. 425-42.
58. Fazeli, A, Dickinson, SL, Hermiston, ML, Tighe, RV, Steen, RG, Small, CG, Stoeckli, ET, Keino-Masu, K, Masu, M, Rayburn, H, Simons, J, Bronson, RT, Gordon, JI, Tessier-Lavigne, M, and Weinberg, RA, Phenotype of mice lacking functional Deleted in Colorectal Cancer (DCC) gene. *Nature*, 1997. 386: p. 796-804.
59. Keino-Masu, K, Masu, M, Hinck, L, Leonardo, ED, Chan, SS, Culotti, JG, and Tessier-Lavigne, M, Deleted in Colorectal Cancer (DCC) encodes a netrin receptor. *Cell*, 1996. 87: p. 175-85.
60. Serafini, T, Colamarino, SA, Leonardo, ED, Wang, H, Beddington, R, Skarnes, WC, and Tessier-Lavigne, M, Netrin-1 is required for commissural axon guidance in the developing vertebrate nervous system. *Cell*, 1996. 87: p. 1001-14.
61. Suli, A, Mortimer, N, Shepherd, I, and Chien, CB, Netrin/DCC signaling controls contralateral dendrites of octavolateralis efferent neurons. *J Neurosci*, 2006. 26: p. 13328-37.
62. Guan, W, and Condic, ML, Characterization of Netrin-1, Neogenin and cUNC-5H3 expression during chick dorsal root ganglia development. *Gene Expr Patterns*, 2003. 3: p. 369-73.
63. Guijarro, P, Simo, S, Pascual, M, Abasolo, I, Del Rio, J. A, and Soriano, E, Netrin1 exerts a chemorepulsive effect on migrating cerebellar interneurons in a Dcc-independent way. *Mol Cell Neurosci*, 2006. 33: p. 389-400.
64. Briancon-Marjollet, A, Ghogha, A, Nawabi, H, Triki, I, Auziol, C, Fromont, S, Piche, C, Enslin, H, Chebli, K, Cloutier, JF, Castellani, V, Debant, A, and Lamarche-Vane, N, Trio mediates netrin-1-induced Rac1 activation in axon outgrowth and guidance. *Mol Cell Biol*, 2008. 28: p. 2314-23.
65. Li, X, Gao, X, Liu, G, Xiong, W, Wu, J, and Rao, Y, Netrin signal transduction and the guanine nucleotide exchange factor DOCK180 in attractive signaling. *Nat Neurosci*, 2008. 11: p. 28-35.
66. Li, X, Meriane, M, Triki, I, Shekarabi, M, Kennedy, TE, Larose, L, and Lamarche-Vane, N, The adaptor protein Nck-1 couples the netrin-1 receptor DCC (deleted in colorectal

- cancer) to the activation of the small GTPase Rac1 through an atypical mechanism. *J Biol Chem*, 2002. 277: p. 37788-97.
67. Li, X, Saint-Cyr-Proulx, E, Aktories, K, and Lamarche-Vane, N, Rac1 and Cdc42 but not RhoA or Rho kinase activities are required for neurite outgrowth induced by the Netrin-1 receptor DCC (deleted in colorectal cancer) in N1E-115 neuroblastoma cells. *J Biol Chem*, 2002. 277: p. 15207-14.
 68. Round, J, and Stein, E, Netrin signaling leading to directed growth cone steering. *Curr Opin Neurobiol*, 2007. 17: p. 15-21.
 69. Shekarabi, M, and Kennedy, TE, The netrin-1 receptor DCC promotes filopodia formation and cell spreading by activating Cdc42 and Rac1. *Mol Cell Neurosci*, 2002. 19: p. 1-17.
 70. Shekarabi, M, Moore, SW, Tritsch, NX, Morris, SJ, Bouchard, JF, and Kennedy, TE, Deleted in colorectal cancer binding netrin-1 mediates cell substrate adhesion and recruits Cdc42, Rac1, Pak1, and N-WASP into an intracellular signaling complex that promotes growth cone expansion. *J Neurosci*, 2005. 25: p. 3132-41.
 71. Hong, K, Nishiyama, M, Henley, J, Tessier-Lavigne, M, and Poo, MM, Calcium signalling in the guidance of nerve growth by netrin-1. *Nature*, 2000. 403: p. 93-8.
 72. Song, H, and Poo, MM, Signal transduction underlying growth cone guidance by diffusible factors. *Curr Opin Neurobiol*, 1999. 9: p. 355-63.
 73. Tang, F, and Kalil, K, Netrin-1 induces axon branching in developing cortical neurons by frequency-dependent calcium signaling pathways. *J Neurosci*, 2005. 25: p. 6702-15.
 74. Wang, G, and Poo, MM, Requirement of TRPC channels in netrin-1-induced chemotropic turning of nerve growth cones. *Nature*, 2005. 434: p. 898-904.
 75. Bouchard, J, Moore, SW, Tritsch, NX, Roux, PP, Shekarabi, M, Barker, PA, and Kennedy, TE, Protein kinase A activation promotes plasma membrane insertion of DCC from an intracellular pool: A novel mechanism regulating commissural axon extension. *J Neurosci*, 2004. 24: p. 3040-50.

76. Moore, S, and Kennedy, TE, Protein kinase A regulates the sensitivity of spinal commissural axon turning to netrin-1 but does not switch between chemoattraction and chemorepulsion. *J Neurosci*, 2006. 26: p. 2419-23.
77. Corset, V, Nguyen-Ba-Charvet, KT, Forcet, C, Moyses, E, Chedotal, A, and Mehlen, P, Netrin-1-mediated axon outgrowth and cAMP production requires interaction with adenosine A2b receptor. *Nature*, 2000. 407: p. 747-50.
78. Ming, G, Song, HJ, Berninger, B, Holt, CE, Tessier-Lavigne, M, and Poo, MM, cAMP-dependent growth cone guidance by netrin-1. *Neuron*, 1997. 19: p. 1225-35.
79. Wu, K, Zippin, JH, Huron, DR, Kamenetsky, M, Hengst, U, Buck, J, Levin, LR, and Jaffrey, SR, Soluble adenylyl cyclase is required for netrin-1 signaling in nerve growth cones. *Nat Neurosci*, 2006. 9: p. 1257-64.
80. Henley, J, and Poo, MM, Guiding neuronal growth cones using Ca^{2+} signals. *Trends Cell Biol*, 2004. 14: p. 320-30.
81. Conklin, M, Lin, MS, and Spitzer, NC, Local calcium transients contribute to disappearance of pFAK, focal complex removal and deadhesion of neuronal growth cones and fibroblasts. *Dev Biol*, 2005. 287: p. 201-12.
82. Estrada, M, Uhlen, P, and Ehrlich, BE, Ca^{2+} oscillations induced by testosterone enhance neurite outgrowth. *J Cell Sci*, 2006. 119: p. 733-43.
83. Tang, F, Dent, EW, and Kalil, K, Spontaneous calcium transients in developing cortical neurons regulate axon outgrowth. *J Neurosci*, 2003. 23: p. 927-36.
84. Lohmann, C, Myhr, KL, and Wong, RO, Transmitter-evoked local calcium release stabilizes developing dendrites. *Nature*, 2002. 418: p. 177-81.
85. Ziv, N, and Spira, ME, Localized and transient elevations of intracellular Ca^{2+} induce the dedifferentiation of axonal segments into growth cones. *J Neurosci*, 1997. 17: p. 3568-79.
86. Wayman, G, Kaech, S, Grant, WF, Davare, M, Impey, S, Tokumitsu, H, Nozaki, N, Banker, G, and Soderling, TR, Regulation of axonal extension and growth cone motility by calmodulin-dependent protein kinase I. *J Neurosci*, 2004. 24: p. 3786-94.

87. Chen, N, Furuya, S, Doi, H, Hashimoto, Y, Kudo, Y, and Higashi, H, Ganglioside/calmodulin kinase II signal inducing Cdc42-mediated neuronal actin reorganization. *Neuroscience*, 2003. 120: p. 163-76.
88. Henley, J, Huang, KH, Wang, D, and Poo, MM, Calcium mediates bidirectional growth cone turning induced by myelin-associated glycoprotein. *Neuron*, 2004. 44: p. 909-16.
89. Price, L, Langeslag, M, ten Klooster, JP, Hordijk, PL, Jalink, K, and Collard, JG, Calcium signaling regulates translocation and activation of Rac. *J Biol Chem*, 2003. 278: p. 39413-21.
90. Aglah, C, Gordon, T, and Posse de Chaves, EI, cAMP promotes neurite outgrowth and extension through protein kinase A but independently of Erk activation in cultured rat motoneurons. *Neuropharmacology*, 2008. 55: p. 8-17.
91. Rodger, J, Goto, H, Cui, Q, Chen, PB, and Harvey, AR, cAMP regulates axon outgrowth and guidance during optic nerve regeneration in goldfish. *Mol Cell Neurosci*, 2005. 30: p. 452-64.
92. Sanchez, S, Jimenez, C, Carrera, AC, Diaz-Nido, J, Avila, J, and Wandosell, F, A cAMP-activated pathway, including PKA and PI3K, regulates neuronal differentiation. *Neurochem Int*, 2004. 44: p. 231-42.
93. Vogt Weisenhorn, D, Roback, LJ, Kwon, JH, and Wainer, BH, Coupling of cAMP/PKA and MAPK signaling in neuronal cells is dependent on developmental stage. *Exp Neurol*, 2001. 169: p. 44-55.
94. Atkins, C, Oliva, A. A., Jr, Alonso, OF, Pearse, DD, Bramlett, HM, and Dietrich, WD, Modulation of the cAMP signaling pathway after traumatic brain injury. *Exp Neurol*, 2007. 208: p. 145-58.
95. Howe, A, Regulation of actin-based cell migration by cAMP/PKA. *Biochim Biophys Acta*, 2004. 1692: p. 159-74.
96. Shabb, J, Physiological substrates of cAMP-dependent protein kinase. *Chem Rev*, 2001. 101: p. 2381-411.

97. Han, J, Han, L, Tiwari, P, Wen, Z, and Zheng, JQ, Spatial targeting of type II protein kinase A to filopodia mediates the regulation of growth cone guidance by cAMP. *J Cell Biol*, 2007. 176: p. 101-11.
98. Ridley, A, and Hall, A, The small GTP-binding protein Rho regulates the assembly of focal adhesions and actin stress fibers in response to growth factors. *Cell*, 1992. 70: p. 389-99.
99. Ridley, A, Paterson, HF, Johnston, CL, Diekmann, D, and Hall, A, The small GTP-binding protein Rac regulates growth factor-induced membrane ruffling. *Cell*, 1992. 70: p. 401-10.
100. Etienne-Manneville, S, and Hall, A, Rho GTPases in cell biology. *Nature*, 2002. 420: p. 629-35.
101. Luo, L, Rho GTPases in neuronal morphogenesis. *Nat Rev Neurosci*, 2000. 1: p. 173-80.
102. Threadgill, R, Bobb, K, and Ghosh, A, Regulation of dendritic growth and remodeling by Rho, Rac, and Cdc42. *Neuron*, 1997. 19: p. 625-34.
103. Kjoller, L, and Hall, A, Signaling to Rho GTPases. *Exp Cell Res*, 1999. 253: p. 166-79.
104. Sander, E, ten Klooster, JP, van Delft, S, van der Kammen, RA, Collard, JG, Rac downregulates Rho activity: reciprocal balance between both GTPases determines cellular morphology and migratory behavior. *J Cell Biol*, 1999. 147: p. 1009-22.
105. Kuhn, T, Meberg, PJ, Brown, MD, Bernstein, BW, Minamide, LS, Jensen, JR, Okada, K, Soda, EA, and Bamburg, JR, Regulating actin dynamics in neuronal growth cones by ADF/cofilin and Rho family GTPases. *J Neurobiol*, 2000. 44: p. 126-44.
106. Lamoureux, P, Altun-Gultekin, ZF, Lin, C, Wagner, JA, and Heidemann, SR, Rac is required for growth cone function but not neurite assembly. *J Cell Sci*, 1997. 110: p. 635-41.
107. Wang, S, Watanabe, T, Noritake, J, Fukata, M, Yoshimura, T, Itoh, N, Harada, T, Nakagawa, M, Matsuura, Y, Arimura, N, and Kaibuchi, K, IQGAP3, a novel effector of Rac1 and Cdc42, regulates neurite outgrowth. *J Cell Sci*, 2007. 120: p. 567-77.

108. Dubreuil, C, Winton, MJ, and McKerracher, L, Rho activation patterns after spinal cord injury and the role of activated Rho in apoptosis in the central nervous system. *J Cell Biol*, 2003. 162: p. 233-43.
109. Moore, S, Correia, JP, Lai Wing Sun, K, Pool, M, Fournier, AE, and Kennedy, TE, Rho inhibition recruits DCC to the neuronal plasma membrane and enhances axon chemoattraction to netrin 1. *Development*, 2008. 135: p. 2855-64.
110. Denker, S, and Barber, DL, Ion transport proteins anchor and regulate the cytoskeleton. *Curr Opin Cell Biol*, 2002. 14: p. 214-20.
111. Jamora, C, and Fuchs, E, Intercellular adhesion, signalling and the cytoskeleton. *Nat Cell Biol*, 2002. 4: p. E101-8.
112. Ramesh, V, Merlin and the ERM proteins in Schwann cells, neurons and growth cones. *Nat Rev Neurosci*, 2004. 5: p. 462-70.
113. Haas, M, Vickers, JC, Dickson, TC, Rho kinase activates ezrin-radixin-moesin (ERM) proteins and mediates their function in cortical neuron growth, morphology and motility in vitro. *J Neurosci Res*, 2007. 85: p. 34-46.
114. Matsui, T, Maeda, M, Doi, Y, Yonemura, S, Amano, M, Kaibuchi, K, Tsukita, S, and Tsukita, S, Rho-kinase phosphorylates COOH-terminal threonines of ezrin/radixin/moesin (ERM) proteins and regulates their head-to-tail association. *J Cell Biol*, 1998. 140: p. 647-57.
115. Mangeat, P, Roy, C., and Martin, M, ERM proteins in cell adhesion and membrane dynamics. *Trends Cell Biol*, 1999. 9: p. 187-92.
116. Heiska, L, Alfthan, K, Gronholm, M, Vilja, P, Vaheri, A, and Carpen, O, Association of ezrin with intercellular adhesion molecule-1 and -2 (ICAM-1 and ICAM-2). Regulation by phosphatidylinositol 4, 5-bisphosphate. *J Biol Chem*, 1998. 273: p. 21893-900.
117. Serrador, J, Alonso-Lebrero, JL, del Pozo, MA, Furthmayr, H, Schwartz-Albiez, R, Calvo, J, Lozano, F, and Sanchez-Madrid, F, Moesin interacts with the cytoplasmic region of intercellular adhesion molecule-3 and is redistributed to the uropod of T lymphocytes during cell polarization. *J Cell Biol*, 1997. 138: p. 1409-23.

118. Yonemura, S, Hirao, M, Doi, Y, Takahashi, N, Kondo, T, Tsukita, S, and Tsukita, S, Ezrin/radixin/moesin (ERM) proteins bind to a positively charged amino acid cluster in the juxta-membrane cytoplasmic domain of CD44, CD43, and ICAM-2. *J Cell Biol*, 1998. 140: p. 885-95.
119. Meima, M, Mackley, JR, and Barber, DL, Beyond ion translocation: structural functions of the sodium-hydrogen exchanger isoform-1. *Curr Opin Nephrol Hypertens*, 2007. 16: p. 365-72.
120. Denker, S, and Barber, DL, Cell migration requires both ion translocation and cytoskeletal anchoring by the Na-H exchanger NHE1. *J Cell Biol*, 2002. 159: p. 1087-96.
121. Denker, S, Huang, DC, Orłowski, J, Furthmayr, H, and Barber, DL, Direct binding of the Na⁺/H⁺ exchanger NHE1 to ERM proteins regulates the cortical cytoskeleton and cell shape independently of H⁺ translocation. *Mol Cell*, 2000. 6: p. 1425-36.
122. Counillon, L, and Pouyssegur, J, The expanding family of eucaryotic Na⁺/H⁺ exchangers. *J Biol Chem*, 2000. 275: p. 1-4.
123. Orłowski, J, and Grinstein, S, Diversity of the mammalian sodium/proton exchanger SLC9 gene family. *Pflugers Arch*, 2004. 447: p. 549-65.
124. Malo, M, and Fliegel, L, Physiological role and regulation of the Na⁺/H⁺ exchanger. *Can J Physiol Pharmacol*, 2006. 84: p. 1081-95.
125. Putney, L, Denker, SP, and Barber, DL, The changing face of the Na⁺/H⁺ exchanger, NHE1: structure, regulation, and cellular actions. *Annu Rev Pharmacol Toxicol*, 2002. 42: p. 527-52.
126. Orłowski, J, and Grinstein, S, Emerging roles of alkali cation/proton exchangers in organellar homeostasis. *Curr Opin Cell Biol*, 2007. 19: p. 483-92.
127. Brett, C, Donowitz, M, and Rao, R, Evolutionary origins of eukaryotic sodium/proton exchangers. *Am J Physiol Cell Physiol*, 2005. 288: p. C223-39.
128. Fliegel, L, Murtazina, R, Dibrov, P, Harris, C, Moor, A, and Fernandez-Rachubinski, FA, Regulation and characterization of the Na⁺/H⁺ exchanger. *Biochem Cell Biol*, 1998. 76: p. 735-41.

129. Fliegel, L, The Na⁺/H⁺ exchanger isoform 1. *Int J Biochem Cell Biol*, 2005. 37: p. 33-7.
130. Baumgartner, M, Patel, H, and Barber, DL, Na⁺/H⁺ exchanger NHE1 as plasma membrane scaffold in the assembly of signaling complexes. *Am J Physiol Cell Physiol*, 2004. 287: p. C844-50.
131. Sardet, C, Franchi, A, and Pouyssegur, J, Molecular cloning, primary structure, and expression of the human growth factor-activatable Na⁺/H⁺ antiporter. *Cell*, 1989. 56: p. 271-80.
132. Ma, E, and Haddad, GG, Expression and localization of Na⁺/H⁺ exchangers in rat central nervous system. *Neuroscience*, 1997. 79: p. 591-603.
133. Tolkovsky, A, and Richards, CD, Na⁺/H⁺ exchange is the major mechanism of pH regulation in cultured sympathetic neurons: measurements in single cell bodies and neurites using a fluorescent pH indicator. *Neuroscience*, 1987. 22: p. 1093-102.
134. Cox, G, Lutz, CM, Yang, CL, Biemesderfer, D, Bronson, RT, Fu, A, Aronson, PS, Noebels, JL, and Frankel, WN, Sodium/hydrogen exchanger gene defect in slow-wave epilepsy mutant mice. *Cell*, 1997. 91: p. 139-48.
135. Seifter, J, and Aronson, PS, Properties and physiologic roles of the plasma membrane sodium-hydrogen exchanger. *J Clin Invest*, 1986. 78: p. 859-64.
136. Aronson, P, Kinetic properties of the plasma membrane Na⁺-H⁺ exchanger. *Annu Rev Physiol*, 1985. 47: p. 545-60.
137. Aronson, P, Nee, J, and Suhm, MA, Modifier role of internal H⁺ in activating the Na⁺-H⁺ exchanger in renal microvillus membrane vesicles. *Nature*, 1982. 299: p. 161-3.
138. Sardet, C, Counillon, L, Franchi, A, and Pouyssegur, J, Growth factors induce phosphorylation of the Na⁺/H⁺ antiporter, glycoprotein of 110 kD. *Science*, 1990. 247: p. 723-6.
139. Sardet, C, Fafournoux, P, and Pouyssegur, J, Alpha-thrombin, epidermal growth factor, and okadaic acid activate the Na⁺/H⁺ exchanger, NHE-1, by phosphorylating a set of common sites. *J Biol Chem*, 1991. 266: p. 19166-71.

140. Fliegel, L, Functional and cellular regulation of the myocardial Na⁺/H⁺ exchanger. *J Thromb Thrombolysis*, 1999. 8: p. 9-14.
141. Slepko, E, Rainey, JK, Sykes, BD, and Fliegel, L, Structural and functional analysis of the Na⁺/H⁺ exchanger. *Biochem J*, 2007. 401: p. 623-33.
142. Takahashi, E, Abe, J, Gallis, B, Aebersold, R, Spring, DJ, Krebs, EG, and Berk, BC, p90(RSK) is a serum-stimulated Na⁺/H⁺ exchanger isoform-1 kinase. Regulatory phosphorylation of serine 703 of Na⁺/H⁺ exchanger isoform-1. *J Biol Chem*, 1999. 274: p. 20206-14.
143. Tominaga, T, and Barber, DL, Na⁺/H⁺ exchange acts downstream of RhoA to regulate integrin-induced cell adhesion and spreading. *Mol Biol Cell*, 1998. 9: p. 2287-303.
144. Tominaga, T, Ishizaki, T, Narumiya, S, and Barber, DL, p160ROCK mediates RhoA activation of Na⁺/H⁺ exchange. *EMBO J*, 1998. 17: p. 4712-22.
145. Bertrand, B, Wakabayashi, S, Ikeda, T, Pouyssegur, J, and Shigekawa, M, The Na⁺/H⁺ exchanger isoform 1 (NHE1) is a novel member of the calmodulin-binding proteins. Identification and characterization of calmodulin-binding sites. *J Biol Chem*, 1994. 269: p. 13703-9.
146. Wakabayashi, S, Bertrand, B, Ikeda, T, Pouyssegur, J, and Shigekawa, M, Mutation of calmodulin-binding site renders the Na⁺/H⁺ exchanger (NHE1) highly H⁺-sensitive and Ca²⁺ regulation-defective. *J Biol Chem*, 1994. 269: p. 13710-5.
147. Wakabayashi, S, Ikeda, T, Iwamoto, T, Pouyssegur, J, and Shigekawa, M, Calmodulin-binding autoinhibitory domain controls "pH-sensing" in the Na⁺/H⁺ exchanger NHE1 through sequence-specific interaction. *Biochemistry*, 1997. 36: p. 12854-61.
148. Aharonovitz, O, Zaun, HC, Balla, T, York, JD, Orłowski, J, and Grinstein, S, Intracellular pH regulation by Na⁺/H⁺ exchange requires phosphatidylinositol 4,5-bisphosphate. *J Cell Biol*, 2000. 150: p. 213-24.
149. Wakabayashi, S, Shigekawa, M, and Pouyssegur, J, Molecular physiology of vertebrate Na⁺/H⁺ exchangers. *Physiol Rev*, 1997. 77: p. 51-74.

150. Barber, D, McGuire, ME, and Ganz, MB, Beta-adrenergic and somatostatin receptors regulate Na-H exchange independent of cAMP. *J Biol Chem*, 1989. 264: p. 21038-42.
151. Borgese, F, Malapert, M, Fievet, B, Pouyssegur, J, and Motais, R, The cytoplasmic domain of the Na⁺/H⁺ exchangers (NHEs) dictates the nature of the hormonal response: behavior of a chimeric human NHE1/trout beta NHE antiporter. *Proc Natl Acad Sci U S A*, 1994. 91: p. 5431-5.
152. Ganz, M, Pachter, JA, and Barber, DL, Multiple receptors coupled to adenylate cyclase regulate Na-H exchange independent of cAMP. *J Biol Chem*, 1990. 265: p. 8989-92.
153. Yao, H, Gu, XQ, Douglas, RM, and Haddad, GG, Role of Na⁺/H⁺ exchanger during O₂ deprivation in mouse CA1 neurons. *Am J Physiol Cell Physiol*, 2001. 281: p. C1205-10.
154. Borgese, F, Sardet, C, Cappadoro, M, Pouyssegur, J, and Motais, R, Cloning and expression of a cAMP-activated Na⁺/H⁺ exchanger: evidence that the cytoplasmic domain mediates hormonal regulation. *Proc Natl Acad Sci U S A*, 1992. 89: p. 6765-9.
155. Higgs, H, and Pollard, TD, Activation by Cdc42 and PIP2 of Wiskott-Aldrich syndrome protein (WASP) stimulates actin nucleation by Arp2/3 complex. *J Cell Biol*, 2000. 150: p. 1311-20.
156. Rohatgi, R, Nollau, P, Ho, HY, Kirschner, MW, and Mayer, BJ, Nck and phosphatidylinositol 4,5-bisphosphate synergistically activate actin polymerization through the N-WASP-Arp2/3 pathway. *J Biol Chem*, 2001. 276: p. 26448-52.
157. Lagana, A, Vadnais, J, Le, PU, Nguyen, TN, Laprade, R, Nabi, IR, and Noel, J, Regulation of the formation of tumor cell pseudopodia by the Na⁺/H⁺ exchanger NHE1. *J Cell Sci*, 2000. 113: p. 3649-62.
158. Cardone, R, Bagorda, A, Bellizzi, A, Busco, G, Guerra, L, Paradiso, A, Casavola, V, Zaccolo, M, and Reshkin, SJ, Protein kinase A gating of a pseudopodial-located RhoA/ROCK/p38/NHE1 signal module regulates invasion in breast cancer cell lines. *Mol Biol Cell*, 2005. 16: p. 3117-27.
159. Paradiso, A, Cardone, RA, Bellizzi, A, Bagorda, A, Guerra, L, Tommasino, M, Casavola, V, and Reshkin, SJ, The Na⁺-H⁺ exchanger-1 induces cytoskeletal changes involving reciprocal RhoA and Rac1 signaling, resulting in motility and invasion in MDA-MB-435 cells. *Breast Cancer Res*, 2004. 6: p. R616-28.

160. Cardone, R, Casavola, V, and Reshkin, SJ, The role of disturbed pH dynamics and the Na^+/H^+ exchanger in metastasis. *Nat Rev Cancer*, 2005. 5: p. 786-95.
161. Bernstein, B, Painter, WB, Chen, H, Minamide, LS, Abe, H, and Bamburg, JR, Intracellular pH modulation of ADF/cofilin proteins. *Cell Motil Cytoskeleton*, 2000. 47: p. 319-36.
162. Schwab, A, Nechyporuk-Zloy, V, Fabian, A, and Stock, C, Cells move when ions and water flow. *Pflugers Arch*, 2007. 453: p. 421-32.
163. Stock, C, and Schwab, A, Role of the Na/H exchanger NHE1 in cell migration. *Acta Physiol (Oxf)*, 2006. 187: p. 149-57.
164. Pouyssegur, J, Sardet, C, Franchi, A, L'Allemain, G, and Paris, S, A specific mutation abolishing Na^+/H^+ antiport activity in hamster fibroblasts precludes growth at neutral and acidic pH. *Proc Natl Acad Sci U S A*, 1984. 81: p. 4833-7.
165. Barber, D, and Ganz, MB, Guanine nucleotides regulate beta-adrenergic activation of Na-H exchange independently of receptor coupling to Gs. *J Biol Chem*, 1992. 267: p. 20607-12.
166. Denker, S, Yan, W, and Barber, DL, Effect of Rho GTPases on Na-H exchanger in mammalian cells. *Methods Enzymol*, 2000. 325: p. 334-48.
167. Vexler, Z, Symons, M, and Barber, DL, Activation of Na^+/H^+ exchange is necessary for RhoA-induced stress fiber formation. *J Biol Chem*, 1996. 271: p. 22281-4.
168. Chijiwa, T, Mishima, A, Hagiwara, M, Sano, M, Hayashi, K, Inoue, T, Naito, K, Toshioka, T, and Hidaka, H, Inhibition of forskolin-induced neurite outgrowth and protein phosphorylation by a newly synthesized selective inhibitor of cyclic AMP-dependent protein kinase, N-[2-(p-bromocinnamylamino)ethyl]-5-isoquinolinesulfonamide (H-89), of PC12D pheochromocytoma cells. *J Biol Chem*, 1990. 265: p. 5267-72.
169. Draushuk, K, Connell, TD, and Higgins, D, Pituitary adenylate cyclase-activating polypeptide and vasoactive intestinal peptide inhibit dendritic growth in cultured sympathetic neurons. *J Neurosci*, 2002. 22: p. 6560-9.

170. Greene, L, and Tischler, AS, Establishment of a noradrenergic clonal line of rat adrenal pheochromocytoma cells which respond to nerve growth factor. *Proc Natl Acad Sci U S A*, 1976. 73: p. 2424-8.
171. Sakai, Y, Hashimoto, H, Shintani, N, Katoh, H, Negishi, M, Kawaguchi, C, Kasai, A, and Baba, A, PACAP activates Rac1 and synergizes with NGF to activate ERK1/2, thereby inducing neurite outgrowth in PC12 cells. *Brain Res Mol Brain Res*, 2004. 123: p. 18-26.
172. Villegas, R, Villegas, GM, Nunez, J, Hernandez, M, and Castillo, C, Neuron-like differentiation of PC12 cells treated with media conditioned by either sciatic nerves, optic nerves, or Schwann cells. *Cell Mol Neurobiol*, 2005. 25: p. 451-61.
173. Yasui, H, Katoh, H, Yamaguchi, Y, Aoki, J, Fujita, H, Mori, K, and Negishi, M, Differential responses to nerve growth factor and epidermal growth factor in neurite outgrowth of PC12 cells are determined by Rac1 activation systems. *J Biol Chem*, 2001. 276: p. 15298-305.
174. Mazzoni, I, and Kenigsberg, RL, Thrombin indirectly affects cholinergic cell expression in primary septal cell cultures in a manner distinct from nerve growth factor. *Neuroscience*, 1991. 45: p. 195-204.
175. Reaume, A, de Sousa, PA, Kulkarni, S, Langille, BL, Zhu, D, Davies, TC, Juneja, SC, Kidder, GM, and Rossant, J, Cardiac malformation in neonatal mice lacking connexin43. *Science*, 1995. 267: p. 1831-4.
176. Xue, J, Douglas, RM, Zhou, D, Lim, JY, Boron, WF, and Haddad, GG, Expression of Na^+/H^+ and HCO_3^- -dependent transporters in Na^+/H^+ exchanger isoform 1 null mutant mouse brain. *Neuroscience*, 2003. 122: p. 37-46.
177. Gu, X, Yao, H, and Haddad, GG, Increased neuronal excitability and seizures in the Na^+/H^+ exchanger null mutant mouse. *Am J Physiol Cell Physiol*, 2001. 281: p. C496-503.
178. Orłowski, J, Heterologous expression and functional properties of amiloride high affinity (NHE-1) and low affinity (NHE-3) isoforms of the rat Na/H exchanger. *J Biol Chem*, 1993. 268: p. 16369-77.
179. Rink, T, Tsien, RY, and Pozzan, T, Cytoplasmic pH and free Mg^{2+} in lymphocytes. *J Cell Biol*, 1982. 95: p. 189-96.

180. Nett, W, and Deitmer, JW, Simultaneous measurements of intracellular pH in the leech giant glial cell using 2',7'-bis-(2-carboxyethyl)-5,6-carboxyfluorescein and ion-sensitive microelectrodes. *Biophys J*, 1996. 71: p. 394-402.
181. Bright, G, Fisher, GW, Rogowska, J, and Taylor, DL, Fluorescence ratio imaging microscopy. *Methods Cell Biol*, 1989. 30: p. 157-92.
182. Bright, G, Fisher, GW, Rogowska, J, and Taylor, DL, Fluorescence ratio imaging microscopy: temporal and spatial measurements of cytoplasmic pH. *J Cell Biol*, 1987. 104: p. 1019-33.
183. Silver, R, Whitaker, M, and Bolsover, SR, Intracellular ion imaging using fluorescent dyes: artefacts and limits to resolution. *Pflugers Arch*, 1992. 420: p. 595-602.
184. Bevensee, M, Schwiening, CJ, and Boron, WF, Use of BCECF and propidium iodide to assess membrane integrity of acutely isolated CA1 neurons from rat hippocampus. *J Neurosci Methods*, 1995. 58: p. 61-75.
185. Baxter, K, Regulation of intracellular pH in cultured fetal rat hippocampal pyramidal neurons. MSc. Thesis. Department of Anatomy, University of British Columbia., 1995.
186. Baxter, K, and Church, J, Characterization of acid extrusion mechanisms in cultured fetal rat hippocampal neurones. *J Physiol*, 1996. 493: p. 457-70.
187. Boron, W, Hogan, E, and Russell, JM, pH-sensitive activation of the intracellular-pH regulation system in squid axons by ATP-gamma-S. *Nature*, 1988. 332: p. 262-5.
188. Roos, A, and Boron, WF, Intracellular pH. *Physiol Rev*, 1981. 61: p. 296-434.
189. Chaillet, J, and Boron, WF, Intracellular calibration of a pH-sensitive dye in isolated, perfused salamander proximal tubules. *J Gen Physiol*, 1985. 86: p. 765-94.
190. Thomas, J, Buchsbaum, RN, Zimniak, A, and Racker, E, Intracellular pH measurements in Ehrlich ascites tumor cells utilizing spectroscopic probes generated in situ. *Biochemistry*, 1979. 18: p. 2210-8.

191. Laemmli, U, Cleavage of structural proteins during the assembly of the head of bacteriophage T4. *Nature*, 1970. 227: p. 680-5.
192. Kwiatkowski, A, Rubinson, DA, Dent, EW, Edward van Veen, J, Leslie, JD, Zhang, J, Mebane, LM, Philippar, U, Pinheiro, EM, Burds, AA, Bronson, RT, Mori, S, Fassler, R, and Gertler, FB, Ena/VASP is required for neuritegenesis in the developing cortex. *Neuron*, 2007. 56: p. 441-55.
193. Ahmad, S, Doweyko, LM, Dugar, S, Grazier, N, Ngu, K, Wu, SC, Yost, KJ, Chen, BC, Gougoutas, JZ, DiMarco, JD, Lan, SJ, Gavin, BJ, Chen, AY, Dorso, CR, Serafino, R, Kirby, M, and Atwal, KS, Arylcyclopropanecarboxyl guanidines as novel, potent, and selective inhibitors of the sodium hydrogen exchanger isoform-1. *J Med Chem*, 2001. 44: p. 3302-10.
194. Demaurex, N, Downey, GP, Waddell, TK, and Grinstein, S, Intracellular pH regulation during spreading of human neutrophils. *J Cell Biol*, 1996. 133: p. 1391-402.
195. Masereel, B, Pochet, L, and Laeckmann, D, An overview of inhibitors of Na⁺/H⁺ exchanger. *Eur J Med Chem*, 2003. 38: p. 547-54.
196. Vigne, P, Frelin, C, Cragoe, EJ Jr, and Lazdunski, M, Ethylisopropyl-amiloride: a new and highly potent derivative of amiloride for the inhibition of the Na⁺/H⁺ exchange system in various cell types. *Biochem Biophys Res Commun*, 1983. 116: p. 86-90.
197. Douglas, R, Schmitt, BM, Xia, Y, Bevensee, MO, Biemesderfer, D, Boron, WF, and Haddad, GG, Sodium-hydrogen exchangers and sodium-bicarbonate co-transporters: ontogeny of protein expression in the rat brain. *Neuroscience*, 2001. 102: p. 217-28.
198. Luo, J, Chen, H, Kintner, DB, Shull, GE, and Sun, D, Decreased neuronal death in Na⁺/H⁺ exchanger isoform 1-null mice after in vitro and in vivo ischemia. *J Neurosci*, 2005. 25: p. 11256-68.
199. Rieder, C, and Fliegel, L, Developmental regulation of Na⁺/H⁺ exchanger expression in fetal and neonatal mice. *Am J Physiol Heart Circ Physiol*, 2002. 283: p. H273-83.
200. Hayashi, H, Aharonovitz, O, Alexander, RT, Touret, N, Furuya, W, Orłowski, J, and Grinstein, S, Na⁺/H⁺ exchange and pH regulation in the control of neutrophil chemokinesis and chemotaxis. *Am J Physiol Cell Physiol*, 2008. 294: p. C526-34.

201. Bell, S, Schreiner, CM, Schultheis, PJ, Miller, ML, Evans, RL, Vorhees, CV, Shull, GE, and Scott, WJ, Targeted disruption of the murine *Nhe1* locus induces ataxia, growth retardation, and seizures. *Am J Physiol*, 1999. 276: p. C788-95.
202. Yao, H, Ma, E, Gu, XQ, and Haddad, GG, Intracellular pH regulation of CA1 neurons in Na^+/H^+ isoform 1 mutant mice. *J Clin Invest*, 1999. 104: p. 637-45.
203. Grinstein, S, Woodside, M, Waddell, TK, Downey, GP, Orlowski, J, Pouyssegur, J, Wong, DC, and Foskett, JK, Focal localization of the NHE-1 isoform of the Na^+/H^+ antiport: assessment of effects on intracellular pH. *EMBO J*, 1993. 12: p. 5209-18.
204. Rojas, J, Sennoune, SR, Maiti, D, Bakunts, K, Reuveni, M, Sanka, SC, Martinez, GM, Seftor, EA, Meininger, CJ, Wu, G, Wesson, DE, Hendrix, MJ, and Martinez-Zaguilan, R, Vacuolar-type H^+ -ATPases at the plasma membrane regulate pH and cell migration in microvascular endothelial cells. *Am J Physiol Heart Circ Physiol*, 2006. 291: p. H1147-57.
205. Dickens, C, Gillespie, JI, and Greenwell, JR, Interactions between intracellular pH and calcium in single mouse neuroblastoma (N2A) and rat pheochromocytoma cells (PC12). *Q J Exp Physiol*, 1989. 74: p. 671-9.
206. Schwiening, C, and Willoughby, D, Depolarization-induced pH microdomains and their relationship to calcium transients in isolated snail neurones. *J Physiol*, 2002. 538: p. 371-82.
207. Willoughby, D, and Schwiening, CJ, Electrically evoked dendritic pH transients in rat cerebellar Purkinje cells. *J Physiol*, 2002. 544: p. 487-99.
208. Tilney, L, Kiehart, DP, Sardet, C, and Tilney, M, Polymerization of actin. IV. Role of Ca^{++} and H^+ in the assembly of actin and in membrane fusion in the acrosomal reaction of echinoderm sperm. *J Cell Biol*, 1978. 77: p. 536-50.
209. Srivastava, J, Barber, DL, and Jacobson, MP, Intracellular pH sensors: design principles and functional significance. *Physiology (Bethesda)*, 2007. 22: p. 30-9.
210. Yonezawa, N, Nishida, E, and Sakai, H, pH control of actin polymerization by cofilin. *J Biol Chem*, 1985. 260: p. 14410-2.

211. Maciver, S, Pope, BJ, Whytock, S, and Weeds, AG, The effect of two actin depolymerizing factors (ADF/cofilins) on actin filament turnover: pH sensitivity of F-actin binding by human ADF, but not of *Acanthamoeba* actophorin. *Eur J Biochem*, 1998. 256: p. 388-97.
212. Gallo, G, and Letourneau, PC, Regulation of growth cone actin filaments by guidance cues. *J Neurobiol*, 2004. 58: p. 92-102.
213. Frantz, C, Karydis, A, Nalbant, P, Hahn, KM, and Barber, DL, Positive feedback between Cdc42 activity and H⁺ efflux by the Na-H exchanger NHE1 for polarity of migrating cells. *J Cell Biol*, 2007. 179: p. 403-10.
214. Lee, H, Bellin, RM, Walker, DL, Patel, B, Powers, P, Liu, H, Garcia-Alvarez, B, de Pereda, JM, Liddington, RC, Volkman, N, Hanein, D, Critchley, DR, and Robson, RM, Characterization of an actin-binding site within the talin FERM domain. *J Mol Biol*, 2004. 343: p. 771-84.
215. Schmidt, J, Zhang, J, Lee, HS, Stromer, MH, and Robson, RM, Interaction of talin with actin: sensitive modulation of filament crosslinking activity. *Arch Biochem Biophys*, 1999. 366: p. 139-50.
216. Renaudin, A, Lehmann, M, Girault, J, and McKerracher, L, Organization of point contacts in neuronal growth cones. *J Neurosci Res*, 1999. 55: p. 458-71.
217. Morgan, J, Di Paolo, G, Werner, H, Shchedrina, VA, Pypaert, M, Pieribone, VA, and De Camilli, P, A role for talin in presynaptic function. *J Cell Biol*, 2004. 167: p. 43-50.
218. Sydor, A, Su, AL, Wang, FS, Xu, A, and Jay, DG, Talin and vinculin play distinct roles in filopodial motility in the neuronal growth cone. *J Cell Biol*, 1996. 134: p. 1197-207.
219. Willoughby, D, Thomas, R, and Schwiening, C, The effects of intracellular pH changes on resting cytosolic calcium in voltage-clamped snail neurones. *J Physiol*, 2001. 530: p. 405-16.
220. Huang, W, Swietach, P, Vaughan-Jones, RD, Ansorge, O, and Glitsch, MD, Extracellular acidification elicits spatially and temporally distinct Ca²⁺ signals. *Curr Biol*, 2008. 18: p. 781-5.

221. Stock, C, Cardone, RA, Busco, G, Krahlting, H, Schwab, A, and Reshkin, SJ, Protons extruded by NHE1: digestive or glue? *Eur J Cell Biol*, 2008. 87: p. 591-9.
222. Schwab, A, Rossmann, H, Klein, M, Dieterich, P, Gassner, B, Neff, C, Stock, C, and Seidler, U, Functional role of Na^+ - HCO_3^- cotransport in migration of transformed renal epithelial cells. *J Physiol*, 2005. 568: p. 445-58.
223. Schwab, A, Ion channels and transporters on the move. *News Physiol Sci*, 2001. 16: p. 29-33.
224. Di Ciano, C, Nie, Z, Szaszi, K, Lewis, A, Uruno, T, Zhan, X, Rotstein, OD, Mak, A, and Kapus, A, Osmotic stress-induced remodeling of the cortical cytoskeleton. *Am J Physiol Cell Physiol*, 2002. 283: p. C850-65.
225. Lewis, A, Di Ciano, C, Rotstein, OD, Kapus, A, Osmotic stress activates Rac and Cdc42 in neutrophils: role in hypertonicity-induced actin polymerization. *Am J Physiol Cell Physiol*, 2002. 282: p. C271-9.
226. Olson, M, Contraction reaction: mechanical regulation of Rho GTPase. *Trends Cell Biol*, 2004. 14: p. 111-4.
227. Lin, S, and Corey, DP, TRP channels in mechanosensation. *Curr Opin Neurobiol*, 2005. 15: p. 350-7.
228. Ramsey, I, Delling, M, and Clapham, DE, An introduction to TRP channels. *Annu Rev Physiol*, 2006. 68: p. 619-47.
229. Nakajima, K, Miyazaki, H, Niisato, N, and Marunaka, Y, Essential role of NKCC1 in NGF-induced neurite outgrowth. *Biochem Biophys Res Commun*, 2007. 359: p. 604-10.
230. Pieraut, S, Laurent-Matha, V, Sar, C, Hubert, T, Mechaly, I, Hilaire, C, Mersel, M, Delpire, E, Valmier, J, and Scamps, F, NKCC1 phosphorylation stimulates neurite growth of injured adult sensory neurons. *J Neurosci*, 2007. 27: p. 6751-9.
231. Li, H, Khirug, S, Cai, C, Ludwig, A, Blaesse, P, Kolikova, J, Afzalov, R, Coleman, SK, Lauri, S, Airaksinen, MS, Keinanen, K, Khiroug, L, Saarma, M, Kaila, K, and Rivera, C, KCC2 interacts with the dendritic cytoskeleton to promote spine development. *Neuron*, 2007. 56: p. 1019-33.

232. Wu, K, Khan, S, Lakhe-Reddy, S, Jarad, G, Mukherjee, A, Obejero-Paz, CA, Konieczkowski, M, Sedor, JR, and Schelling, JR, The NHE1 Na⁺/H⁺ exchanger recruits ezrin/radixin/moesin proteins to regulate Akt-dependent cell survival. *J Biol Chem*, 2004. 279: p. 26280-6.
233. Paglini, G, Kunda, P, Quiroga, S, Kosik, K, and Caceres, A, Suppression of radixin and moesin alters growth cone morphology, motility, and process formation in primary cultured neurons. *J Cell Biol*, 1998. 143: p. 443-55.
234. Poinat, P, De Arcangelis, A, Sookhareea, S, Zhu, X, Hedgecock, EM, Labouesse, M, and Georges-Labouesse, E, A conserved interaction between beta1 integrin/PAT-3 and Nck-interacting kinase/MIG-15 that mediates commissural axon navigation in *C. elegans*. *Curr Biol*, 2002. 12: p. 622-31.
235. Shirai, Y, Murakami, T, Kuramasu, M, Iijima, L, and Saito, N, A novel PIP2 binding of epsilonPKC and its contribution to the neurite induction ability. *J Neurochem*, 2007. 102: p. 1635-44.
236. Baumgartner, M, Sillman, AL, Blackwood, EM, Srivastava, J, Madson, N, Schilling, JW, Wright, JH, and Barber, DL, The Nck-interacting kinase phosphorylates ERM proteins for formation of lamellipodium by growth factors. *Proc Natl Acad Sci U S A*, 2006. 103: p. 13391-6.
237. Bretscher, A, Edwards, K, and Fehon, RG, ERM proteins and merlin: integrators at the cell cortex. *Nat Rev Mol Cell Biol*, 2002. 3: p. 586-99.
238. Tomasevic, N, Jia, Z, Russell, A, Fujii, T, Hartman, JJ, Clancy, S, Wang, M, Beraud, C, Wood, KW, and Sakowicz, R, Differential regulation of WASP and N-WASP by Cdc42, Rac1, Nck, and PI(4,5)P2. *Biochemistry*, 2007. 46: p. 3494-502.
239. Sin, W, Haas, K, Ruthazer, ES, and Cline, HT, Dendrite growth increased by visual activity requires NMDA receptor and Rho GTPases. *Nature*, 2002. 419: p. 475-80.
240. Cooper, D, Schell, MJ, Thorn, P, and Irvine, RF, Regulation of adenylyl cyclase by membrane potential. *J Biol Chem*, 1998. 273: p. 27703-7.
241. Willoughby, D, and Cooper, DM, Organization and Ca²⁺ regulation of adenylyl cyclases in cAMP microdomains. *Physiol Rev*, 2007. 87: p. 965-1010.

242. Yamada, R, Matsuki, N, and Ikegaya, Y, cAMP differentially regulates axonal and dendritic development of dentate granule cells. *J Biol Chem*, 2005. 280: p. 38020-8.
243. Willoughby, D, Masada, N, Crossthwaite, AJ, Ciruela, A, and Cooper, DM, Localized Na^+/H^+ exchanger 1 expression protects Ca^{2+} -regulated adenylyl cyclases from changes in intracellular pH. *J Biol Chem*, 2005. 280: p. 30864-72.
244. Chen, Y, Cann, MJ, Litvin, TN, Iourgenko, V, Sinclair, ML, Levin, LR, and Buck, J, Soluble adenylyl cyclase as an evolutionarily conserved bicarbonate sensor. *Science*, 2000. 289: p. 625-8.
245. Litvin, T, Kamenetsky, M, Zarifyan, A, Buck, J, and Levin, LR, Kinetic properties of "soluble" adenylyl cyclase. Synergism between calcium and bicarbonate. *J Biol Chem*, 2003. 278: p. 15922-6.
246. Wang, D, Hu, J, Bobulescu, IA, Quill, TA, McLeroy, P, Moe, OW, and Garbers, DL, A sperm-specific Na^+/H^+ exchanger (sNHE) is critical for expression and in vivo bicarbonate regulation of the soluble adenylyl cyclase (sAC). *Proc Natl Acad Sci U S A*, 2007. 104: p. 9325-30.
247. Ren, X, Ming, GL, Xie, Y, Hong, Y, Sun, DM, Zhao, ZQ, Feng, Z, Wang, Q, Shim, S, Chen, ZF, Song, HJ, Mei, L, and Xiong, WC, Focal adhesion kinase in netrin-1 signaling. *Nat Neurosci*, 2004. 7: p. 1204-12.
248. Li, W, Lee, J, Vikis, HG, Lee, SH, Liu, G, Aurandt, J, Shen, TL, Fearon, ER, Guan, JL, Han, M, Rao, Y, Hong, K, and Guan, KL, Activation of FAK and Src are receptor-proximal events required for netrin signaling. *Nat Neurosci*, 2004. 7: p. 1213-21.
249. Liu, G, Beggs, H, Jurgensen, C, Park, HT, Tang, H, Gorski, J, Jones, KR, Reichardt, LF, Wu, J, and Rao, Y, Netrin requires focal adhesion kinase and Src family kinases for axon outgrowth and attraction. *Nat Neurosci*, 2004. 7: p. 1222-32.
250. Klein, M, Seeger, P, Schuricht, B, Alper, SL, and Schwab, A, Polarization of Na^+/H^+ and $\text{Cl}^-/\text{HCO}_3^-$ exchangers in migrating renal epithelial cells. *J Gen Physiol*, 2000. 115: p. 599-608.